NTNU
Norwegian University of
Science and Technology

Doubly-Fed Induction Machine for use in Mini-Hydro Power Plants

Brage Iversen

Master of Energy and Environmental Engineering
Submission date: June 2016
Supervisor: Trond Toftevaag, ELKRAFT

Norwegian University of Science and Technology
Department of Electric Power Engineering

Doubly-fed Induction Machine for use in Mini-Hydro power plants

The main objective of this Masters thesis work is to further develop and evaluate the performance of a laboratory set-up of a DFIG in mini-hydropower system. The work represents a continuation of a Masters thesis project from 2015, in which a simulation model for this type of system was developed, and the performance of the model checked by carrying out simulation at different operating conditions [7]. The overall idea is to investigate whether or not the efficiency of this type of hydro power generation system can be improved by running the system at a speed so that the optimum efficiency can be achieved at different operating points. The DFIG solution will be implemented in lab using an existing lab setup with a generator/motor set, two back-to-back IGBT converters, and a Speedgoat controller which can run Simulink models in real-time. The control system will be built from scratch. The induction motor in the generator/motor set is used for simulating the hydro turbine behaviour at different operating points.

Preface

This work is based on the idea of implementing a doubly fed induction generator (DFIG) into a small hydro power plant. The first master thesis on this subject was given in the spring of year 2015. The work contained developed control models, simulations, and the beginning of a lab setup. This master thesis is used as a basic for this work. During the fall of 2015, I studied the theoretical background for the DFIG and in the spring of 2016 the work with the master thesis was started.

The original topic was to increase the efficiency of the hydro power plant by adding the possibility of operating at variable speed. The DFIG is used for wind power applications, and its control system is well known. However, it is not yet used in hydro power applications. As mentioned, the behavior of such a system was simulated in earlier an master thesis, but the idea was not verified by appling the theory in lab.

The main goal of this master thesis therfore became to make a lab setup which could be used for simulating the hydro power plant with a DFIG using real machines. The DFIG requires two back-to-back connected voltage source converters for supplying energy to the rotor circuit. Lots of time was spent on making this control system.

When the control system is to be designed, most of the ideas are well known in terms of theory. However, the actual implementation in real life has some difficulties that are not described in the theoretical descriptions. Therefore, a control system was developed during its construction at the lab. The converters and machine setup existed from earlier, but all signal conditioning, instrumentation, construction and programming was made from scratch. The first version of the control system was a messy system where all the components were exposed to noise, making it impossible to use for the given application. Also, if someone else was going to take over the setup in the future, the system would have to be redone due to complexity and bad solutions.

The first version was torn apart, and a new design using existing components from the service lab was made. Finally, the setup started to work as expected. It was now ready for programming the control system. The programming was done using Matlab/Simulink real time environment. After weeks of trial and error, each part of the control system started to work properly. At the beginning of June 2016, the system was running good enough to do some measurements for use in this master thesis.

All this experimentation in the laboratory takes time. Waiting for new parts to arrive, thinking about how to do things and then actually do it, before realizing that it was a really bad idea, causing you to start all over again. However, this process has been very useful for learning how to do things and to understand how things work. This thesis focuses on the road to the target and not the target itself. Most of the ideas and experience gathered from this project, are given throughout this document. Hopefully, it might also be useful for others in the future.

Summary

In hydro power applications, the synchronous generator is widely used. As the speed of the synchronous generator is fixed to the frequency of the grid, the hydro turbine must operate at fixed speed independent of load and water flow. Earlier studies of the topic have concluded that the efficiency of the turbine can be increased by introducing a variable speed generator.

The doubly-fed induction generator (DFIG) is widely used in wind power applications and is capable of operating at speeds $\pm 30\%$ around synchronous speed. However, this introduces a power electronic converter for controlling the rotor currents and slip rings are used for transferring the power into the rotor circuit. This adds complexity to the system which may cause needs for more maintenance and more expensive equipment.

This work continues a work started in a Master thesis in 2015, where the control strategies for a DFIG used in hydro power applications were developed. Simulations were used to study the behavior of the configuration, and a lab setup where a asynchronous motor was used as turbine was made.

The lab setup is improved and the complete control system is rebuilt. A Speedgoat real-time controller is chosen as the controller for the lab setup. The programming of the controller is done by the use of Simulink, which is a well known tool for simulations. The signal conditioning system for speed, voltage and current measurements and solutions for interfacing the converters are made from scratch. The motor drive controlling the asynchronous motor which is used for simulating the turbine, is controlled by the Speedgoat controller.

Through lab tests, the functionality of the lab setup is verified by changing speed and torque. The result of the work, is a lab setup which can be used for testing the DFIG in a hydro power application. Since the hardware is made and found to be working well, it is possible to develop the setup further in the future mainly by doing improvements in software.

Acknowledgements

I would like to thank Trond Toftevaag for being my supervisor on this project, and giving me the opportunity to mainly focus on laboratory work. In an academic environment where simulations are more and more used, it is great that lab work still can be used.

I would also like to thank power electronic virtuous Kjell Ljøkelsøy. Without him, it would have been impossible to have running lab setup. His knowledge and experience from real life is extremely useful while figuring out how to do things properly in the laboratory.

Without the service lab personnel it would have been impossible to do this work. Many thanks to Aksel Andreas Reitan Hanssen, Bård Almås, Vladimir Klubicka and Svein Erling Norum. Also, thanks to Anders Gytri for help with software challenges and for interesting discussions.

I would also like to thank Atle Rygg for providing good ideas for measurements and instrumentation in Simulink and discussions about the control system. A big thanks to Eirik Haustveit for good discussions and ideas about controllers and PWM techniques.

Lastly, I would like to thank my dear friend Ingunn for helping me completing this work.

Brage Iversen

Table of Contents

List of Tables

List of Figures

Chapter 1

Introduction

1.1 Background

The background for this work is an idea presented in an earlier master thesis, where the idea was to implement a doubly-fed induction generator (DFIG) into a small scale hydro power plant for increasing efficiency at operating points different from the best efficiency point. Traditionally, hydro power plants are built using synchronous generators where the speed is fixed to the frequency of the grid. By introducing a variable speed generator, the turbine designer is allowed to vary the rotational speed of the turbine which potentially can increase the efficiency. The speed variation can be $\pm 30\%$ around synchronous speed. However, by introducing the DFIG, a power electronic converter must be used to control the rotor voltage. This converter introduces additional complexity and increases power loss in the system. The slip rings and brushes used for transferring power into the rotor circuit also increase the need for more maintenance. However, the DFIG is widely used in wind power applications and its control system is well known, making it easier to adopt the technology for use with a hydro turbine.

1.2 Objective

The objective for this work is to use ideas developed earlier to make a laboratory setup for testing the DFIG used in a small hydro power system. The best choice for such a laboratory setup is to include a real hydro turbine so that the real turbine characteristics are included in the result, however this would require a DFIG with ratings fitting the turbines used in the hydro power laboratory. For Francis turbines, these model turbines are quite big, and with power ratings up to a few hundred kilowatts. This also require a corporation with the hydro power laboratory. Therefore, a standard induction motor is used for simulating turbine behavior in the lab setup. The size of the machines can then be chosen to fit to existing power sources in the laboratory, and old machines can be reused.

In addition to the machines, the control system of the DFIG will be studied and made.

This includes the choice of which digital platform to use to implement the control system, in addition to making reliable instrumentation to measure the variables in the system, and interface power electronic converters. When these parts are made and their functionality is verified, tests can be performed to document their behavior.

It will be focused on the lessons learned from real life problems that often occur when building such a setup, and hopefully this document (and lab setup) will be useful for someone else in the future.

1.3 Scope of work

In such a project, it is impossible to take everything in account. The time is limited, and it is important to determine goals for the project that fit into the time available. If there is time left after the main goal is reached, one might expand the project further.

In this project the main goal is to design and build the control system for a generator-motor set which can be used to simulate a DFIG connected to a hydro turbine. When each part of the control system is made, its functionality is verified, before moving on the next part. This makes it possible for someone else to continue the work, if time consuming problems occurs.

When the lab setup is working, its functionality can be verified by doing measurements on the setup. It is impossible to make a lab setup that works 100% correct with the time and equipment available, but if each part of the setup is working satisfactory and close to the theory, the goal of the project is reached. If the setup is working, it is possible to continue the development by someone else without the need of rebuilding the system.

1.4 Software

For controlling the lab setup, the Speedgoat X-PC target computer was chosen. This machine is able to run Simulink models in real-time, which can control hardware by using input and output blocks in the model. By the use of Simulink, the level of complicity is reduced to a minimum as most students are familiar with its use during the studies. In addition, the Simulink environment uses visual programming where block diagrams are made, making the readability of the programming better. Simulink also hides most of the complex computer algorithms which are not necessary to know for a power engineer who wants to focus on actual machines more than details of computer algorithms.

For projects where a simulation model is made, the model can be used as a control model without big changes. This can reduce the time spent on developing control models, since the simulation model exists before the lab is made. If a complete simulation model is not made, the Simulink environment makes it possible to test algorithms by testing the behavior of the syste, without actually controlling the machine. This is very useful when errors in models can damage equipment or similar. Some systems must be well tuned to be stable and this tuning can then be done by simulations (via the control model) without using the actual equipment.

1.5 About this report

This report is structured in the following way:

1. First, the background of the work is described.
2. The theoretical background of the doubly fed induction machine and its control system is described. This includes the transient and steady state analysis, the voltage source converters, the vector control principles, techniques for tuning the controllers and information about the turbine concept. As most of the content is well known from literature, the focus has been on keeping the text brief and clear. Still, the basics for understanding the control system are included.
3. The digital Speedgoat controller and its modules are described. This creates a fundamental understanding of how the controller works and is useful knowledge before looking into the laboratory setup description.
4. The laboratory setup is described in detail. Every part of the setup has its own section. First, all the hardware parts of the laboratory setup is described, before the details of how the control system is implemented in Simulink is given.
5. When dealing with practical work, some problems must be solved. Calibration of instrumentation, noise and other physical phenomenons are described in this chapter. Some of the special implementations in Simulink which are not described in the previous chapter, is further described here.
6. In this chapter, the measured results of the setup is given.
7. A discussion of the results, and some thoughts about the configuration.
8. The conclusion. Including a summary of the work, in addition to some ideas and thoughts for future work.
9. Appendices. Pinouts, status codes and and an instruction of how to run the laboratory setup is given here.

Chapter 2

Theoretical description

This chapter will give the theoretical background for the doubly fed induction generator (DFIG) and its control system. First, the steady state and dynamic model is established, before the control system with converters and controllers are examined. In the end, the turbine is described.

The DFIG and its control system is well documented in literature [1][2][3][7]. It is therefore only necessary to include the parts that is important for this project.

2.1 Doubly fed induction generator - DFIG

The DFIG consist of a stator and a rotor, where the stator is equal to the one used for normal induction machines and synchronous machines. The rotor consists of a star connected three phase winding which is connected to three slip rings at the end of the machine. These machines are traditionally used as motor for applications that requires high startup torque. During normal operation, the rotor was short circuited, while during startup a variable resistance was inserted in series with the rotor windings developing high torque and lower currents at slow speeds. However, in this work the DFIG is used as a generator which provides active power to the grid instead of consuming active power. The stator is directly connected to the grid while the rotor is connected to the grid using a bidirectional variable frequency and voltage converter. By varying the frequency in rotor, and thereby the slip, the generator can be operated at different speeds. Usually, this configuration is made for a speed deviation of $\pm$ 30% around synchronous speed. The limiting factor is the size of the converter. When the slip increases, the power rating of the converter is increasing as well. An advantage of this configuration is that the rotor circuit can supply active power to the grid when the machine is running at speeds higher than synchronous speed. This will increase the possible maximum active power without increasing the stator power ratings. This will keep the machine smaller and less expensive. The drawback is the slip rings used to supply the rotor circuit which will require more maintenance.

2.2 DFIG - Steady state

2.2.1 Basic description

As mentioned over, the DFIG consists of two sets of three-phase windings. Each three phase winding consists of three windings 120°shifted from each other and can have p pole pairs, one in stator and one in rotor. The stator can be connected as either Δ or Y and the user can choose the connection based on available voltage and the ratings of the given DFIG. It is common to use a Y connected rotor, but there is usually only three slip rings, as the neutral point is not needed outside the rotor.
The flux produced by the stator is rotating at synchronous speed given by the number of poles and frequency of the currents in the stator and is given by [2]

$$n_s = \frac{60 \cdot f_s}{p} \tag{2.1}$$

where f_s is the frequency in the stator and p is the number of pole pairs. The speed of the stator flux is then given by n_s, and is given in revolutions per minute (rpm). The stator flux will induce a voltage in the rotor windings. This voltage will depend on the difference in stator and rotor speed. The angular frequency of currents and voltages in the rotor is given by

$$\omega_r = \omega_s - \omega_m \tag{2.2}$$

where ω_s is the angular frequency of currents and voltages in the stator and ω_m is the mechanical angular frequency of the rotor. This relation implies two important properties of the system:

- If the rotor does not rotate, the machine acts similar to a transformer with equal frequency in rotor and stator.
- If the rotor operates at synchronous speed, the rotor frequency is zero.

The mechanical angular frequency of the rotor must be given in electrical radians per second. In a two pole machine, the mechanical and electrical angular frequency is the same. In a system with other numbers of pole pairs, the rotor angular frequency is given by

$$\omega_m = p \cdot \Omega_m \tag{2.3}$$

where Ω_m is the angular frequency of the rotor in mechanical radians per second.

It is common to use the term $slip$ to denote the relationship between the stator and rotor speed. It is defined as

$$s = \frac{\omega_s - \omega_m}{\omega_s} \tag{2.4}$$

The properties of the slip is given as

- $s > 0$: Subsynchronous operation
- $s < 0$: Hypersynchronous operation
- $s = 0$: Synchronous operation

The ratio between the stator and rotor angular frequencies given by the slip are given by

$$\omega_r = \omega_s \cdot s \tag{2.5}$$

and hence, the frequencies of the stator and rotor given by the slip are

$$f_r = f_s \cdot s \tag{2.6}$$

2.2.2 Equivalent circuit

The equivalent circuit of the DFIG is similar to the equivalent circuit of the induction machine, but has an additional voltage source in the rotor part of the circuit. It is common to divide the rotor resistance and voltage source into two parts to show which part that is dependent of slip and which part that is not. All quantities are referring to the stator side. The circuit is shown in figure 2.1.

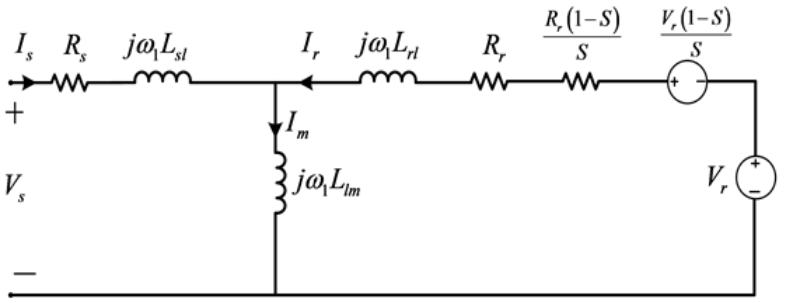

Figure 2.1: Equivalent circuit of DFIG

The equivalent circuit contains the following:

- Stator leakage inductance (L_{ls})
- Rotor leakage inductance (L_{lr})
- Magnetizing inductance (L_m)
- Stator resistance (R_s)
- Rotor resistance (R_r)

The known inductances for a DFIG is the stator inductance (L_s), rotor inductance (L_r) and magnetizing inductance (L_m). The relation between the leakage inductances and the actual inductances is given by

$$L_s = L_m + L_{ls} \tag{2.7}$$

$$L_r = L_m + L_{lr} \tag{2.8}$$

The rotor and stator flux can be written in phasor form as

$$\bar{\lambda_s} = L_s \cdot \bar{I_s} + L_m \cdot \bar{I_r} \tag{2.9}$$

$$\bar{\lambda_s} = L_m \cdot \bar{I_s} + L_r \cdot \bar{I_r} \tag{2.10}$$

By applying Kirchhoff's voltage law on the equivalent circuit, the steady state voltage can be found as

$$\bar{V_s} = R_s \bar{I_s} + j\omega_s \bar{\lambda_s} \tag{2.11}$$

$$\bar{V_r} = R_r \bar{I_r} + j\omega_r \bar{\lambda_r} \tag{2.12}$$

2.2.3 Active power relations

As described in the introduction of this chapter, the power can be exchanged both through rotor and stator, depending on the operating mode. By convention, the power is positive when entering the machine (motoring) and negative when it is extracted from the machine. The total power balance for the DFIG is [2]

$$P_s + P_r = P_{cu,r} + P_{cu,s} + P_{mech} \tag{2.13}$$

where

- P_s and P_r is stator and rotor power
- $P_{cu,s}$ and $P_{cu,r}$ is copper loss in stator and rotor
- P_{mech} is mechanical power

For the steady state analysis, the copper losses can be neglected since they are very small compared to the stator and rotor power. The stator and rotor powers are found as

$$P_s = \Re\{\bar{V_s} \cdot \bar{I_s^*}\} \tag{2.14}$$

$$P_r = \Re\{\bar{V_r} \cdot \bar{I_r^*}\} \tag{2.15}$$

If the mechanical losses (friction and windage) are neglected the mechanical power is

$$P_{mech} = T_{em}\Omega_m = T_{em}\frac{\omega_m}{p} \tag{2.16}$$

Where T_{em} is the electromagnetic torque developed in the machine. When the active power relations in the equivalent circuit are examined, the mechanical power can be expressed as

$$P_{mech} = 3R_r\left(\frac{1-s}{s}\right)|\bar{I_r}|^2 - 3\left(\frac{1-s}{s}\right) \cdot \Re(\bar{V_r} \cdot \bar{I_r^*}) \tag{2.17}$$

In the steady state analysis, it is possible to find approximated power relations between stator and rotor. The copper losses in both stator and rotor are neglected [2].

$$P_r = -sP_s \tag{2.18}$$

$$P_{mech} = P_s - sP_r = (1-s)P_s \tag{2.19}$$

2.2.4 Reactive power relations

The steady state reactive power relations of the DFIG, are similar to the equations for active power and are extracted from the equivalent circuit [3].

$$\begin{aligned} Q_s &= \Im\{\bar{V}_s \cdot \bar{I}_s^*\} \\ &= 3\omega_s L_s |\bar{I}_s|^2 + 3\omega_s L_m \cdot \Re(\bar{I}_r \cdot \bar{I}_s^*) \end{aligned} \tag{2.20}$$

$$\begin{aligned} Q_r &= \Im\{\bar{V}_r \cdot \bar{I}_r^*\} \\ &= 3s\omega_s L_r |\bar{I}_r|^2 + 3s\omega_s L_m \cdot \Re(\bar{I}_s \cdot \bar{I}_r^*) \end{aligned} \tag{2.21}$$

2.2.5 Four quadrant operation

As for the induction machine, the DFIG can be operated in four quadrant mode, origo of the four quadrants is moved from the intersection between mechanical speed and electromagetic torque to the intersection between synchronous speed and electromagnetic torque. This is shown in figure 2.2.

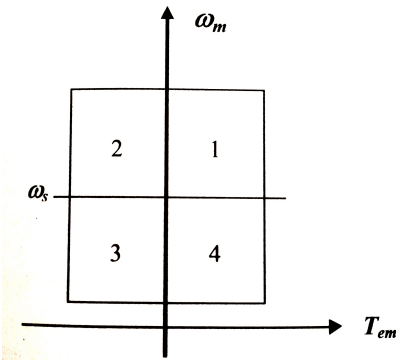

Figure 2.2: Four Quadrant Operation of DFIG

The four quadrants representing two quadrants for motoring (2, 3) and two quadrants for generation (1, 4). In addition subsynchronous (1, 2) and hypersynchronous (3, 4) modes are possible. In terms of slip, mechanical power, stator power and rotor power, the different operating modes are summed up in table 2.1. It can be noted that in generator mode running at hypersynchronous speed, active power can be delivered to the grid. This gives the possibility to increase the active power above nominal power.

Table 2.1: Operating modes of the DFIG

Mode	Speed	P_{mech}	P_s	P_r
Motor	$s < 0$ $\omega_m > \omega_s$ (Hypersynchronism)	> 0	> 0	> 0
Generator	$s < 0$ $\omega_m > \omega_s$ (Hypersynchronism)	< 0	< 0	< 0
Generator	$s > 0$ $\omega_m < \omega_s$ (Subsynchronism)	< 0	< 0	> 0
Motor	$s > 0$ $\omega_m < \omega_s$ (Subsynchronism)	> 0	> 0	< 0

2.3 Space vector analysis

The three phase system with three axes $120°$ spread can be difficult to use when analyzing the dynamic behaviour of the DFIG. The space vector notation is therefore introduced to simplify the dynamic behavior of the system. In the following subsections the theoretical description of the space vector is given for a general variable x which can present voltages, currents or fluxes in the DFIG [2][3].

2.3.1 The space vector

The three phase quantities can be expressed as three sinusoidal varying quantities with $120°$ phase shift and can be mathematically expressed as

$$\begin{aligned} x_a &= \hat{X}\cos(\omega t + \Phi) \\ x_b &= \hat{X}\cos(\omega t + \Phi - \frac{2\pi}{3}) \\ x_c &= \hat{X}\cos(\omega t + \Phi - \frac{4\pi}{3}) \end{aligned} \tag{2.22}$$

where the frequency is given by ω, the amplitude by $\hat{X}$ and phase shift by Φ. Each of the three quantities is varying in their respective axis. These three axes are $120°$ shifted and are defined as a, b and c. The projection of each instantaneous magnitude forms a rotating vector with length equal to the amplitude $\hat{X}$. This is shown in figure 2.3.

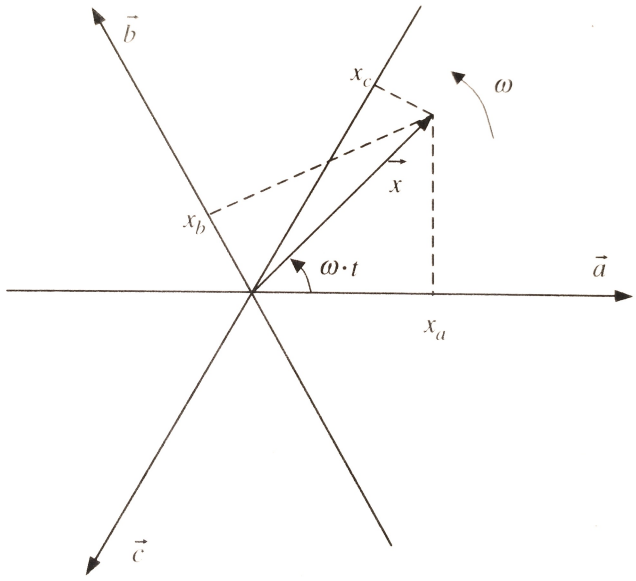

Figure 2.3: Space vector representation

The space vector is mathematically expressed as

$$\vec{x} = |\vec{x}|e^{j(\omega t+\Phi)} \tag{2.23}$$

This is a more compact way of expressing the three phase quantities.

2.3.2 $\alpha\beta$ transformation

Above, the space vector was presented by the projection in each phase of the three phase system. The vector can be expressed as one real and one imaginary component called α and β. This is shown in figure 2.4. As for the abc-coordinate system, the $\alpha\beta$ coordinate system is stationary, giving sinusoidal varying $\alpha\beta$ components of the space vector [2].

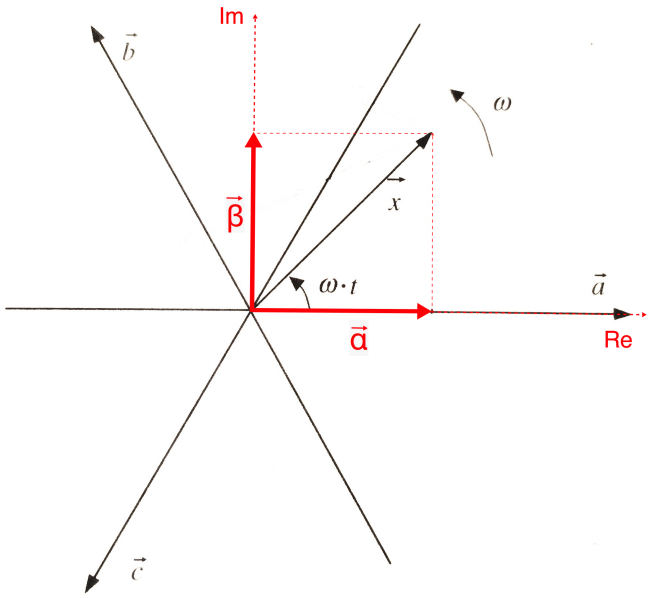

Figure 2.4: $\alpha\beta$ transformation

It can be seen that the α-component is equal to the a-component. Mathematically, the space vector can be presented by

$$\vec{x} = x_\alpha + jx_\beta = \frac{2}{3}(x_a + ax_b + a^2x_c) \tag{2.24}$$

where

$$a = e^{j(2\pi/3)} \tag{2.25}$$

It can be mentioned that the scaling factor of $2\frac{2}{3}$ is used for having the same amplitudes in both coordinate systems. In matrix form the transformation can be expressed as

$$\vec{x}^s = \begin{bmatrix} x_\alpha \\ x_\beta \end{bmatrix} = \frac{2}{3}\begin{bmatrix} 1 & -\frac{1}{2} & -\frac{1}{2} \\ 0 & \frac{\sqrt{3}}{2} & -\frac{\sqrt{3}}{2} \end{bmatrix} \cdot \begin{bmatrix} x_a \\ x_b \\ x_c \end{bmatrix} \tag{2.26}$$

The superscript s denotes that the space vector is rotating at synchronous speed. The transformation is called Clarke transformation. The inverse Clarke transformation is expressed as:

$$\begin{bmatrix} x_a \\ x_b \\ x_c \end{bmatrix} = \begin{bmatrix} 1 & 0 \\ -\frac{1}{2} & \frac{\sqrt{3}}{2} \\ -\frac{1}{2} & -\frac{\sqrt{3}}{2} \end{bmatrix} \cdot \begin{bmatrix} x_\alpha \\ x_\beta \end{bmatrix} \tag{2.27}$$

To calculate power using $\alpha\beta$ coordinates, complex power expression is used:

$$S = P + jQ \tag{2.28}$$

Using space vectors, the complex power is expressed as

$$S = \frac{3}{2}(\vec{v} \cdot \vec{i}^*) \tag{2.29}$$

Inserting $\alpha\beta$ components:

$$S = \frac{3}{2}[(v_\alpha + jv_\beta)(i_\alpha - ji_\beta)] \tag{2.30}$$

$$= \frac{3}{2}[(v_\alpha i_\alpha + v_\beta i_\beta) + j(v_\beta i_\alpha - v_\alpha i_\beta)] \tag{2.31}$$

If this is inserted equation into (2.28), the results for P and Q is

$$P = \frac{3}{2}(v_\alpha i_\alpha + v_\beta i_\beta) \tag{2.32}$$

$$Q = \frac{3}{2}(v_\beta i_\alpha - v_\alpha i_\beta) \tag{2.33}$$

2.3.3 dq-transformation

If the $\alpha\beta$-coordinate system described in the last subsection is rotated with the same speed as the space vector, the components will become constant. This is shown in figure 2.5. The coordinate system used is the dq-coordinate system.

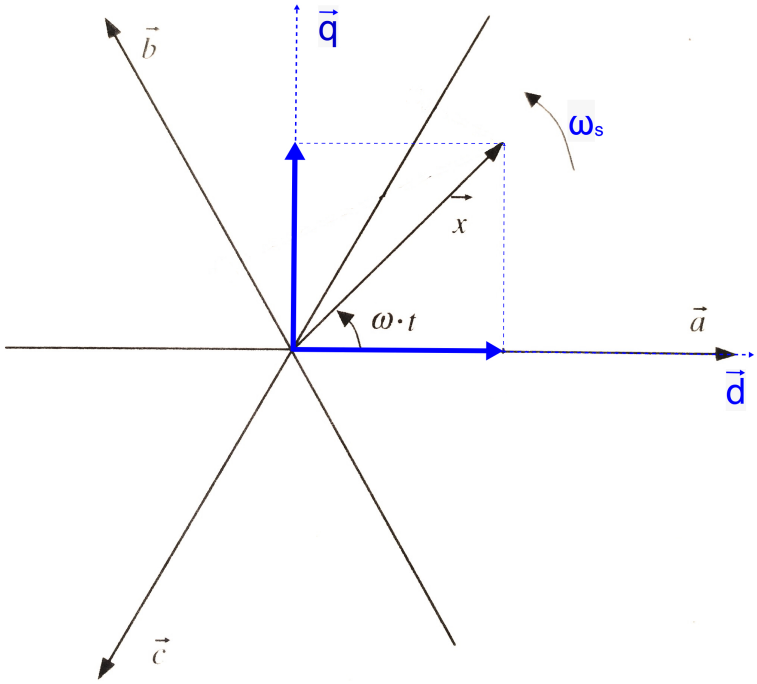

Figure 2.5: dq transformation

The subscript a denotes that the space vector is referred to the synchronously rotating coordinate system. The transformation used for transforming $\alpha\beta$ to dq components is called Park transformation. It must be highlighted that this transformation require the angle of the given space vector.

$$\vec{x}^a = \begin{bmatrix} x_d \\ x_q \end{bmatrix} = \begin{bmatrix} \cos(\theta_s) & -\sin(\theta_s) \\ \sin(\theta_s) & \cos(\theta_s) \end{bmatrix} \cdot \begin{bmatrix} x_\alpha \\ x_\beta \end{bmatrix} \tag{2.34}$$

The Park transformation also has an inverse Park transformation

$$\vec{x}^s = \begin{bmatrix} x_\alpha \\ x_\beta \end{bmatrix} = \begin{bmatrix} \cos(\theta_s) & \sin(\theta_s) \\ -\sin(\theta_s) & \cos(\theta_s) \end{bmatrix} \cdot \begin{bmatrix} x_d \\ x_q \end{bmatrix} \tag{2.35}$$

To convert between stator reference frame and synchronously rotating frame, the following equation can be used [2]

$$\vec{x}^a = e^{-j\theta_s}\vec{x}^s \tag{2.36}$$

$$\vec{x}^s = e^{-j\theta_r}\vec{x}^r \tag{2.37}$$

Using the relation in equation (2.36), the expressions for active and reactive power can be

found to be:

$$P = \frac{3}{2}(v_d i_d + v_q i_q) \tag{2.38}$$

$$Q = \frac{3}{2}(v_q i_d - v_d i_q) \tag{2.39}$$

It must be highlighted that the d- and q-axis components are DC variables. This is very useful when the control system for the DFIG is designed. In the following sections the dynamic model of the DFIG and the grid will be made for both dq and $\alpha\beta$ reference frames.

2.4 Dynamic model of the DFIG

As discussed for the steady state model, the ideal DFIG consists of two sets with three phase windings. One in rotor and one in stator [2][3]. This setup is shown in figure 2.6.

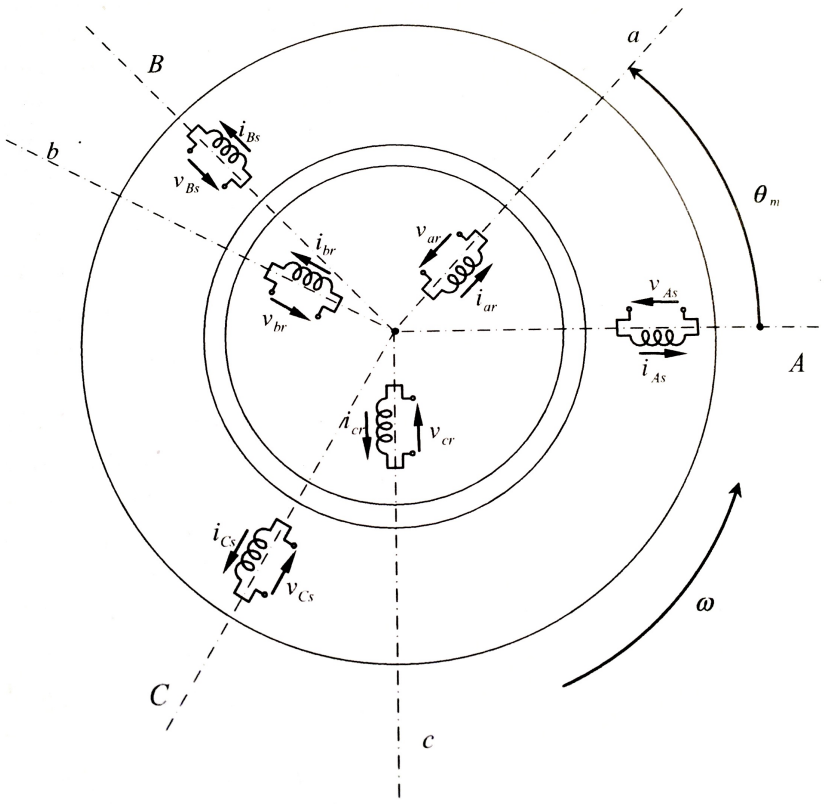

Figure 2.6: Ideal windings of the DFIG

The stator and rotor windings are assumed to be inductances with resistance in series. The instantaneous stator voltage can then be expressed as [2]

$$v_{as} = R_s i_{as}(t) + \frac{d\lambda_{as}(t)}{dt} \tag{2.40}$$

$$v_{bs} = R_s i_{bs}(t) + \frac{d\lambda_{bs}(t)}{dt} \tag{2.41}$$

$$v_{cs} = R_s i_{cs}(t) + \frac{d\lambda_{cs}(t)}{dt} \tag{2.42}$$

where R_s is the stator resistance, i_{as}, i_{bs}, and i_{cs} are the phase currents of each phase, and λ_{as}, λ_{bs}, and λ_{cs} are the stator fluxes for each phase. When the machine operates at steady state, the stator fluxes, voltages and currents are varying sinusiodally with the stator frequency ω_s. The rotor is similar to the stator. For simplifying the analysis, the rotor parameters are referred to the stator side. For machines with equal turns ratio in stator and rotor, the parameters are equal when they are seen from rotor or stator. The rotor voltage is presented as

$$v_{ar} = R_r i_{ar}(t) + \frac{d\lambda_{ar}(t)}{dt} \tag{2.43}$$

$$v_{br} = R_r i_{br}(t) + \frac{d\lambda_{br}(t)}{dt} \tag{2.44}$$

$$v_{cr} = R_r i_{cr}(t) + \frac{d\lambda_{cr}(t)}{dt} \tag{2.45}$$

where R_r is the rotor resistance, i_{ar}, i_{br}, and i_{cr} are the phase currents of each phase, and λ_{ar}, λ_{br}, and λ_{cr} are the rotor fluxes for each phase. At steady state, the fluxes, voltages and currents in the rotor is varying sinusiodally with the rotor frequency ω_r.

2.4.1 $\alpha\beta$ model

For now, the dynamic equations has been described for the actual three phase system. Since the fluxes, currents and voltages can be expressed by space vectors, it is possible to express them as $\alpha\beta$ coordinates. By applying the Clarke transformation given in equation (2.26) on equation (2.40)-(2.42) and (2.43)-(2.45), the $\alpha\beta$ representation of the stator and rotor is:

$$\vec{v_s}^{\,s} = R_s \vec{i_s}^{\,s} + \frac{d\vec{\lambda_s}^{\,s}(t)}{dt} \tag{2.46}$$

$$\vec{v_r}^{\,r} = R_r \vec{i_r}^{\,r} + \frac{d\vec{\lambda_r}^{\,r}(t)}{dt} \tag{2.47}$$

The superscript r for the rotor means that the space vector for the rotor is referred to the rotor reference frame. This gives different reference frames for rotor and stator. It is more convenient to have the same reference system for both rotor and stator to simplify the analysis. To be able to do so, the currents and inductances must be referred to the stator reference frame. The stator and rotor fluxes given as space vectors are

$$\vec{\lambda_s}^{\,s} = L_s \vec{i_s}^{\,s} + L_m \vec{i_r}^{\,s} \tag{2.48}$$

$$\vec{\lambda_r}^r = L_m \vec{i_s}^r + L_r \vec{i_r}^r \tag{2.49}$$

As for steady state modeling, L_m is magnetizing inductance, L_s is stator inductance and L_r is rotor inductance. Now, by the use of the Clarke transformation, it can be found that [2]

$$\vec{\lambda_s}^s = L_s \vec{i_s}^s + L_m \vec{i_r}^s = L_s \vec{i_s}^s + L_m e^{j\theta_m} \vec{i_r}^r \tag{2.50}$$

$$\vec{\lambda_r}^r = L_m \vec{i_s}^r + L_r \vec{i_r}^r = L_m e^{j\theta_m} \vec{i_s}^s + L_r \vec{i_r}^r \tag{2.51}$$

If equation (2.47), which represents the rotor voltage in the rotor reference frame, is multiplied with $e^{j\theta_m}$, the dynamic expression of the DFIG in the stator reference frame becomes:

$$\vec{v_s}^s = R_s \vec{i_s}^s + \frac{d\vec{\lambda_s}^s(t)}{dt} \tag{2.52}$$

$$\vec{v_r}^s = R_r \vec{i_r}^s + \frac{d\vec{\lambda_r}^s(t)}{dt} - j\omega_m \vec{\lambda_r}^s \tag{2.53}$$

$$\vec{\lambda_s}^s = L_s \vec{i_s}^s + L_m \vec{i_r}^s \tag{2.54}$$

$$\vec{\lambda_r}^s = L_m \vec{i_s}^s + L_r \vec{i_r}^s \tag{2.55}$$

The powers for rotor and stator in stator reference frame can then be calcualated by inserting the α and β components into equation (2.32) and (2.33), giving

$$P_s = \frac{3}{2}\Re(\vec{v_s} \cdot \vec{i_s}^*) = \frac{3}{2}(v_{\alpha s} i_{\alpha s} + v_{\beta s} i_{\beta s}) \tag{2.56}$$

$$Q_s = \frac{3}{2}\Im(\vec{v_s} \cdot \vec{i_s}^*) = \frac{3}{2}(v_{\beta s} i_{\alpha s} - v_{\alpha s} i_{\beta s}) \tag{2.57}$$

$$P_r = \frac{3}{2}\Re(\vec{v_r} \cdot \vec{i_r}^*) = \frac{3}{2}(v_{\alpha r} i_{\alpha r} + v_{\beta r} i_{\beta r}) \tag{2.58}$$

$$Q_r = \frac{3}{2}\Im(\vec{v_r} \cdot \vec{i_r}^*) = \frac{3}{2}(v_{\beta r} i_{\alpha r} - v_{\alpha r} i_{\beta r}) \tag{2.59}$$

2.4.2 dq model

Now, the model will be presented in the synchronous rotating frame. As introduced in equation (2.36) and (2.37), the transformation form $\alpha\beta$ to dq reference frames, can be done by multiplying with $e^{j\theta_s}$ and $e^{j\theta_r}$ for stator and rotor respectively. The origial $\alpha\beta$ voltage equations are transformed into dq-components, giving

$$\vec{v_s}^a = R_s \vec{i_s}^a + \frac{d\vec{\lambda_s}^a(t)}{dt} + j\omega_s \vec{\lambda_s}^a \tag{2.60}$$

$$\vec{v_r}^a = R_r \vec{i_r}^a + \frac{d\vec{\lambda_r}^a(t)}{dt} + j\omega_r \vec{\lambda_r}^a \tag{2.61}$$

$$\tag{2.62}$$

The same can be done for the flux expressions.

$$\vec{\lambda_s}^a = L_s \vec{i_s}^a + L_m \vec{i_r}^a \tag{2.63}$$

$$\vec{\lambda_s}^a = L_m \vec{i_s}^a + L_r \vec{i_r}^a \tag{2.64}$$

As shown in equation (2.38) and (2.39), the active and reactive power equations will be equal to the $\alpha\beta$ power expressions

$$P_s = \frac{3}{2}\Re(\vec{v_s} \cdot \vec{i_s}^*) = \frac{3}{2}(v_{ds}i_{ds} + v_{qs}i_{qs}) \tag{2.65}$$

$$Q_s = \frac{3}{2}\Im(\vec{v_s} \cdot \vec{i_s}^*) = \frac{3}{2}(v_{qs}i_{ds} - v_{ds}i_{qs}) \tag{2.66}$$

$$P_r = \frac{3}{2}\Re(\vec{v_r} \cdot \vec{i_r}^*) = \frac{3}{2}(v_{dr}i_{qr} + v_{dr}i_{qr}) \tag{2.67}$$

$$Q_r = \frac{3}{2}\Im(\vec{v_r} \cdot \vec{i_r}^*) = \frac{3}{2}(v_{qr}i_{dr} - v_{dr}i_{qr}) \tag{2.68}$$

2.5 Dynamic model of the grid system

Between the grid converter and the grid, there is a filter located for smoothing out the switched currents. For modeling purposes, this filter is assumed to be an inductor with inductance L_f and resistance R_f. The grid is assumed to be stiff. Using the space vector notation developed for the DFIG in the last sections, the $\alpha\beta$ and dq models will be developed.

2.5.1 $\alpha\beta$ model

The three phase circuit with the converter, filter inductance and grid can be described similar to the rotor and stator of the DFIG. The three phase voltage balance is given by

$$v_{af} = R_f \cdot i_{ag} + L_f \cdot \frac{di_{ag}}{dt} + v_{ag} \tag{2.69}$$

$$v_{bf} = R_f \cdot i_{bg} + L_f \cdot \frac{di_{bg}}{dt} + v_{bg} \tag{2.70}$$

$$v_{cf} = R_f \cdot i_{cg} + L_f \cdot \frac{di_{cg}}{dt} + v_{cg} \tag{2.71}$$

where v_{af}, v_{bf} and v_{cf} are the phase voltages of the converter, i_{ag}, i_{bg} and i_{cg} are the current flowing to the grid, and v_{ag}, v_{bg} and v_{cg} are the phase voltages of the grid. By applying the Clarke transformation, the $\alpha\beta$ voltage balance is given by:

$$v_{\alpha f} = R_f i_{\alpha g}(t) + L_f \frac{di_{\alpha g}(t)}{dt} + v_{\alpha g} \tag{2.72}$$

$$v_{\beta f} = R_f i_{\beta g}(t) + L_f \frac{di_{\beta g}(t)}{dt} + v_{\beta g} \tag{2.73}$$

The $\alpha\beta$ equations can be presented in compact form as [2]

$$\vec{v_f}^s = R_f \vec{i_g}^s + L_f \frac{d\vec{i_g}^s}{dt} + \vec{v_g}^s \tag{2.74}$$

2.5.2 dq model

The dq model is found by multiplying (2.74) with $e^{-j\theta_s}$.

$$\vec{v_f}^s \cdot e^{-j\theta_s} = R_f \vec{i_g}^s \cdot e^{-j\theta_s} + L_f \frac{d\vec{i_g}^s}{dt} \cdot e^{-j\theta_s} + \vec{v_g}^s \cdot e^{-j\theta_s} \tag{2.75}$$

The solution is found as:

$$v_{df} = R_f i_{dg}(t) + L_f \frac{di_{dg}(t)}{dt} + v_{dg} - \omega_a L_f i_{qg} \tag{2.76}$$

$$v_{qf} = R_f i_{qg}(t) + L_f \frac{di_{qg}(t)}{dt} + v_{qg} + \omega_a L_f i_{dg} \tag{2.77}$$

Equation (2.76) and (2.77) is the fundamental equation for applying vector control to the grid converter. This will be described later in the chapter.

2.6 Voltage source converter

For generating the variable frequency and voltage for rotor circuit and for supplying the grid with AC power from the rotor when the DFIG is running at hypersynchronous speed, two equal voltage source converters are used. The voltage source converter (VSC) is made out of six switches and a capacitor bank. The setup is shown in figure 2.7.

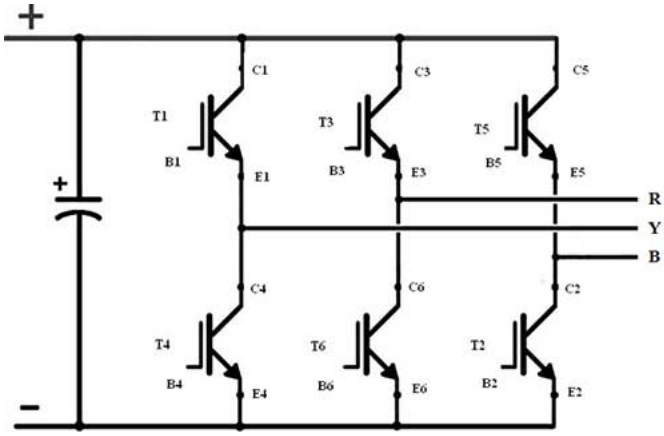

Figure 2.7: Two-level voltage source converter

In each leg with a lower and upper switch, only one switch can be conducting at the time. The voltage at the point between the two switches can then be either 0 or V_{dc}. Three signals are used to trigger the three legs of switches. When the trigger signal is HIGH, the upper transistor is conducting, while if the trigger signal is LOW, the lower transistor is conducting. If the trigger signals are varied in a sinusoidal fashion, the average voltage at a leg will be close to sinusoidal. This can be used to create variable frequency and voltage. An expression for the phase voltage is now made.

2.6.1 Converter model

The voltage between the the zero voltage point in the DC link and the output of a switching leg can either be 0 or V_{dc}. If a switching signal S_j, which can be either 0 or 1, is defined, the voltage at leg j can be expressed as [2]

$$v_{jo} = V_{dc} S_j \tag{2.78}$$

where j can be phase a, b or c. The voltage between phase j and and zero voltage at the DC link can be expressed as

$$v_{an} = v_{ao} - v_{no} \tag{2.79}$$
$$v_{bn} = v_{bo} - v_{no} \tag{2.80}$$
$$v_{cn} = v_{co} - v_{no} \tag{2.81}$$

where v_{no} is the voltage between the neutral point of the three phase system and zero volt in the DC link. From the three phase theory, it is known that the sum of phase voltage at a given time is zero

$$v_{an} + v_{bn} + v_{cn} = 0 \tag{2.82}$$

If (2.79)-(2.81) is inserted in (2.82), the neutral to DC link zero can be found as

$$v_{no} = \frac{1}{3}(v_{ao} + v_{bo} + v_{co}) \tag{2.83}$$

If (2.79)-(2.81) is inserted into (2.83), the phase voltage becomes

$$v_{an} = \frac{2}{3} v_{ao} - \frac{1}{3}(v_{bo} + v_{co}) \tag{2.84}$$
$$v_{bn} = \frac{2}{3} v_{bo} - \frac{1}{3}(v_{ao} + v_{co}) \tag{2.85}$$
$$v_{cn} = \frac{2}{3} v_{co} - \frac{1}{3}(v_{bo} + v_{ao}) \tag{2.86}$$

If (2.78) is inserted in the last equation, the phase voltages in terms of switching states is given as

$$v_{an} = \frac{V_{dc}}{3}(2 \cdot S_a - S_b - S_c) \tag{2.87}$$
$$v_{bn} = \frac{V_{dc}}{3}(2 \cdot S_b - S_a - S_c) \tag{2.88}$$
$$v_{cn} = \frac{V_{dc}}{3}(2 \cdot S_c - S_a - S_b) \tag{2.89}$$

It can be seen that the phase-to-neutral voltage can take up to five different voltage levels, while the line-to-line voltage can have only two voltages. The combination of the three switching states gives eight different switching states, where six is generating output voltage, while the last two are zero vectors, giving zero voltage.

Each of the switches, which usually are insulated-gate bipolar transistors (IGBT), has an antiparallel diode connected in parallel with the switch. That means that the DC link

is charged up to a voltage equal to the amplitude of the sinusoidal voltage applied at the AC of the converter. It is therefore possible to use the converter as a diode rectifier if no control pulses are applied. It must be noted that the power flow can only be from the grid to the DC link in such a case.

2.6.2 Filters

The switching generates currents with high overharmonic content. In order to smooth out the current to something close to sinusoidal waveform, filters are used. For the grid converter, a filter consisting of a pure inductance can be used. This gives more sinusoidal waveforms. There is one inductor for each phase. The rotor circuit can also have a inductive filter, but it is more important to have a dv/dt filter for reducing the voltage at the rotor terminals of the DFIG. The converter can produce overvoltages which can be harmful to the winding insulation. This filter can be e.g series RC filter or RLC filter with R in parallel with L. In some cases, the parasitic resistance of the inductor, is used instead of an actual resistance[2].

2.6.3 PWM modulation techniques

Different pulse with modulation (PWM) techniques exists for controlling the switches of the VSI. These includes:

- Sinusoidal PWM.
- Sinusoidal PWM with third harmonic injection.
- Space vector modulation.

In this work, sinusoidal PWM with third harmonic injection is used. It utilizes the DC link voltage 15% better than traditional sinusoidal PWM, and is mathematically easier to perform than space vector PWM. The harmonic content of the generated voltage is lower than for sinusoidal PWM, but it is a little bit higher than for space vector PWM. The different modulation techniques are presented in detail in literature [2]. From now on, only the sinusoidal PWM with third harmonic injection is described.

The PWM signals are generated by comparing a reference value to a triangular wave. If the reference signal is greater than the triangle wave, the output is on. When the reference signal is lower than the triangle wave, the output is off. For the VSI, the lower transistor is conducting if the signal is off, and the upper transistor is conducting if the signal is on. That means that if the upper and lower transistors are on for the same amount of time, the averange is zero volts. For a three phase VSI, three signals are generated with three different reference signals. These signals are called v_a*, v_b* and v_c* where the subscript is corresponding to phase a, b and c.

If these reference signals are varied in a sinusoidal fashion, the average of the output voltage is sinusoidal.

As mentioned in this work, sinusoidal PWM with third harmonic injection is used. The phase voltage references are generated in the control system, and in the modulator, a third harmonic signal is added. This gives some better use of the available DC link voltage.

The maximal amplitude of the fundamental component of the phase voltage is [2]

$$V_{1,max} = \frac{V_{dc}}{\sqrt{3}} \tag{2.90}$$

To generate the third harmonic component, the properties of the three phase systems are used. The maximum and minimum of the three sinusoidal varying reference signals are divided by 2 and subtracted from the references. This gives an easy method for third harmonic injection. This is shown matematically as:

$$V_3 = -\frac{\min(v_a^*, v_b^*, v_c^*) + \max(v_a^*, v_b^*, v_c^*)}{2} \tag{2.91}$$

Schematically, it is shown in figure 2.8.

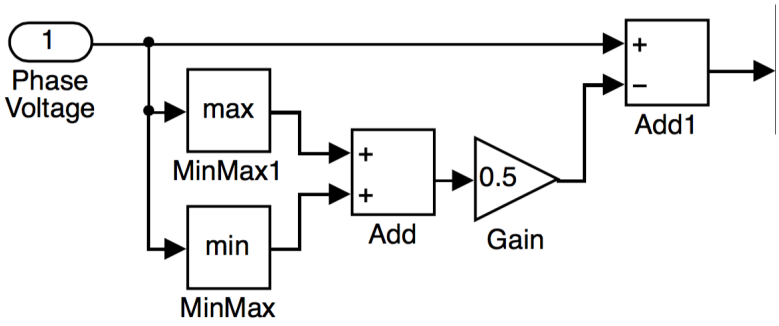

Figure 2.8: SPWM with third harmonic injection

2.7 Vector control principle

The two back-to-back connected converters are responsible for generating voltages with correct magnitude, frequency and phase for the rotor circuit, and for ensuring that power can be exchanged between the rotor circuit and grid in both directions. The system is shown schematically in figure 2.9.

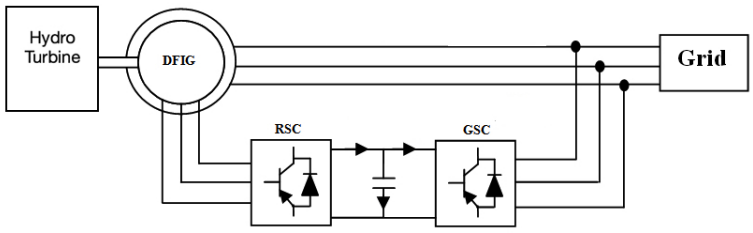

Figure 2.9: DFIG system with hydro turbine

The idea behind vector control is to control the d and q axis currents of the converter in such a way that the setup is working properly. The basic functionality can be summed up as follows:

- The three phase currents of the converter are measured and converted to its d and q components using Clarke and Park transformations. The Park transformation needs an angle varying with the same frequency as the phase currents. The angle can be measured and aligned to the grid voltage or to the stator flux.

- In vector control, the d- and q-axis currents should be controlled to be some desired values, defined by the user. This is done by comparing the measured dq currents to some wanted dq currents values. Proportional + Integral (PI) controllers are used to control the currents.

- The output of the dq current controllers, are the d- and q-axis components of the voltage that should be produced by the converter. The dq voltage values are transformed to abc voltages, which is used as reference for the sinusoidal PWM modulator which controls the converter. The angle for the Park transformations used is the same as for the current transformation described above.

The main idea is to control the dq currents using the dq voltages. In the next two sections, the vector control for each converter is described. The dq currents is very useful seen from the control perspective.

2.8 Vector control of grid side converter

The rotor side converter is responsible for maintaining the DC link voltage at a fixed level, and thereby ensuring bidirectional power flow over the DC link. The reactive power production of the grid converter can also be controlled. The required vector control equations are given in the following subsections.

2.8.1 Vector control equations for the grid side converter

For controlling the grid side converter, the d-axis of the synchronously rotating frame is aligned to the grid voltage space vector. This means that the q-axis voltage is zero. The dq model of the grid system ends up with the following two equations:

$$v_{df} = R_f i_{dg}(t) + L_f \frac{di_{dg}(t)}{dt} + v_{dg} - \omega_a L_f i_{qg} \tag{2.92}$$

$$v_{qf} = R_f i_{qg}(t) + L_f \frac{di_{qg}(t)}{dt} + v_{qg} + \omega_a L_f i_{dg} \tag{2.93}$$

Using the fact that

$$v_{qg} = 0 \tag{2.94}$$

the equations can be simplified to

$$v_{df} = R_f i_{dg}(t) + L_f \frac{di_{dg}(t)}{dt} + v_{dg} - \omega_a L_f i_{qg} \tag{2.95}$$

$$v_{qf} = R_f i_{qg}(t) + L_f \frac{di_{qg}(t)}{dt} + \omega_a L_f i_{dg} \tag{2.96}$$

Further on, power calculations can be redone. The active power can be represented as

$$P_g = \frac{3}{2}\Re(\vec{v_g} \cdot \vec{i_g}^*) = \frac{3}{2}(v_{dg} i_{dg} + v_{qg} i_{qg}) \tag{2.97}$$

which can be simplified to

$$P_g = \frac{3}{2} v_{dg} i_{dg} = \frac{3}{2} |\vec{v_g}^s| i_{dg} \tag{2.98}$$

The same is valid for the reactive power. Reactive power can then be expressed as

$$Q_g = \frac{3}{2}\Im(\vec{v_g} \cdot \vec{i_g}^*) = \frac{3}{2}(v_{qg} i_{dg} - v_{dg} i_{qg}) \tag{2.99}$$

which can be simplified to

$$Q_g = -\frac{3}{2} v_{dg} i_{qg} = -\frac{3}{2} |\vec{v_g}^s| i_{qg} \tag{2.100}$$

From the active power and reactive power relations, is can be seen directly that the d-axis current is responsible for active power control and the q-axis is responsible for reactive power control. By controlling the dq currents, active and reactive power can be controlled separately. However, if (2.95) and (2.96) are examined, the d-axis current is not dependent of the d-axis voltage alone. In the controller, the cross-coupling terms are usually added as feed-forward terms at the output of the PI controllers.

2.8.2 Phase locked loop

The phase locked loop (PLL) is used for obtaining the angle of the grid. It can be realized in a number of ways. This includes:

- Synchronize an oscillator to the zero crossing of the positive sequence a-axis of the voltage. Calculate frequency of the oscillator by using the duration of the last period.
- Convert the three phase voltages to space vector form using the Clarke transformation. Then obtain the angle by calculate the arcus tanges of the $\alpha\beta$ components of the voltage.
- Convert the three phase voltages to space vector form using the Park transformation. By feeding the d-axis voltage in a PI controller as the error, and let the output of the PI controller be the angular frequency. This frequency can be integrated to get the angle. This angle is fed into the Park transformation. By having accurate tunings, the PI controller will force the d-axis component to be zero, which will ensure that the d-axis is in phase with the grid voltage space vector.

The PLL is responsible for obtaining the grid angle without loosing track due to voltage and/or frequency variations. The three methods described above is just a basic description of possible ways of doing it. The actual PLLs requires more complex details to be able to obtain the grid frequency in a good manner. For more details on this subject, it is referred to the literature [2].

2.8.3 DC link voltage controller

As stated above, the d-axis current is controlling the active power flow of the converter. The energy flow over the DC link must be in equilibrium for having a constant voltage at the DC link. When the DFIG is running as a generator and the speed is subsynchronous, the power flows from the grid, through the grid converter, over the DC link, through the rotor converter and into the rotor of the DFIG. In this mode, the grid converter acts as a rectifier while the rotor converter act as an inverter. It is possible to run the grid converter without any control at this operating point. If the speed is increased to a speed above synchronous speed, the rotor circuit will supply power to the DC link. If the grid converter is running as a rectifier, there is no way the active power can be fed back to the grid, and the DC link voltage will increase. However, if the grid converter is started to work as an inverter, the active power can be fed back to the grid. This can be controlled by the d-axis current of the converter.

For ensuring bidirectional power flow, the actual DC link voltage is compared to a fixed DC voltage that is determined by the user. A PI controller which controls the d-axis current reference can then be used to keep the DC link voltage constant. The magnitude of the DC link voltage must be higher than the voltage a standard diode rectifier will make. By having a constant DC link voltage, the power flow over the DC link is in equilibrium and the grid converters can smoothly change from rectifiers to inverters.

2.9 Vector control of rotor side converter

The rotor converter controls the active and reactive stator power, by adjusting the dq currents of the rotor circuit. The active power control is used for controlling the speed of the DFIG. The necessary vector control equations is given in this section.

2.9.1 Alignment of the rotating dq coordinate system

There are two ways of aligning the rotating reference system of the rotor converter. This includes:

- Stator flux orientation
- Grid voltage orientation

If the stator flux orientation is used, the stator flux is estimated, and the d-axis of the synchronous rotating frame is aligned to the stator flux space vector. This is the traditional way of controlling the DFIG. However, for voltage variations of the grid, the rotating speed

is not constant, adding a disturbance in the angle. This method is most accurate for stiff grids.

If grid voltage orientation is used, the d-axis of the synchronous rotating frame is aligned to the grid voltage space vector. The grid angle is just a stiff as the frequency of the grid. This makes this method more capable of withstanding voltage dips. Another feature of this method, is that the grid voltage is easy to measure and no estimation is necessary. The PLL is used to obtain the grid angle. In this work, grid oriented vector control is used for the rotor converter.

2.9.2 Vector control equations for the rotor side converter

The rotor side converter controls the d and q-axis currents of the rotor circuit. The power expressions for the stator is generally written as:

$$P_s = \frac{3}{2}\Re(\vec{v_s} \cdot \vec{i_s}^*) = \frac{3}{2}(v_{ds}i_{ds} + v_{qs}i_{qs}) \tag{2.101}$$

$$Q_s = \frac{3}{2}\Im(\vec{v_s} \cdot \vec{i_s}^*) = \frac{3}{2}(v_{qs}i_{ds} - v_{ds}i_{qs}) \tag{2.102}$$

By aligning the d-axis of the synchronous rotating reference frame, the q-axis voltage of the stator becomes zero. Using this fact, the power equations are reduced to:

$$P_s = \frac{3}{2}v_{ds}i_{ds} \tag{2.103}$$

$$Q_s = -\frac{3}{2}v_{ds}i_{qs} \tag{2.104}$$

This gives the active power only dependent of the d-axis stator current and the reactive power only dependent of the q-axis stator current [1]. An expression for stator based on rotor current is needed for understanding how the system should be controlled. The stator flux is shifted $90°$ behind the stator voltage. Since the d-axis is aligned with the stator voltage space vector, the flux in the d-axis is zero. That means that the dq-model of the stator flux becomes:

$$L_s i_{ds} + u_{dr}L_m = 0 \tag{2.105}$$

$$L_s i_{qs} + u_{qr}L_m = \lambda_s \tag{2.106}$$

By rearranging (2.105) and (2.106), we can express the dq stator currents as:

$$i_{ds} = -\frac{L_m}{L_s}i_{dr} \tag{2.107}$$

$$i_{qs} = \frac{\lambda_s - L_m i_{qr}}{L_s} \tag{2.108}$$

If these components are inserted in the power expressions (2.103) and (2.104), the active and reactive power of the stator can be expressed as:

$$P_s = -\frac{3}{2}\frac{L_m}{L_s} \cdot v_{ds} i_{dr} \tag{2.109}$$

$$Q_s = -\frac{3}{2}\left[\frac{\lambda_s}{L_s} v_{ds} - \frac{L_m}{L_s} v_{ds} i_{qr}\right] \tag{2.110}$$

If the stator resistance is neglected, the stator voltage is expressed as

$$\hat{V_s} = v_{ds} = \lambda_s \cdot \omega_s \tag{2.111}$$

By inserting the last equations in the power expressions, the final expressions for active and reactive power becomes:

$$P_s = -\frac{3}{2}\frac{L_m}{L_s} \cdot v_{ds} i_{dr} \tag{2.112}$$

$$Q_s = \frac{3}{2}\left[\frac{L_m}{L_s} v_{ds} i_{qr} - \frac{v_{ds}^2}{2 \cdot \omega_s L_s}\right] \tag{2.113}$$

As seen from the equations above, the active power is proportional to d-axis rotor current, while the reactive power can be controlled by the q-axis rotor current, but has an additional term dependent of voltage and frequency. The reactive power control is then limited by the current ratings of the rotor and the active power demand.

The voltage and current relations is the stator must be used to design the control system of the rotor converter. From the dynamic modelling of the rotor, the following relations was found for the dq reference frame

$$v_{dr} = R_r i_{dr} - \omega_r \lambda_{qr} + \frac{d}{dt}\lambda_{dr} \tag{2.114}$$

$$v_{qr} = R_r i_{qr} + \omega_r \lambda_{dr} + \frac{d}{dt}\lambda_{qr} \tag{2.115}$$

Since the stator flux is zero in the d-axis, the dq flux expressions becomes

$$\lambda_{dr} = (L_r - \frac{L_m^2}{L_s}) i_{dr} \tag{2.116}$$

$$\lambda_{qr} = (L_r - \frac{L_m^2}{L_s}) i_{qr} + \frac{L_m}{L_s}\lambda_{qs} \tag{2.117}$$

By the use of the leakage factor σ, the flux equations can be simplified to

$$(L_r - \frac{L_m^2}{L_s}) = L_{ls} + \frac{L_m L_{ls}}{L_m + L_{ls}} = \sigma L_r \tag{2.118}$$

where

$$\sigma = 1 - \frac{L_m^2}{L_r L_s} \tag{2.119}$$

This finally gives the following relation for the voltages and currents:

$$v_{dr} = R_r i_{dr} - \omega_r \sigma L_r i_{qr} + \omega_r \frac{L_m}{L_s} \lambda_{qs} + \frac{d}{dt}(\sigma L_r i_{dr}) \tag{2.120}$$

$$v_{qr} = R_r i_{qr} + \omega_r \sigma L_r i_{dr} + \frac{d}{dt} \frac{L_m}{L_s} \lambda_{qs} + \frac{d}{dt}(\sigma L_r i_{qr}) \tag{2.121}$$

Now, the plant for control design can be chosen [2].

- The derivative of the stator flux given in the q-axis equation is zero during normal operation. However, this is not the case for voltage variations at the stator terminals.
- The cross-coupling terms is added as feed-foreward terms after the PI current regulators.
- The stator flux term for the d-axis equation, is constant and can be compensated in the controllers.

The final plant equations then becomes:

$$v_{dr} = R_r i_{dr} - \omega_r \sigma L_r i_{qr} + \sigma L_r \frac{d}{dt} i_{dr} \tag{2.122}$$

$$v_{qr} = R_r i_{qr} + \omega_r \sigma L_r i_{dr} + \sigma L_r \frac{d}{dt} i_{qr} \tag{2.123}$$

These equations can further be Laplace-transformed and controller tunings can be chosen.

2.9.3 Angle calculation for the rotor side converter

The Park transformations used for the stator side converter, require the angle of the rotor. It is possible to estimate the rotor angle, but it is common to measure the angle by the use of an encoder [2]. The frequency of the rotor currents is given by

$$\omega_r = \omega_s - \omega_m \tag{2.124}$$

where ω_s is the stator angular frequency and ω_m is the mechanical angular frequency as electric radians per second. The angle of the rotor follows the same concept:

$$\theta_r = \theta_s - \theta_m \tag{2.125}$$

The grid angle θ_s is obtained from the PLL, while the mechanical angle θ_m is given from the encoder located at the rotor shaft.

2.9.4 Speed controller

As shown above, the d-axis current is controlling the active stator power. The turbine can be seen as a torque controlled motor having no control over the speed. The runaway speed of a hydro turbine can be $1.5 - 2.5$ times higher than the nominal speed, giving a need for speed control. Usually, the hydro power plants use synchronous generators which run

at fixed speed controlled by a speed governor. The governor increases the water flow to increase the production of mechanical power when the generator load is increased. In this case the DFIG should control the speed by adjusting the active stator power.

A simple PI controller measures the rotational speed of the DFIG and controls the d-axis current of the rotor converter to control the active stator power. The speed is obtained by taking the derivative of the mechanical rotor angle given by the encoder at the rotor shaft. The speed can then be chosen by the turbine governor to operate the hydro turbine at the optimal speed. This is briefly described in the next section.

2.10 Turbine

The prime mover in the hydro power plant is the hydro turbine. Different designs exists for different head and flow. They can be controlled by guide vanes or needle valves to produce the desired power. The three most used turbines are:

- Pelton turbine (600m $<$ Head)
- Francis turbine (30m $<$ Head $<$ 600m)
- Kaplan turbine (5m $<$ Head $<$ 70m)

These three turbine types are well described in literature [3][7], and only the relevant features for this work will be included here. In this work, the Francis turbine is considered. It consist of three main parts:

- Turbine runner
- Guide vanes
- Spiral casing

The spiral casing is located around the guide vanes and the turbine runner. It is responsible for supplying water to the turbine around the periphery of the turbine runner. The water flow is limited by a set of guide vanes located between the runner and the spiral casing. The angle of these guide vanes can be adjusted to give the right flow which will control the power delivered by the turbine. The water hits the turbine blades, flows through the turbine and flowes out axially through the draft tube. Since the runner rotates in the water flow, there is no air involved. This makes it possible to utilize the head from the runner to the tailwater. This means that the turbine can utilize all the available head and the efficiency can be up to 95-96%.

However, the efficiency is best at a certain guide vane angle. At operating points different from the best efficiency point (BEP), the efficiency decreases. The efficiency can be seen as the contours in the Hill diagram, given in figure 2.10. The horisontal axis gives the rotational speed. while the vertical axis gives the water flow. In this diagram, the flow and speed is given as specific parameters. This is useful for comparing prototypes to model turbines. For a more detailed description, it is referred to the literature [3]. The dotted lines across the Hill diagram shows the different guide vane angles for all the different efficiencies.

For power plants which use synchronous generators, the speed is fixed to the vertical line which goes through BEP. All the possible operating points are located along the line. For a power plant using the DFIG, the speed can be varied. If it is possible to move along a non-vertical path when a change in flow is given, the efficiency can be better. This gives the turbine designer more freedom to design a turbine which can run on different speeds, and possibly increase efficiency. Some operating points might be impossible at fixed speed due to cavitation problems. Some of these can be eliminated by running at different speeds.

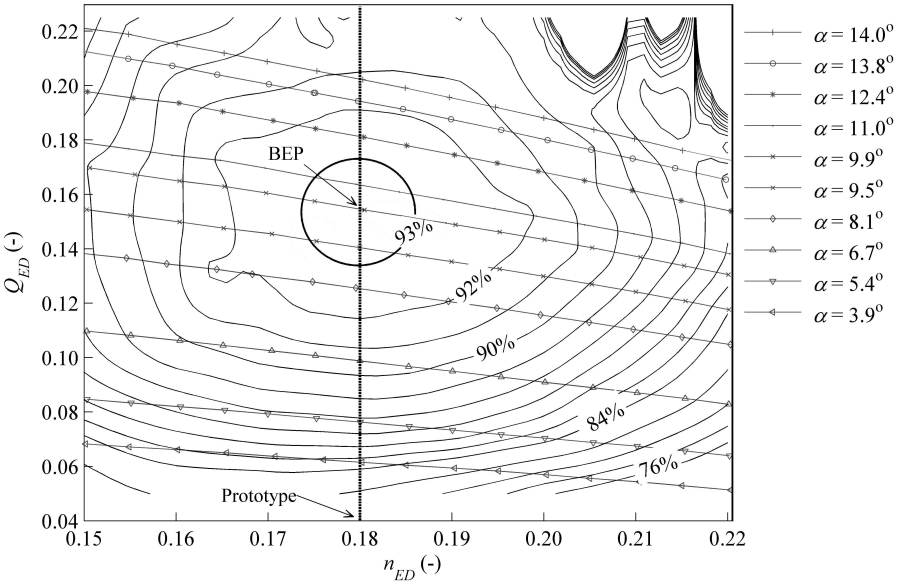

Figure 2.10: Hill diagram of a Francis turbine

Chapter 3

Software - Simulink Real Time

For controlling the laboratory setup, a Speedgoat realtime target controller is used. The system consists of a computer with analog and digital inputs and outputs for measurements and controllers in the setup. Simulink is running at an additional computer where the control system is developed. The Simulink models are then compiled inside the computer and transferred to the real time target computer for execution of the control model in real time.

3.1 Simulink

Simulink is used for developing the control model for the system. Simulink is a part of MATLAB and is used for simulation of systems. Programming of models is based on connecting together functional blocks and creating block diagrams of the given system. Therefore, there is no need for direct coding of the control models. This makes the development of models fast and will move focus to the actual model development instead of programming complicated code algorithms. This makes the platform well suited for users who want to focus on developing physical models instead of coding. A visual representation of the system increase the understanding of the models. Simulink is used for simulation of systems in both academic environments and industrial environments.

For this work, the models of the hardware parts are removed and replaced by input and output blocks to actual hardware. The model will then contain all the controllers, protection and monitoring of the laboratory setup. A special set of IO blocks are supplied with the Speedgoat, and it is then makes it possible to install the blockset for any computer running MATLAB under Windows.

3.2 Speedgoat X-PC target computer

The Speedgoat X-PC target computer is a modular computer with slots for different IO-cards used for interfacing the hardware in the setup. This machine has the following

IO-cards installed:

- 2x PWM modules (IO311)
- 1x Analog to digital module (IO106)
- 1x Digital to analog module (IO110)
- 1x Digital IO module (IO203)
- 1x Real time Ethernet module (IO703)

The two PWM modules are based on a Xilinx Virtex-II FPGA and each board have six PWM channels, three encoder inputs, three pulse inputs, one interrupt, one negation channel and six standard digital IO. Each of the two converters used for controlling the DFIG has one dedicated PWM module. The analog to digital (ADC) module have either 64 singel ended or 32 differential input channels. These ADC channels are used for measuring voltages and currents in the system. The digital to analog (DAC) module has 32 output channels. These signals are used for analog control of the asynchronous motor and for four debug channels for use with an extern oscilloscope. The digital IO module has 64 channels and each channel can be either output or input. These lines are used for controlling relays in the setup. The real time ethernet module is not used in this work and will not be explained any further. The Speedgoat X-PC target computer is shown is figure 3.1.

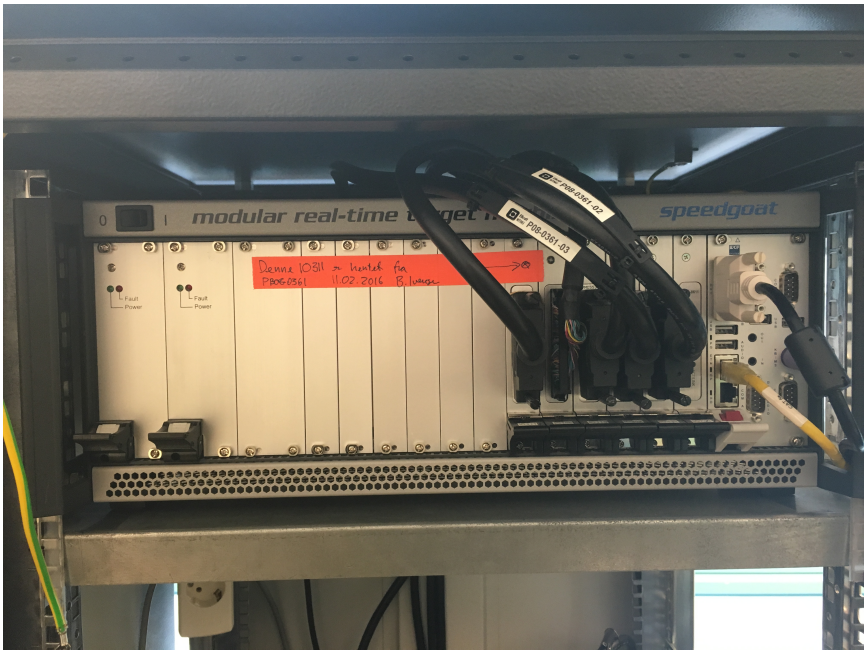

Figure 3.1: Speedgoat X-PC target computer

Each of the IO cards has its own multicore cable which is connected to a breakout board with connections for each pin. These breakout boards are discussed in detail in chapter 4.

In addition to the IO cards, the Speedgoat has the following features:

- DVI connector for monitoring the running application
- PS-2 connector for standard keyboard
- Two gigabit ethernet connectors for communication with the host computer
- Four RS-232 Serial lines which also can be used for communication with the host computer
- USB connectors
- Dual power supply

At the time of writing, the Speedgoat requires MATLAB release 2010a or 2010b to work. This is a rather old MATLAB release and the X-PC real time environment has changed to Simulink Real Time in newer releases. Without any upgrades of the Speedgoat, it will only be possible to run models created using MATLAB release 2010a or 2010b.

In the following sections, the different modules are discussed more in detail. Only the important data for this work is included. For more information about the functionality of each module, it is referred to the Speedgoat documentation [8].

3.2.1 311 PWM Module

This module is used for generating pulse width modulated (PWM) signals for the converters, receive status data from the converters and capturing encoder signals. It is based on the Xilinx Virtex-II Field Programmable Gate Array (FPGA) and is preprogrammed from the manufacturer. Since the FPGA is preprogrammed, all the functionality is fixed and can not be change unless the FPGA code is changed. This code can not be produced by Simulink, and the manufacture can provide custom code on request. The default setting features the following:

- 6x PWM outputs which can be synchronized.
- 3x Encoder inputs with A, B And Z (index) channels.
- 1x Capture input for capturing pulse signals or determining PWM duty cycles.
- 1x Negation input for inverting a signal
- 6x Standard digital IO
- 5V Logic level
- 33 MHz clock

FPGA's provide very fast execution of code and is very useful for time critical parts of the control system. In digital signal processor (DSP) based programming the instructions are executed in a sequence one by one. This takes some time, and it is necessary to have very fast processors to accurately do the desired task at exactly the right time. In the FPGA,

programmable logic cells are wired together creating the functionality the designer wants. This gives much faster execution times than DSP-based programming.

The six PWM signals are used for controlling the six transistors in each converter. PWM signals are created by comparing a given value to a counter. The counter is 32-bit and runs at 33 MHz. The PWM logic is based around one counter and two compare values, A and B. These modules can be confiured to work together in synchronism. There is three PWM modules giving the totalt of 6 PWM outputs. Each module also have a trigger output which can be used for synchronizing analog measurements to the PWM. The PWM modules can be configured differently by a number of parameters given in the Speedgoat documentation.

The encoder inputs takes the three signals from the mechanical encoder mounted on the end of the DFIG. These signals are decoded into a counter that will reset every one turn of machine. The counter can then be used to find the angle and speed of the machine. Three signals are supported:

- Channel A: Gives a number of pulses per revolution
- Channel B: Same as channel A, but 90 degrees phase offset. Used for determining direction of rotation.
- Channel Z: Gives a pulse every one turn. Used for resetting the position counter.

The digital IO is standard input/output. Each channel can be configured as input or output. Status, enable and reset signals from the converters can be controlled using this input/output ports.

3.2.2 106 Analog to digital module

The analog to digital converter (ADC) board is used for measuring voltages fast for use in the model. All channels have dedicated ADC's resulting in high speed operation. The ADC module has the following features:

- 64 single ended inputs, 62 pseudo differential inputs or 32 differential inputs.
- Multiple voltage ranges. All inputs are using the same voltage range.
- Fast conversion times.
- Possible synchronizing with PWM

In this work, all measurements are done as fast as possible in each sample period of the control model. That means that there is no synchronization between PWM signals and measurements. As described in chapter 4, this will introduce the need of filters, especially on the the current measurements. It is worth mentioning that the current measurements must be converted to voltage signals before they can be measured using the ADC module. The measured voltages appear as real voltages in the Simulink model.

3.2.3 110 Digital to analog module

The digital to analog converter (DAC) module is used for generating analog signals for external devices. The DAC module has the following features:

- 32 Singel ended outputs
- 16-bit resolution
- 3 μs update time
- Individual voltage range for each channel

Two DAC channels are used for analog control of torque and torque limit of the motor driver for the asychronous motor. Four additional outputs are used for debugging signals for an external oscilloscope. This is extremely useful for debugging the control system during runtime.

3.2.4 203 Digital IO module

This module consists of standard digital inputs and/or outputs. It has the following features:

- 64 Singel ended TTL or CMOS compilant inputs or outputs.
- 3.3V Logic level
- Low latency

This module is used for controlling the relays which controls the main breakers for the converters.

3.2.5 Speedgoat monitor

The Speedgoat X-PC target computer can be used with a standard DVI screen for monitoring real time data. The monitor supports either soft oscilloscopes or numerical representation of the model data. In the X-PC Simulink Blockset, these data representation blocks are called Scope. These scopes are useful for monitoring currents, voltages, rpm, and other variables. The screen will atomatically zoom each scope so that all the scopes in the model are visible at all times. There is no way to access any data in the model during runtime using these scopes, but it is possible to zoom at spesific scope to have a better look at each scope. A scope can either be a numerical representation or have an oscilloscope-like behavior.

3.3 Simulink external mode

As mentioned in section 3.2.5, the Speedgoat has no control surface for manipulating data during runtime. If ”External mode” is used in the Simulink model after the model is uploaded to the Speedgoat, it is possible to change some blocks during runtime. These blocks include:

- Manual switches
- Constant blocks
- Gain blocks
- Slider gains

Figure 3.2 shows the control surface for the laboratory setup. A number of switches are used to control the different breakers, converters, controllers and other boolean operations. Constant blocks and slider gains are used for changing setpoints for controllers and adjusting limits for the protection system. Internal routing of measurement values using manual switches is useful when the monitor fills up with many scopes. Also, changing gains during runtime is useful for controller tunings as well. It is worth mentioning that the ”Display” block works well in ”external mode”, but might be slow and are therefore useful for status codes and similar applications which does not require high update speeds.

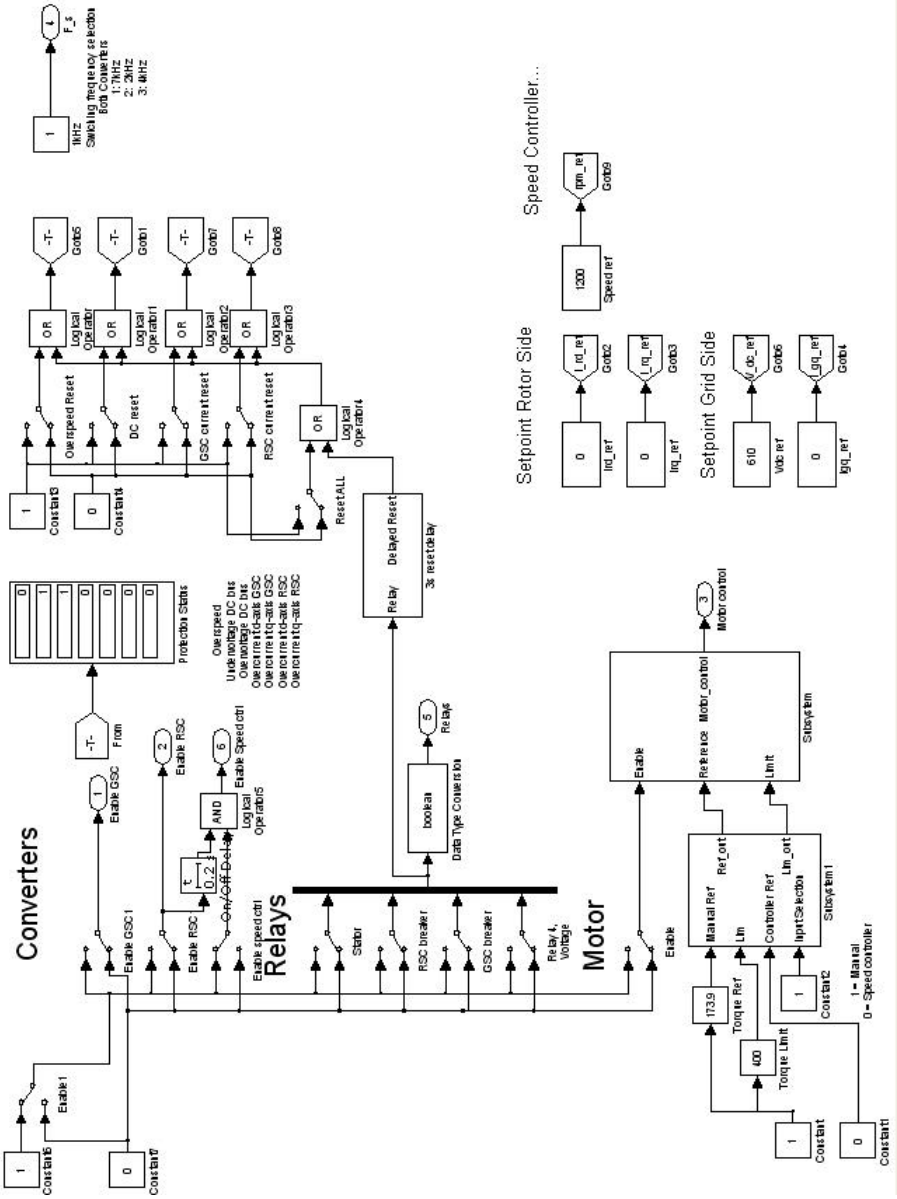

Figure 3.2: Simulink control panel

Chapter 4

Laboratory Setup

The laboratory setup for simulation of the Francis turbine, DFIG and control system consists of the following parts:

- A 15kW asynchronous motor with torque control for turbine simulation.
- A 15kVA doubly fed induction machine as generator
- Two 20kVA back-to-back connected voltage source converters for control of the rotor circuit
- A Speedgoat X-PC target computer with IO connections for controlling the system

The generator-motor set is mounted on a steel frame, and is standing freely. The generator and motor are connected together on the same shaft using a mechanical connection. Encoders are mounted on each machine for angle measurements for the respective controllers. Next to the machine setup, there is three racks on wheels. One for the back-to-back converter, one for the control system and one for the motor controller. All power connections for the DFIG is located in the bottom of the converter rack along with breakers for rotor and stator circuits. Current measurements are located on each converter, while the voltage measurements are located in the rack for the control system. In the control system rack, the Speedgoat controller and signal conditioning equipment are located. The controller is on the top, while signal conditioning and connections are located in the middle. The motor controller is a standard 20kVA vector control based motor controller and has its own control system. It is remotely controlled by the Speedgoat controller, but can also be controlled locally. In figure 4.1, the generator-motor set, converter rack and controller rack is shown. In the following parts, each part of the lab setup will be discussed in detail.

4.1 Generator-motor set

The DFIG and the motor is mounted together on a steelframe as seen in figure 4.1b. A mechanical coupling with a rubber ring is used to connect the shafts of each machine

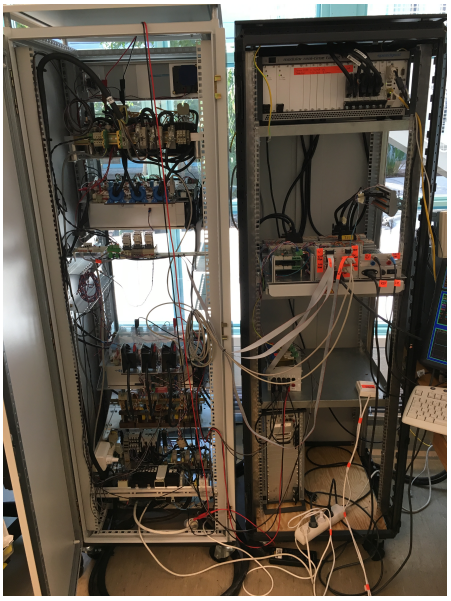

(a) Converter to the left and control system to the right

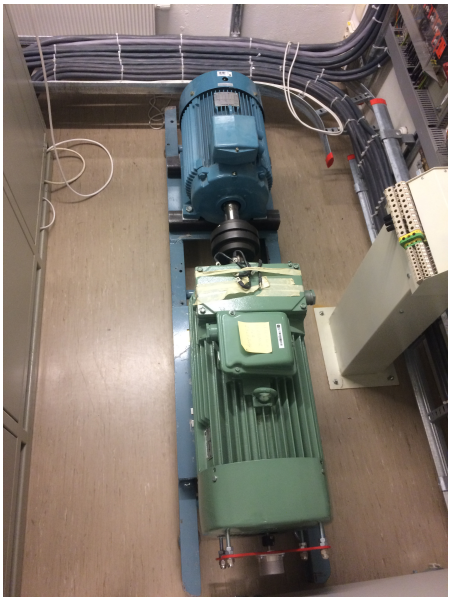

(b) Generator-motor set

Figure 4.1: Laboratory setup

together. Because of bearings in both ends of each machine, perfect alignment of the shafts is difficult, and the rubber ring adds some freedom to the alignment. This is very common and is used for larger hydromachines and other mechanical applications as well.

4.1.1 DFIG

The green machine in figure 4.1b is the DFIG. The box at the upper end of the machine is where the slipsrings are mounted. The connection to the rotor circuit is inside this box. The box next the hook on the top of the machine is the connection for stator circuit. There is six connection points - two for each winding. Therefore, it is possible to choose either star or delta connection of the stator. The rotor is delta connected and this cannot be changed. The red device in the lower end of the DFIG is the mechanical encoder which is used for angle and speed measurements. The DFIG parameters is given in table 4.1.

Table 4.1: DFIG parameters

Nominal power: 15 kW	Nominal I_r: 33A
Nominal speed: 1470 rpm	$R_s = 0.12\Omega$
4 poles	$R_r = 0.14\Omega$
Nominal V_s: 380/220V (Y/Δ)	$L_s = 13.74\text{mH}$
Nominal I_s: 32/55A (Y/Δ)	$L_r = 13.74\text{mH}$
Nominal V_r: 280V	$L_m = 13.54\text{mH}$

4.1.2 Motor

The blue machine in figure 4.1b. This is a standard squirrel cage induction motor and it is going to simulate the turbine behaviour. The machine parameters are similar to the DFIG and is given in table 4.2.

Table 4.2: Motor parameters

Nominal power: 15 kW	Nominal V_s: 380V (Y)
Nominal speed: 1450 rpm	Nominal I_s: 31A (Y)
4 poles	Cos ϕ: 0.82

4.1.3 Motor controller

For controlling the motor, a torque controlled motor drive is used. This is a standard 20kVA Sintef/NTNU voltage source converter with a FPGA-based control system. The drive can be used for both synchronous permanent magnet machines as well as induction machines. A flexible menu system provides easy configuration of the drive. It is possible to use the drive with or without speed controller. This is very useful when configuring the DFIG control system. A fixed speed can be set on the motor driver and the parameters can be tuned without problems with rise in mechanial speed. When the speed controller is disabled, the machine is torque controlled.
Before using the drive, it is necessary to set some parameters [6]. This can be set in the menu system of the converter.

- Encoder resolution
- Phase sequence of the drive
- Positive speed direction
- Speed or torque control mode
- Rated current of the motor
- Rotor time constant
- Max slip frequency
- Magnetization current

The drive has a protection system that must be set accordingly to ensure safe operation. This include

- Maximum speed limit
- Maximum current limits
- Maximum DC link voltage

With all the given parameters set, it is possible to set the drive into operation. This can be done by starting the drive from the LCD display and setting the speed or torque reference different from zero. It is worth noting that the converter uses the values -1000 to 1000 as -1 to 1 per unit. This is done for having integer values in the control system. This gives 0.1% accuracy, which should be good enough for most applications. The speed controller uses rpm as setpoint while the torque controller uses 0-1000 for zero to rated torque. Both negative speed and torque can be set, which will correspond to reverse the direction of rotation.

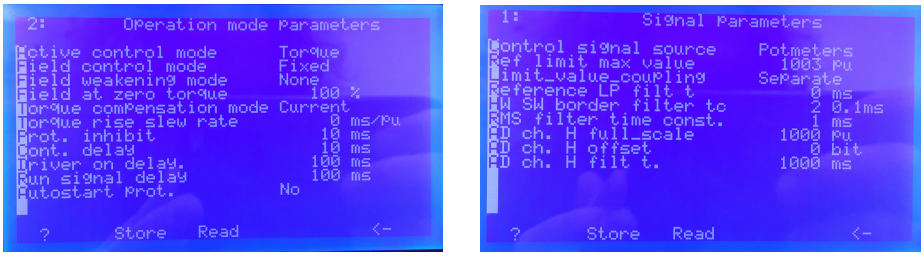

(a) Setting for torque or speed controller **(b)** Setting source for reference

Figure 4.2: Controller settings for the motor controller

In figure 4.2a it is shown where to select speed or torque mode of the drive. The first line can be changed into either ”Speed” or ”Torque” using the navigation buttons on the controller. Figure 4.2b shows where source for the speed or the torque reference can be set. It is possible to set the reference from a fixed value, by analog input (potmeters), by CAN-bus, or by setting the value from the menu using the navigation buttons. Both torque and speed shares the same reference setting, but since this project only remotely control the torque reference, the speed reference is not discussed any further.
Since the Speedgoat controllers does not have any CAN-bus interface, the torque reference must be controlled by an analog signal. When the torque reference is to be controlled by analog input, it is required to have a reference limit on an additional analog input. These two signals are generated using the digital-to-analog channels of the Speedgoat controller. These signals can then be connected to the drive by the use of two shielded BNC cables. The two analog inputs is located next to the LCD display on the drive. These connections is shown in figure 4.3a. Input C is the reference, while input D is the limit.
The analog inputs is 0-5V and the zero is offset at 2.5V. A positive reference is then above 2.5V and a negative reference is below 2.5V. There is also a dead band around 2.5V to clearly define zero reference.

(a) Analog inputs

(b) LCD display and analog outputs

Figure 4.3: Front panel of the drive

In figure 4.3b the front panel of the drive is shown. To the right, four BNC connectors are located. These are the 0-5 V analog outputs of the drive. It is possible to route almost every variable in the drive to these outputs using the menu system. This can be very useful for monitoring variables on an oscilloscope while tuning controllers and can also be used to show i.e. torque, speed and DC link voltage during normal operation.

4.2 Voltage Source Converters

The voltage source converters (VSI) used is a standard type 20 kVA converter developed at Sintef/NTNU. These converters are mounted on a standard 19" rack tray with gate drivers, protection, capacitors, IGBT transistors, snubber circuits, power supply, current measurements and heat sink. Both converters for the DFIG are identical. It is also the same converter used for the motor controller. The gate driver interface board applies necessary dead time between upper and lower transistors to ensure that only one transistor in each leg is conducting at all times. Over-current protection for each transistor is located in the respective gate driver. Capacitors are located in the middel of the converter between the heat sink and the gate driver boards. All these features in a single tray, makes the converter very compact and easy to use. There is no need to know all the practical details around how to build a converter, and this makes it very useful for academic applications where time is limited. Figure 4.4 shows the converter module.

4.2.1 Transistors

In each converter there are four Semikron SKM400GB125D Insulated-gate bipolar transistor (IGBT) transistors [5]. Three are used for phase a, b and c while the fourth is used for a breaking chopper. The breaking chopper can be used to limit the DC link voltage. Since there are two back to back mounted converters used, bi-directional power flow is obtained and thereby it is possible to control the DC link voltage by the use of the grid converter. Therefore it is not necessary to use the breaking chopper, and it will not be discussed any further. The transistors has the following data:

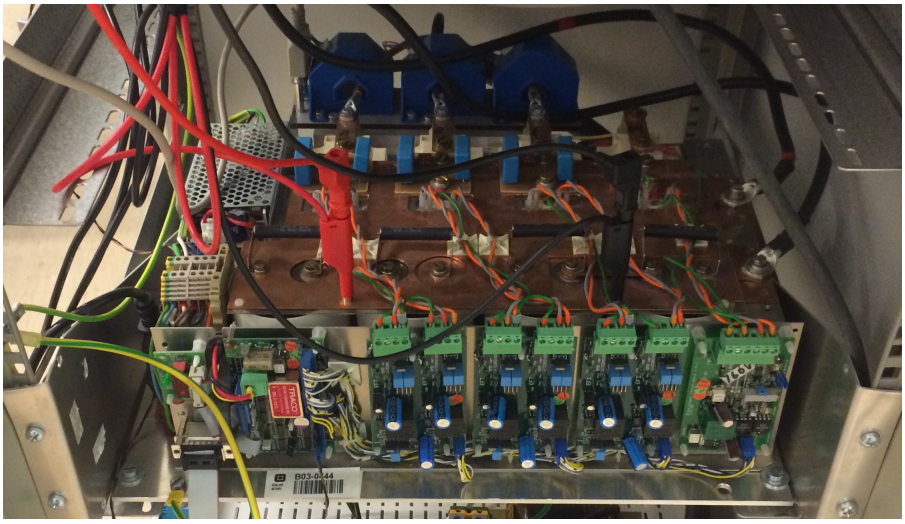

Figure 4.4: Converter module

- Nominal voltage 1200V
- Nominal current 400A
- 0-25kHz switching frequency

Over the DC connections of each leg there is located a snubber circuit for reducing noise from the antiparallel diodes in each leg. The snubber is made out of a capacitive snubber i parallel with a RC snubber. The RC snubber damp out oscillations, while the capacitive snubber damp out voltage transients. The capacitiv snubber is 10 nF while the RC snubber is 22 nF / 1 Ω [5].

The maximum power transfer through the converter is limited by the capacity of the heat sink. This will vary with the switching frequency and DC link voltage. In this work, the switching frequency is 7 kHz and the DC link voltage is around 600V. Using data from the documentation [5], this correspond to about 60-65 A without overheating the converter. The transistors are shown schematically in figure 4.6.

4.2.2 Capacitor bank

The capacitor bank of the converter consists of four 3300 μF 350V capacitors [5]. Two in series, two in parallel. If one capacitor has the capacitance C, the total capacitance will be:

$$Total\ capacitance = \frac{1}{\frac{1}{C}+\frac{1}{C}} + \frac{1}{\frac{1}{C}+\frac{1}{C}} = \frac{2C}{2} = C \tag{4.1}$$

This gives a total of 3300 μF and 700V. The capacitors has 47 kΩ resistors per capacitor for ensuring that the voltage is equally divided voltage between the capacitors. The capacitors are located between the gate driver cards and the heat sink and can be seen in figure 4.4.

4.2.3 Gate drivers

The gate driver cards and the gate driver interface is located on the front side of the converter. Each gate driver board drives both the upper and lower transistors in each leg. The gate driver cards are connected to a common interface card that controls the converter. A number of protections is included in the gate driver system [5]:

- Each gate driver card has short circuit protection for the respective transistors. This is done by measuring the voltage between collector and emitter, and a large voltage drop over the IGBT will occur when a large collector-emitter current is present. If a high current is measured, a trip signal is sent to the driver interface card which will trip all the transistors. The short circuit protection is tuned to trip at a level just above rated current (400A). Because of this, the short circuit protection will act as a over-current protection as well.
- A thermistor located in the heat sink provides overload protection. When the temperature in the heat sink increases over a given limit, a trip signal to the transistor is generated.
- The DC link voltage is measured, and if the voltage reach a given threshold, a trip signal for the transistors is generated.
- To ensure that two transistors in the same leg never is conducting at the same time, two functions are implemented:
  - If the upper transistor is turned on, it is not possible to turn on the lower transistor even if control signal is on.
  - A dead time of about 3μs is applied when turning on a transistor to be sure that the other transistor is off.

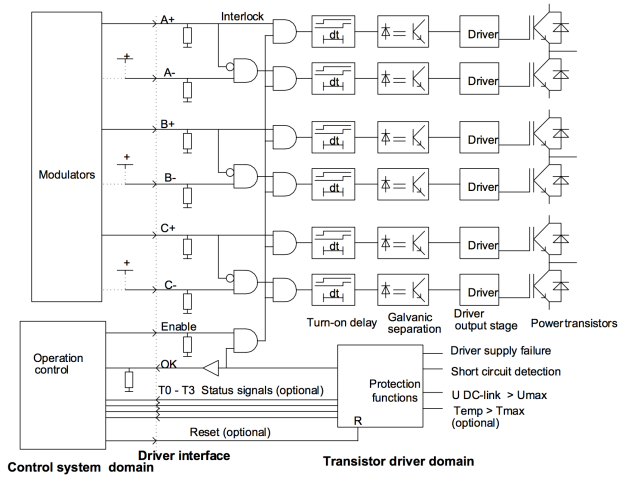

Figure 4.5: Gate driver schematic

All the described functionality is shown schematically in figure 4.5. A feature that can simplify the PWM controller is to connect the control signal of the three lower transistors to +5V, while switching only the upper transistors. The protection for shoot-through in the transistor leg will then take care for turning the right transistors on and off.

In addition to the six gate signals, there are a few more signals for controlling the converter:

- OK-signal for the converter to the control system. When there is no error detected and the converter is ready to be started, this signal is true (HIGH).
- Four lines for status feedback to the control system. Each line represent a bit in a 4 bit hexadecimal status code of the converter. The status code is given in appendix C. The logic is inverting, giving a OK-signal on all lines TRUE (HIGH). This is done because of when the 5V power supply has failed, all lines are LOW giving a number of hexadecimal F which corresponds to 5V error message.
- Enable transistors. When this signal is TRUE the transistors can be controlled by the gate signals. Useful for turning the converter on and off.
- Reset converter (after a fault). Turning this signal to TRUE will reset the error latch and the converter is ready for operation again.

All signals has 5V CMOS and cannot be used with 3.3V signals. The signal grounding is isolated from the grounding of the power system.

4.2.4 Filters

At each converter there is located a LCL filter for smoothing out the currents and reducing the harmonics produced by the converters. The following components are used [6]:

- Converter side inductor: $L_1 = 1$ mH, $I_{sat} = 200$ A
- Capacitor: $C = 25$ μF, 700V DC.
- Grid side inductor: $L_2 = 0.6$ mH

The filter, transistors and DC link is shown in figure 4.6.

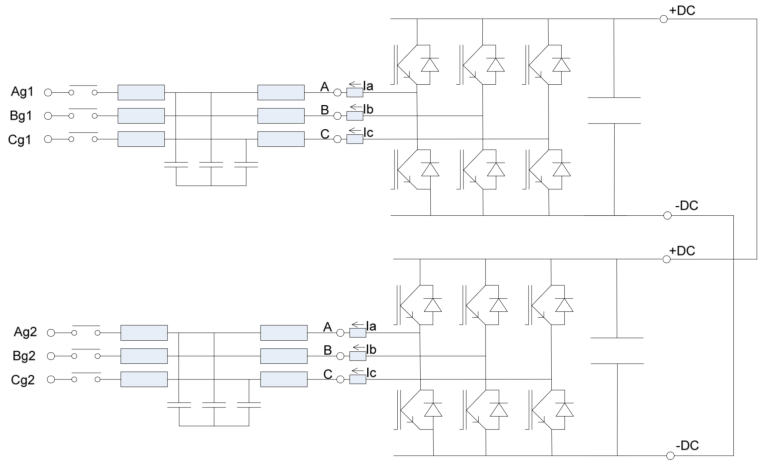

Figure 4.6: Back-to-back connected converter

4.3 Relays and breakers

For controlling the breakers for the stator, grid converter and rotor converter, a setup with three relays is used. The breaker is controlled by 230V AC signals, and the relays are controlled by 12V DC. The digital IO signals from the Speedgoat controller must be amplified to be able to control the relays.

4.3.1 Relay drivers

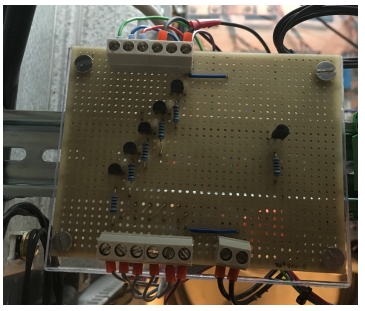

(a) 5ch Relay driver board

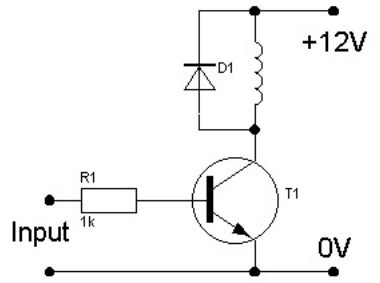

(b) Relay driver circuit

Figure 4.7: Relay driver

For controlling the relays it is necessary to amplify the 3.3V signals from the Speedgoat controller to 12V signals. This is done by the use of a BC337 NPN transistor. A 1 kΩ gate

resistor is used. The input to the driver can then be connected directly to the Speedgoat controller digital output. The circuit is shown in figure 4.7b. The fly-back diode shown in the driver circuit is located in the relay itself. Five of these drivers are soldered on a veroboard and mounted next to the relays in the converter rack. A flat cable with a D-SUB 9 connector is used for interfacing the digtal outputs from the Speedgoat controller. The 5ch driver board is shown in figure 4.7a. On the output of the relays, Phoenix connectors are used for connecting the control signals for the main breakers.

4.3.2 Relay and breakers

There are three main breakers in the control system for the DFIG. These are indicated with a red square and a number in figure 4.8. There is one breaker between the stator and the grid (1), one between the rotor converter and the rotor itself (2), and one between the grid and the grid converter (3). Each breaker is a standard Eaton contactor with 230V

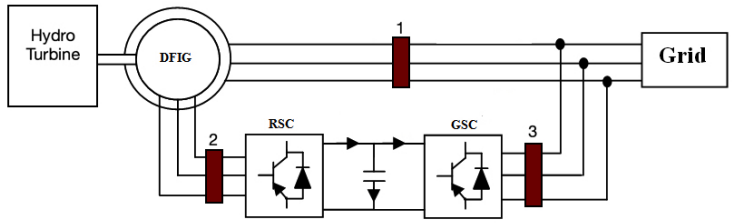

Figure 4.8: Breakers in the DFIG control system

AC coil. The control voltage for each breaker is controlled by the relays. There is one relay for each contactor. For reducing the current while charging up the DC link, there is a seperat contactor with 47 Ω / 50 W resistors connected to a separat diode rectifier which is connected to the DC link. The main breaker is delayed with about 3s so that the capacitors is fully charged when the main breaker closes. This are equivalent for both converters [6].

4.4 Measurement equipment

For controlling the DFIG it is necessary to measure voltages, currents and rotor position. The measurements points are shown in figure 4.9 and are as follows:

- Voltage and current on the AC side of the grid converter.
- DC link voltage.
- Voltage and current on the AC side of the rotor converter. The voltage is not necessary for the control system, but can be useful for debugging and experimentation.
- Rotor position (and speed).

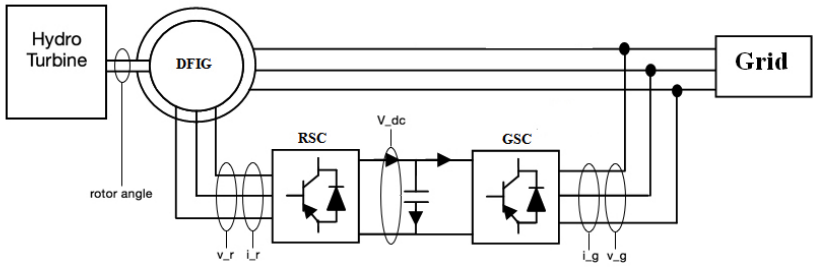

Figure 4.9: Measurements in the DFIG control system

In the following parts, voltage, current and encoder measurements are described in detail.

4.4.1 Current measurements

For current measurements Lem LA 205-S current transducers are used. It is a hall effect based transducer with a maximum primary current of 200 A. The secondary current is the measurement signal which is proportional with the primary, and with a ratio of 1:2000. In this case, the primary wires are turned two times around the core giving a ratio of 1:1000 and a maximum current of 100 A. The current transducer requires a $\pm$15 V power supply. The secondary current can then be converted to a voltage by the use of a measurement resistor R_m. This resistor can be choosen by applying Ohm's law. If a $\pm$5 V signal is perfered and a maximum primary current of 100 A is needed, the resistor can be found from

$$R_m = \frac{U_m}{I_m} = \frac{5\ V}{100\ A \cdot \frac{1}{1000}} = 50\ \Omega \tag{4.2}$$

The details of the further signal conditioning is described in section 4.5.3. Three of these transducers are mounted on the AC side of each converter. A D-SUB9 connector is used for easy connection between the transducers and the measurement cards. The transducers require $\pm$15 V to operate.

4.4.2 Voltage measurements

For measuring voltages Lem LV 25-800 (DC link and grid voltage) and Lem LV 25-600 (rotor voltage) are used. These two voltage transducers are practically the same, but with different measuring range. A measuring resistor is added between the two points where the voltage should be measured. This results in a current flowing through the resistor. This current is measured with a Lem LV 25-p hall effect based current transducer. The current transducer has a ratio of 10:25, resulting in a 25 mA secondary current if the primary current is 10 mA. Maximum current at the primary side is 10 mA. The secondary current can then be translated to a voltage by the use of another measuring resistor. Therefore, two measurement resistors must be chosen to fit the application. This is done by applying Ohm's law as for the current transducers. The LV 25-800 is made for measuring up to 800V. The resistors can then be found:

$$R_{pri,800} = \frac{V_{m,max}}{I_{m,max}} = \frac{800\ \text{V}}{10\ \text{mA}} = 80\ \text{k}\Omega \tag{4.3}$$

For LV 25-600, the measuring range is up to 600 V, giving:

$$R_{pri,600} = \frac{V_{m,max}}{I_{m,max}} = \frac{600\ \text{V}}{10\ \text{mA}} = 60\ \text{k}\Omega \tag{4.4}$$

At maximum voltage for the transducer, the secondary current is then 25 mA. The secondary resistor must be chosen to fit for voltage range of the analog inputs of the control system. The signal conditioning board can use ± 5 V signals. The measurement resistor for the secondary side can then be calculated as:

$$R_{sec} = \frac{V_{ADC,max}}{I_{transducer,max}} \frac{5\ \text{V}}{25\ \text{mA}} = 200\ \Omega \tag{4.5}$$

For the LV 25-800, five units are mounted inside a box. A D-SUB 15 connector is used for connecting the transducers to power supply and signal conditioning card. Banana connectors are used for input of the voltage to be measured (figure 4.10). Three LV 25-600 are mounted on a single PCB board. Berg electronics connectors, which fits to the signal conditioning boards, are used for the measured signals. Phonenix connectors are used for input on the primary side. The transducers require ± 15 V to operate.
For the rotor and grid voltage measurement, the phase voltage is measured. This is done by connecting the negative terminals of the transducers together creating a neutral point, while the phases are connected to the positive inputs. This is useful for the control system, since there is no need to offset the measured grid angle for control of the grid converters.

4.4.3 Encoder measurements

For measuring the mechanical angle of the rotor, an incremental Heidenhain rotary encoder is used. It features

- 5V differential logic signals
- 2048 pulses per revolution

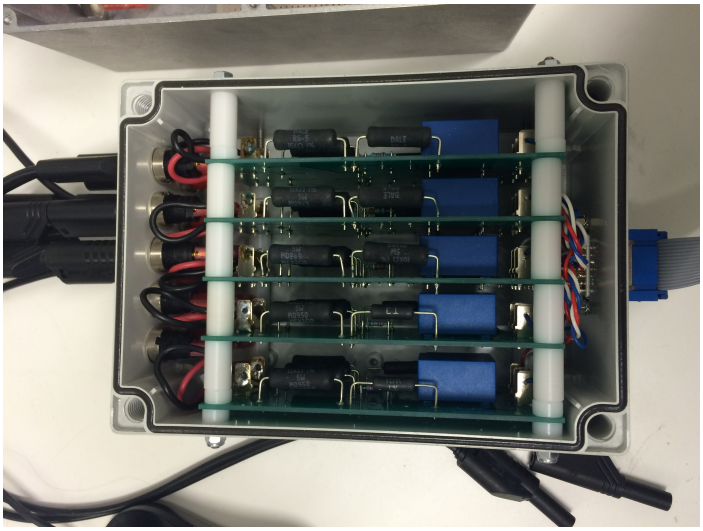

Figure 4.10: LV 25-800 voltage transducer box

- Channel A and B for determining direction
- Index channel (Z) for resetting position counter
- Directly connected to the DFIG rotor

An incremental encoder is made up of a disc with holes which rotates with the shaft of the device. A light emitting diode (LED) lights through the holes in the disc. When the LED lights at a point between two holes in the disc no light gets through the disc. On the other side of the disc, a phototransistor is mounted. This will turn on when it is lit, and turn off when the light is shut off. This will create a pulse train which has a frequency proportional to the rotational speed. If there is n holes in the disc, there will be n pulses per revolution. There are two equal setups with LED and phototransistors, but they are $90°$ out of phase with each other. These two signals are usually called A and B. This can be used for determining the direction of the rotation. If channel A changes from logic 0 to 1 and channel B is 0, the direction is one positive. If channel A changes from logic 0 to 1 and channel B is 1, the direction is one negative. A counter can be programmed to increment for every positive pulse, and decrement for every negative pulse. A third set of a LED and a phototransistor is used for detection of exactly one revolution. Instead of having n holes around the disc, this has only one hole giving one pulse per revolution. This channel is called Z or Index channel. This can further be used to reset the counter to an initial value. In this case each revolution presents 2048 pulses. At 2000 rpm, the frequency of channel A and B is then

$$2048 \text{ per revolution} \cdot \frac{2000 \text{ rev/min}}{60 \text{ min/s}} = 68.267 \text{ kHz} \tag{4.6}$$

These are fast signals, which is smart to implement in FPGA chips. The Speedgoat controller has dedicated inputs for encoders, making it really easy to interface them in soft-

ware. A special 12 pin encoder connector connects the encoder to the control system. The differential signals must be converted to single ended signals, and this is described in section 4.5.4. The encoder is shown in figure 4.11

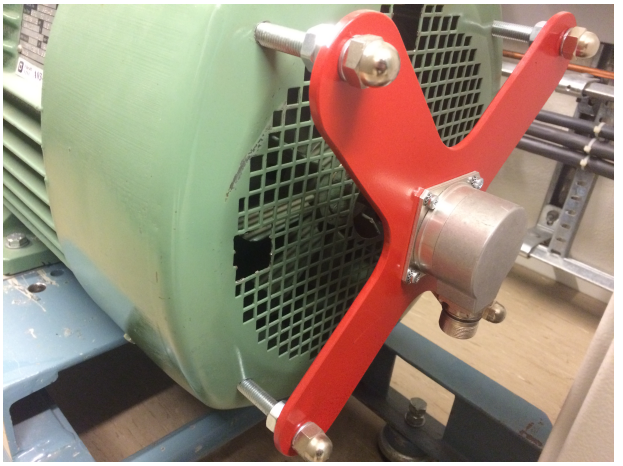

Figure 4.11: DFIG encoder

4.5 Signals conditioning

The signals to the converters, from the voltage and current transducers, and from the encoders require to have a proper connection with good electrical ground to prevent noise. Some of the signals also need some kind of signal conditioning before they are fed into the Speedgoat controller. A setup of connections, power supplies, signal conditioning boards and interface cards for the Speedgoat controller is mounted on a standard 19 inch rack tray. This setup is shown in figure 4.12.

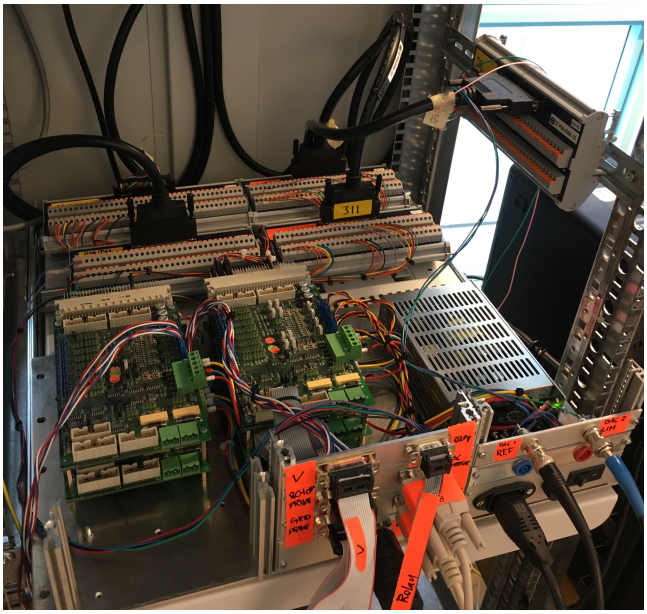

Figure 4.12: Signal conditioning setup

The setup features the following:

- Connections for all signals and power.
- Four equal signal conditioning cards for voltage, current and encoder signals.
- Power supply with $\pm$15V and +5V voltage levels.
- Interface cards for the Speedgoat controller.

4.5.1 Signal connections

In the front panel of the rack tray, all the connections to the system are placed. This section will give an overview over which connectors are used and where they are connected. The panel is shown in figure 4.13.

- The D-SUB 15 connector marked ”V” is five channels consiting of LV 25-800 voltage transducers. This is current signals for the grid voltage and DC link voltage.
- The D-SUB 9 connector marked ”Relay” is five digital signals straight from the interface board for the digital IO in the Speedgoat controller. This is the control signals for the relay driver.
- The D-SUB 15 connector marked ”Rotor driver” (below ”V”) is the control signals for the rotor converter. This includes status signals and gate driver signals. The signals is futher connected to the rotor converter signal conditioning board.
- The D-SUB 15 connector below ”Rotor driver” is the same signal as for the ”Rotor driver”, but for the grid converter. It is marked ”Grid Driver”. It is connected to the grid converter signal conditioning board.
- The D-SUB 9 connectors marked ”RSC current” and ”GSC current” is the current signals for the current transducers at each converter. The signals are connected to the rotor side and grid side converter signal conditioning board respectively.
- The round black connector at the bottom left side is the DFIG rotor encoder input. The signals is futher connected to the encoder inputs on the grid converter signal conditioning board.
- The four BNC connectors on the top right side is four analog outputs connected directly to the DAC interface board of the Speedgoat controller. Useful for debugging with a oscilloscope.
- The two BNC connectors marked ”DAC 1 REF” and ”DAC 2 LIM” are the analog output signals for the motor controller. Connected directly to the DAC interface board of the Speedgoat controller.
- The blue and red banana connectors are not used.
- Eurocable connector is power input for the power supply. A fuse and a switch are located at the same panel.
- Note: The rotor voltage transducers do not have a dedicated D-SUB 15 connector. They are directly connected to the rotor voltage signal conditioning card.

All the connectors are grounded in the chassis except for the current and voltage transducers. This separates the digital and analog grounding, which may remove noise from the analog signals.

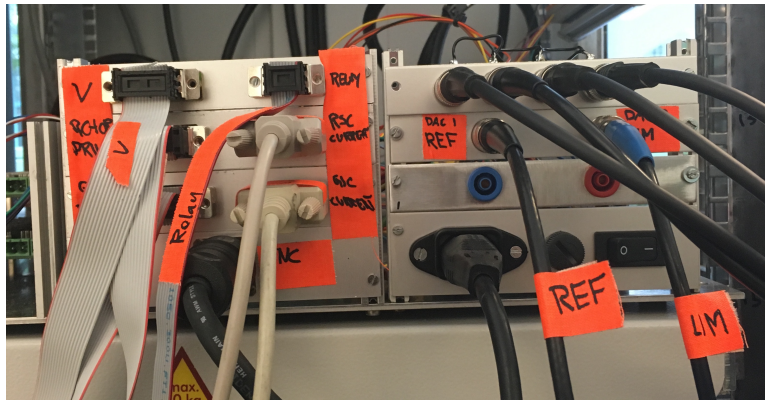

Figure 4.13: Connections

4.5.2 Signal conditioning boards

The board provides buffering of signals and converting of differential signals to singel ended signals. If the controllers run at 3.3V, the board can act as a level shifter to 5V for both inputs and outputs. Analog filtering can be used if required. A number of different configurations is possible, and these options are set using jumpers. The four signal conditioning boards used in the setup are all equal and has the same features [4]:

- 4x current inputs for LEM-transducers.
- 8x Analog/digital input
- 2x Relay driver outputs 15V
- Encoder connection (Heidenhain ROD420)
- Converter driver interface
- 2x 16 bit IO
- $\pm$15V and +5V power inputs.
- Multipin euro connector for connection to the Speedgoat controller.

For this project, the current inputs, converter driver interface and encoder inputs are used. The current inputs can be used for both voltage and current transducers. The four boards are shown in figure 4.14. To identify which board is which, they have numbers and names.

1. Grid side converter current card. (Bottom, right side)
    - Grid side current measurement
    - Grid side converter control signals
    - DFIG rotor encoder signals

2. Rotor side converter current card. (Top, right side)
    - Rotor side current measurement
    - Rotor side converter control signals
3. Grid side converter voltage card. (Bottom, left side)
    - Grid voltage
4. Rotor side converter voltage card. (Top, left side)
    - Rotor voltage

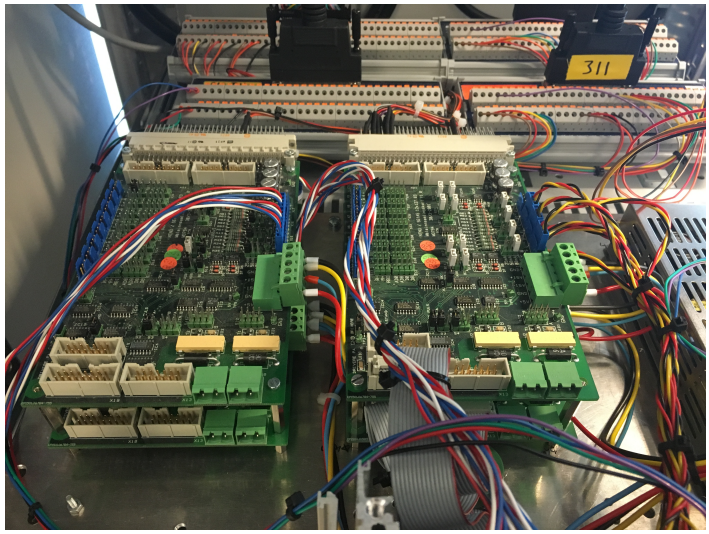

Figure 4.14: Signal conditioning cards

From the back end of the boards, wires are connected to the correct Speedgoat interfaces which are located at the back side of the signal conditioning cards. The wires are soldered to a female euro connector which fits in at the back of the board. All wires attached to the boards are connected with connectors so it is easy to remove a card for accessing the underlaying card. At the same time, all the messy cable connections are kept in one place, between the signal conditioning cards and Speedgoat interface. This makes it easier to debug the system if something does not work.

4.5.3 Current inputs

The four LEM current transducer inputs are located at the right side of the board in the setup. There are four 4-pin Berg connectors with +15 V and -15 V voltage and the current signal in each. The current signal are then converted to voltage signals using a burden resistor. There are three different resistors avaliable, 50 Ω, 100 Ω and 200 Ω. These resistors can be chosen by setting the right jumper. The choice of resistors is based on having a ±5 V voltage at ±100 mA, ±50 mA and ±25 mA. For this project, 50 Ω is used for the current transducers and 200 Ω for the voltage transducers. The voltage signal is then filtered with a RC-filter with 1 μs time constant. It is possible to have a time constant of 100 μs by setting a jumper. The filtered signal is then buffered through an op-amp buffer. The buffered signal is then offset to +2.5 V by the use of a voltage divider between the signal and +5V. This gives a 0-5 V signal with 2.5 V offset. This signal is then buffered with a new op-amp buffer. The signal can then be routed to the desired output pin in the euro connector by the use of jumpers.

4.5.4 Encoder interface

For connecting the encoder connector to the board, a flat-cable connector is used. The three encoder signals (A,B,Z) are differential signals which need to be converted to single ended signals since the Speedgoat controller does not have any differential inputs. A four channel MAX3095 receiver circuit is used to convert the differential signals to single ended signals. It is possible to do an XOR of the A and B signals, doubling the frequency of the signal but for this work only plain channel A, B and Z is used. The signals are routed directly to the Euro connector.

4.5.5 Converter interface

There is a 16 pin flat cable connector dedicated for the converter interface. It is the same pinout as for the gate driver interface card used in the converters. The signal is lowpass filtered with a time constant of 1 μs to remove noise in the signal. The signal is buffered, and it is possible to use both 3.3V and 5V signal levels. The signals are routed directly to the Euro connector of the board.

4.5.6 Connection to Speedgoat IO modules

As mentioned in chapter 3, there are five different IO modules in the Speedgoat controller. Each of these modules has its own multipin connector for connection of the signals. For easy connection, a breakout board with all the signals available in two rows exists for each module. The breakout board used is the same for each module, except for the one connected to the ADC module which has slightly more pins. From these breakout boards all signals are connected to the signal conditioning boards and to the connectors in the front of the signal conditioning tray using single color coded cables. All the pinouts and colors are given in appendix. Figure 4.15 shows the breakout boards.

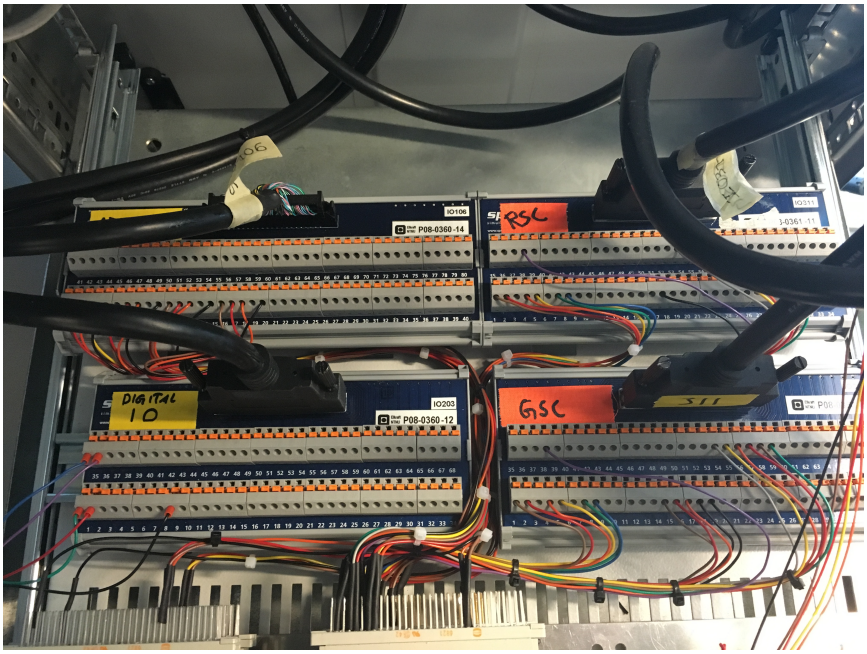

Figure 4.15: Speedgoat connection boards

4.6 Implementation in Simulink

This section will describe the different methods used in the Simulink control model for the Speedgoat controller. Most literature does not describe practical solutions which need to be included to have a system working, especially during start and stop of controllers. The total control system is shown in figure 4.16

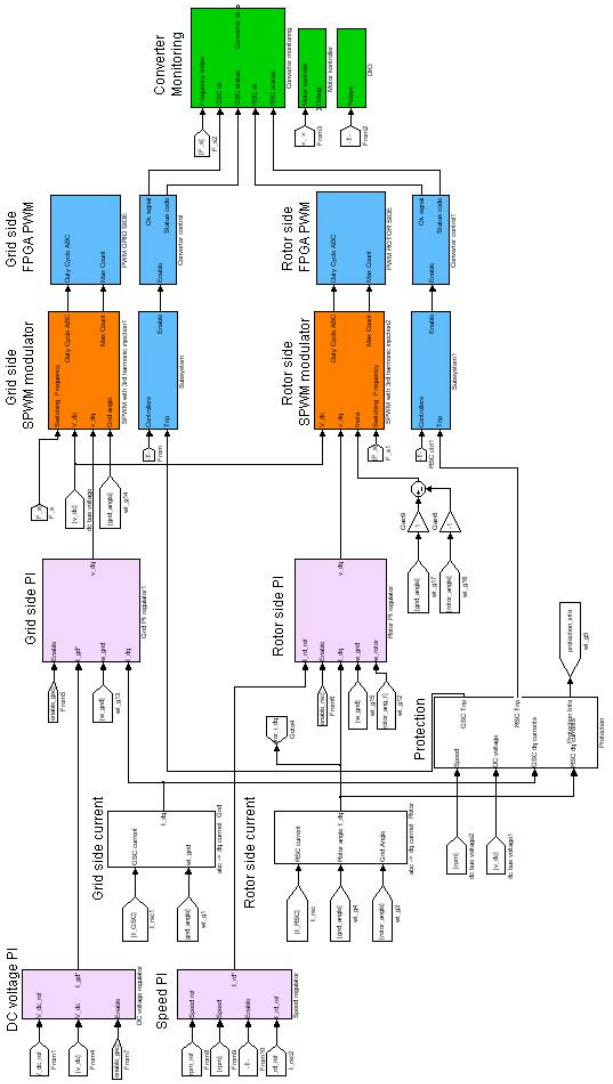

Figure 4.16: Simulink block diagram

4.6.1 Voltage and current measurements

The voltage and current signals are 0-5 V signals which is centered at 2.5 V. The analog to digital converter (ADC) need two simulink blocks. One block is used for configuration of the ADC. Voltage range and number of inputs can be set using this block. The upper blue block in figure 4.17 is the setup block. The lower blue block is the ADC read block, which provides a vector with all ADC channels. The output signals is of type double and presents the real voltage at the ADC inputs. The 2.5V offset is removed and the gain is adjusted to correspond to the actual unit of the signals. This is shown in figure 4.18. The calibration is done by using an oscilloscope. The DC link voltage and the current signals are filtered by a low pass filter after the calibration. For the current signals, the time constant is 0.3 ms while for the DC link it is 10 ms. All currents and voltages (except for the DC link voltage) are converted to root mean square (RMS) signals before they are published to the output of the block. Both RMS values and actual values are published. The three terminated signals at the output of the ADC read block is the fourth current input on conditioning board 1, 2 and 4. These are not used for any measurements.

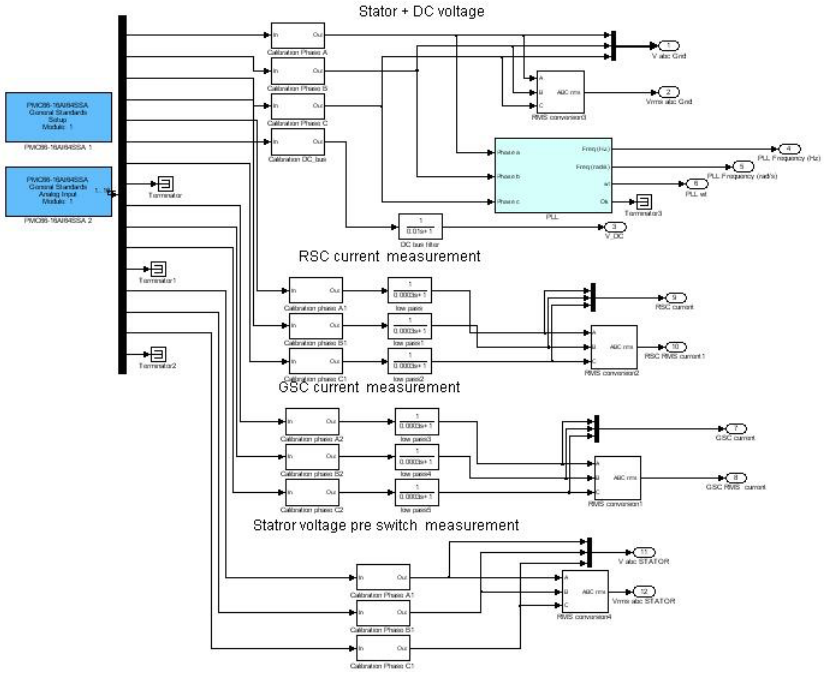

Figure 4.17: Voltage and current measurements

4.6.2 Phase locked loop

The phase locked loop (PLL) is shown in figure 4.19. It is located in the voltage/current measurement block and is shows in figure 4.17 as the light blue block connected to the grid

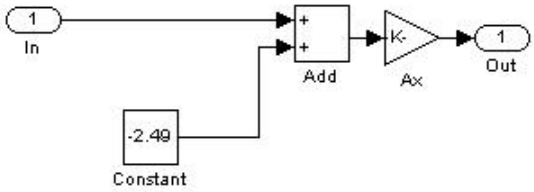

Figure 4.18: Calibration of voltages and currents

voltage measurement. The phase locked loop is responsible for measuring the grid voltage angle and is used as angle reference in both converters. It works by converting the three phase voltages into positive, negative and zero sequence components and synchronizing the positive sequence zero crossing to a ramp generator. The block require signals with amplitude of about 1 making it necessary to scale the voltage at the input of the PLL. The output frequency is given in hertz and is published in both hertz and in radians per second. The angle is given in radians and a direction switch and offset is implemented. The offset is used for calibrating the rotating dq-frame in the Park transformations used in the model. The direction switch is used for inverting the angle which can be turned around due to wrong signs in the measurement system.

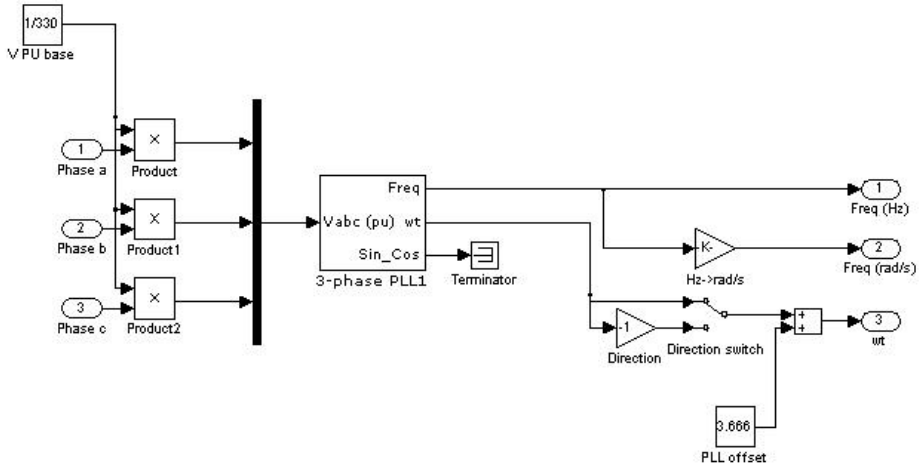

Figure 4.19: Phase locked loop

4.6.3 Encoder measurements

The encoder measurements is done in the Speedgoat 311 FPGA module. The encoder signals are converted into a counter which resets every revolution. The encoder interface in Simulink uses two blocks. One block for configuration where signal type and counter setting can be set, and one block for pulishing the counter value. This block also provides the index found signal which is used for verifying that the counter is correct. The counter signal is then used for calculation of rotor angle and rotor speed in both radians per second and as revolutions per minute (RPM). The number of poles is necessary for converting the measured angle from mechanical radians to electric radians. This is only used for the angle and angular frequency of the rotor. The number of revolutions per minute is the same for any number of poles. The setup is shown in figure 4.20.

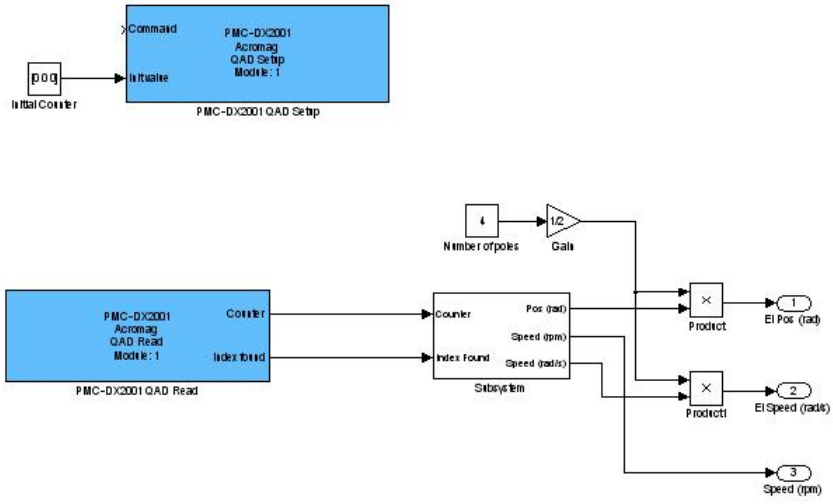

Figure 4.20: Encoder interface

The calculation of rotor angle and speed is shown in figure 4.21. The angle is calculated by converting the $0 - 2048$ counter into $0 - 2\pi$. This is calculated using

$$\theta_{rotor} = p \cdot \frac{2\pi}{2048} + O \tag{4.7}$$

where ω_{rotor} is the electrical position of the rotor, p is the number of pole pairs, and O is the encoder offset. This offset must be calibrated so the rotor voltage is only in the d-axis, giving zero q-axis rotor voltage.

For calculating the rotational speed, a simple approximation of the time derivative of the counter is used. The counter value is measured and kept. After ten more samples, the counter is measured again and is compared to the old counter value. Since the sampling frequency and counter resolution is known, it is possible to convert the difference between the new and the old counter value for calculation of the rotational speed. The algoritm is:

- The sign of the counter is checked. A direction signal is either true or false for positive or negative counter values. Then the sign of the counter value is removed. The counter will now always increase independent of the direction of rotation.
- The signal is sent to a ten-sample delay block which will store the signal for ten samples.
- After ten samples, the delayed signal is compared to the most current signal of the counter.
  - If the current counter value is less than the old counter value, the counter has overflown and has started at zero again. Then, if n denotes the counter value at a given time, the difference between them, Δn, can be calculated using

$$\Delta n = 2048 + n_{old} - n_{new} \tag{4.8}$$

  - If the most current counter value is greater than the old value, the difference can be found directly using

$$\Delta n = n_{new} - n_{old} \tag{4.9}$$

- When the difference Δn is known, the speed in revolutions per minute can be calculated by

$$Speed[rpm] = \frac{\Delta n \cdot 60}{N_{enc} \cdot T_s \cdot D} \tag{4.10}$$

  where N_{enc} is the encoder resolution (2048), T_s is the sampling time (0.1 μs) and D is the number of sample delays between the counter samples (10). Using the known properties, the formula is simplified to

$$Speed[rpm] = \Delta n \frac{60000}{2048} \tag{4.11}$$

- The calculated speed is then low pass filtered using a 1st order lowpass filter with 20 ms time constant. The result is rounded to keep integer speed.
- The direction signal is then used to give correct sign to the speed measurement.
- The electric angular frequency is then calculated with the use of

$$\omega_{rotor} = \frac{p}{2} \cdot \frac{2\pi}{60} \tag{4.12}$$

- Both speed and angle measurement is 0 until the ”Index found” signal is true.
- Note: During calibration - which was done using the tachometer in the motor drive - it was necessary to add a 3.5 offset to the speed measurement. This gives exact integer speed measurement in the range from 1000 to 1700 rpm. An small error exist for speeds lower than 1000 rpm.

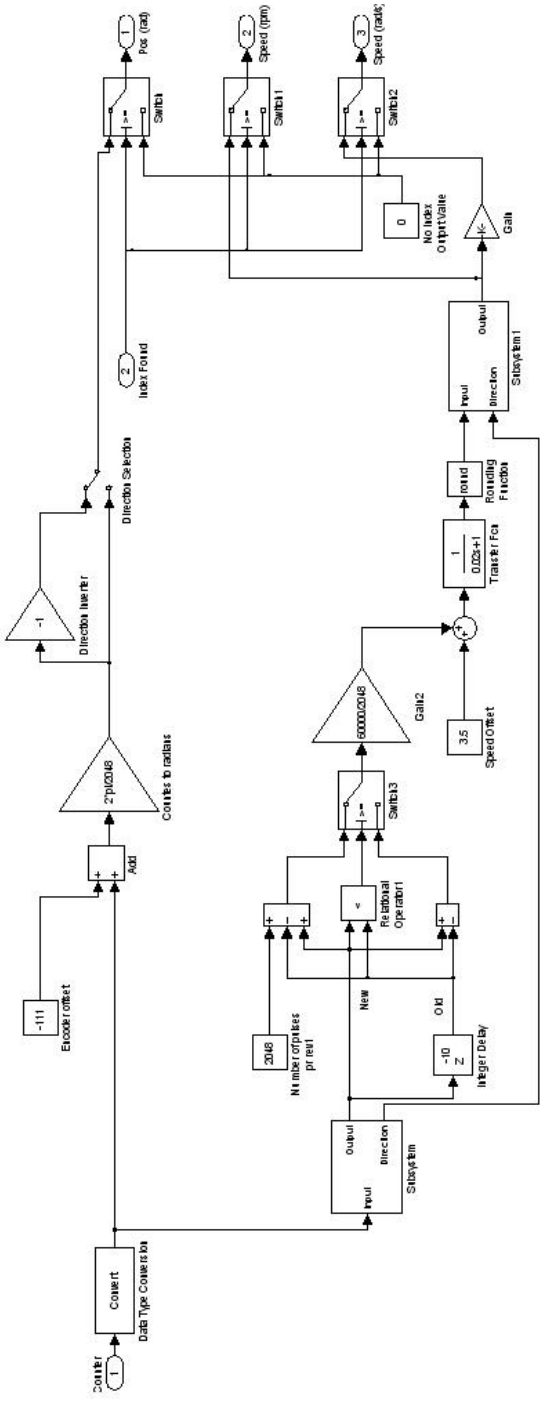

Figure 4.21: Calculation of rotor speed and angle

4.6.4 PWM generation

The PWM generation blocks is equal for both converters. It consists of two main blocks:

- PWM modulator block: Takes in the dq components and the angle of the desired output voltage and the DC link voltage. These values are processed and duty cycles for each converter are computed. The duty cycles are scaled to fit the compare values needed for PWM generation in the PWM output block.

- PWM output block: The phase A,B and C duty cyles are given and are converted to integer values for the compare inputs of the Speedgoat 311 PWM block. Other controls for the PWM generation is implemented here.

The modulator block is shown in figure 4.22. The dq voltages are transformed to a per unitized phase voltage which is used as input for the sinusoidal PWM generator. The sinusoidal PWM generator requires the maximum count of the PWM counter to be able to produce compare values for the triangular wave used in the FPGA module. A set of predetermined switching frequencies is made and it is possible to choose frequency from a list. The index of this list is the input to the switching frequency selection block. The output of the block is then the maximum counter value and is used in both the sinusoidal PWM generator and the FPGA interface in the PWM output block. This system is shown in figure 4.22.

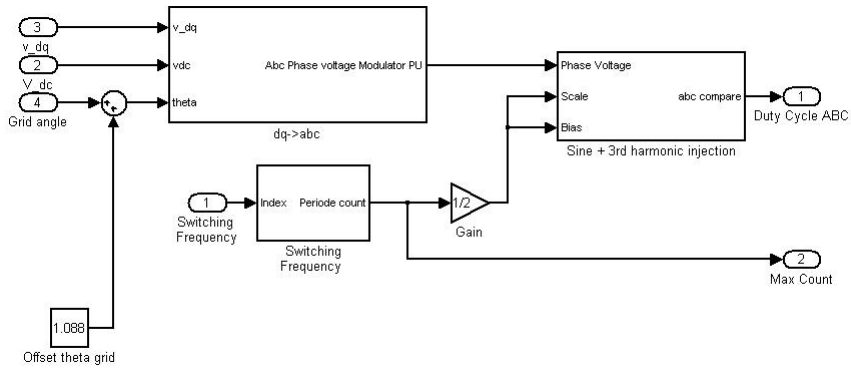

Figure 4.22: Modulator block

It can be noted that the angle input of the inverse dq-transformation has a offset parameter given. This is due to alignment of the dq-frame, and the inserted value is a result of calibration. Inside the dq-abc block, which is shown in figure 4.23, there is a gain for per unitization of the input signals. It is possible to scale the output voltage to the actual DC link voltage, but this feature is not actually used in the model.

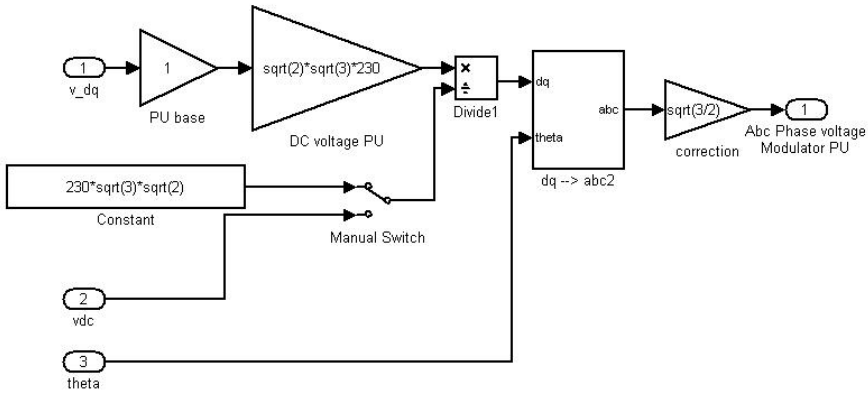

Figure 4.23: dq to adc transformation

The generation of duty cycles is done in the sinusoidal PWM block. The method used is sinusoidal PWM with third harmonic injection. This makes it possible to utilize the DC link voltage better than for pure sinusoidal PWM. The algorithm is shown in figure 4.24. Maximum and minimum values are added to the fundamental sinus signal generating a third harmonic component. The output of this operation is scaled to have a amplitude of ± 1.0. Since the PWM output block does not support negative counter values, the signal must be offset to the value which makes zero average voltage at the output of each bridge leg of the converter. This is 50% duty cycle which corresponds to a compare value of half the maximum count. For having maximum output without overmodulation, the scale of the signal is half the maximum count. This will correspond to a compare value at 0 for a input of -1 and max count for a input of 1.

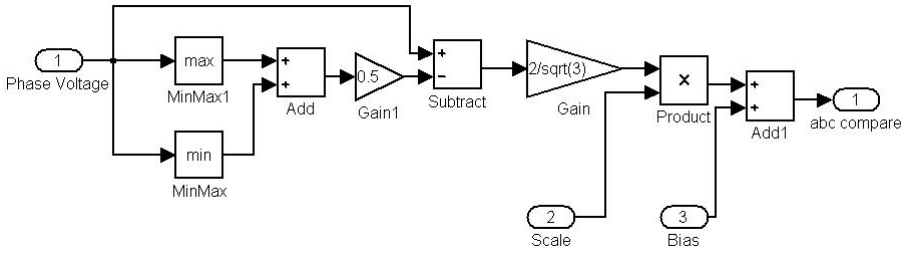

Figure 4.24: Sinusoidal PWM with 3rd harmonic injection

The PWM output block is shown in figure 4.25. This block is used for interfacing the Speedgoat 311 FPGA module. The upper blue block is used for setup of the PWM signal while the lower blue block is the input of the compare values and control signals. The start/stop signal is for turning on/off the PWM action. It is set to always on, since the same function is built in the gate driver interface card. The A and B compare count inputs is a vector of length 3 with compare values for each PWM channel. Compare A controls the upper transistors and compare B controls the lower. Therefore, the same signal is

applied to both upper and lower. The signal for the lower transistors is inverted in the setup block. The phase of the compare values can be changed, but is by default set to ABC. The maximum count for each PWM channel is set using the period compare count input. This controls the frequency of the PWM. When max count of all PWM channels is set using a vector with all numbers the same, the PWM for all three phases is guaranteed to be in synchronism with each other.

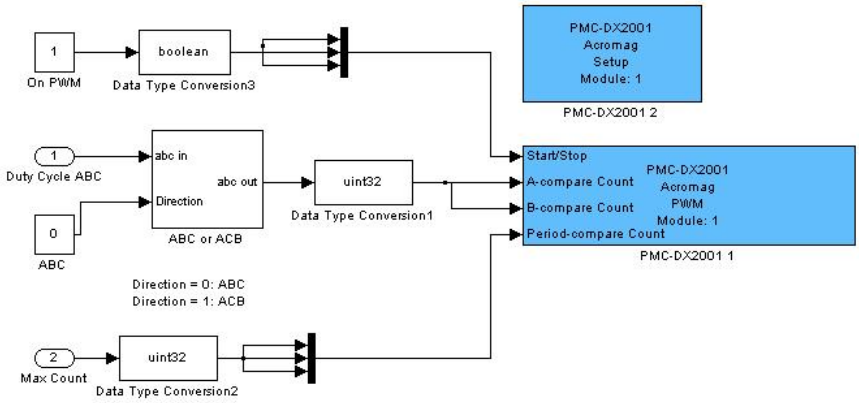

Figure 4.25: PWM blocks

4.6.5 Converter control signals

The converter has some control signals which is needed for correct operation. The Speedgoat 311 FPGA module has some standard 5V digital IO which is used for these signals. In figure 4.26, the input and output block of the 311 module is shown. The only output signal is the enable signal. For the input there is a "OK" signal and four status code signals named T_0 to T_3. These signals are inverted logic meaning that zero volts is logic true and vice versa. A status code block generates the four-bit status code for the converter.

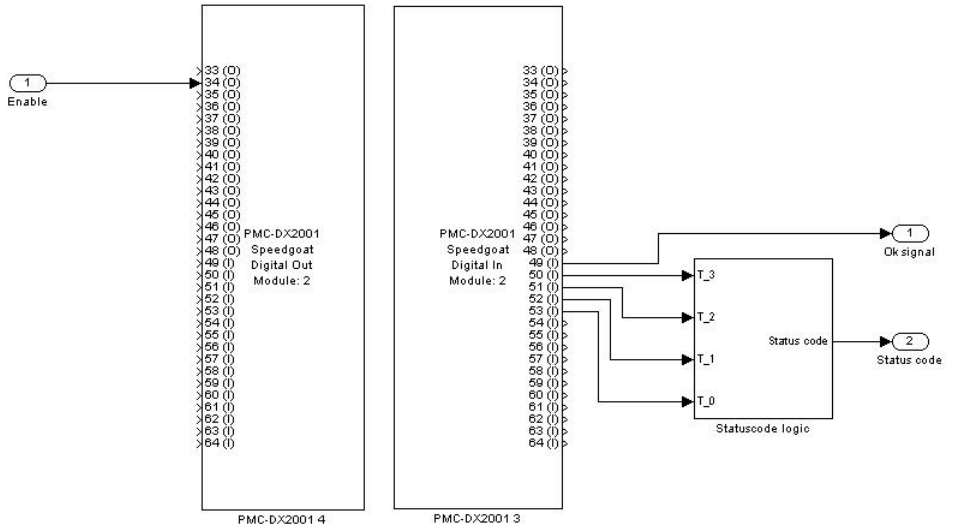

Figure 4.26: Control signals for the converters

4.6.6 GSC current controllers

The grid side current controllers, which is shown in figure 4.27, is made up of two PI controllers, smooth start for the d-axis controller and the feed-foreward cross-coupling terms. The integrator and controller limits are set to 1.2 pu. When the controllers are enabled, both integrators are reset. The integrator in the d-axis is reset to a value corresponding to producing a d-axis voltage which is equal to the grid voltage. Without this, the transistor protection will trip the converter. This value is found from trial and error using variable grid voltage by the use of a variac. The reset value for the q-axis integrator is zero. When the current regulators were tuned, it was found out that if the d-axis current error was ramped up in about 500 ms, the integrator would stabilize better not causing the converter protection to trip. Therefore, and variable is ramped up from 0 to 1 in 500 ms and multiplied with the error of the d-axis current controller. The cross-coupling terms are made, but not used at the time of this writing.

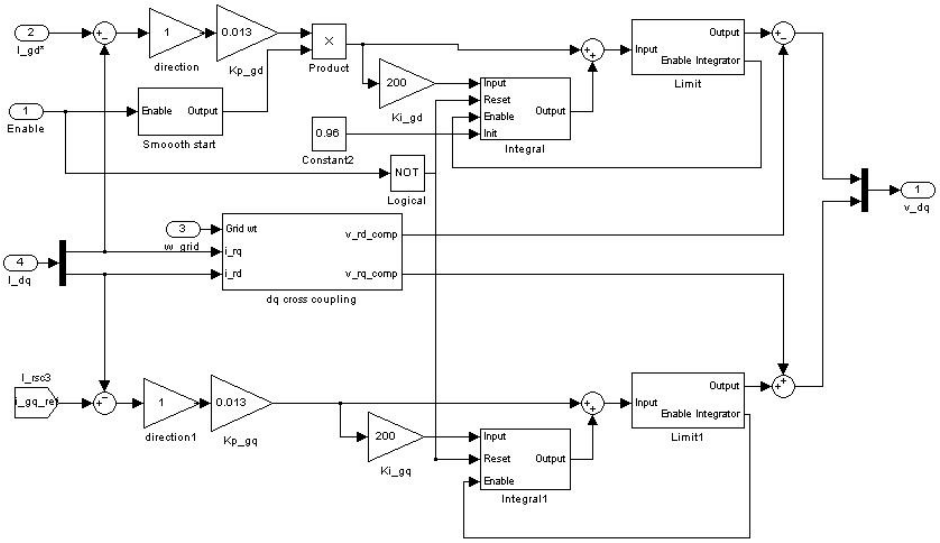

Figure 4.27: Grid side converter current controllers

4.6.7 DC link voltage controller

This controller is a standard PI controller. The limits are the same for the integrator and the output of the controller. The enable signal sets the error from 0 to the actual error and resets the integrator with a value of about -0.15. This value is found to a stable operating point without any voltage controller. The controller is enabled at the same time as the grid converter. It is shown in figure 4.28.

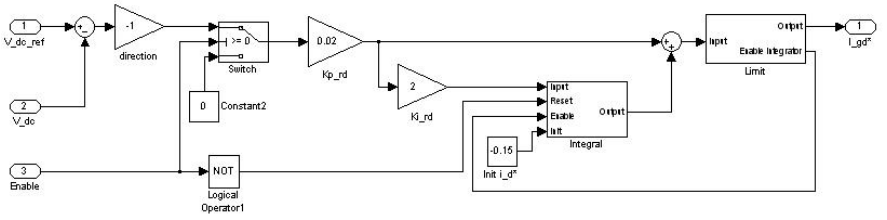

Figure 4.28: DC link voltage controller

4.6.8 RSC current controllers

The current controllers for the rotor is two PI controllers shown in figure 4.29. It is similar to the grid controller, but there is no smooth start or inital values for the integrator. When the controller is enabled, the integrators are reset to zero. Limits for both integrators and output of the controller is set to 1.2 pu. The cross-coupling terms are used for this controller. The q-axis setpoint is controlled directly from the control panel, while the d-axis setpoint is controlled by the speed controller.

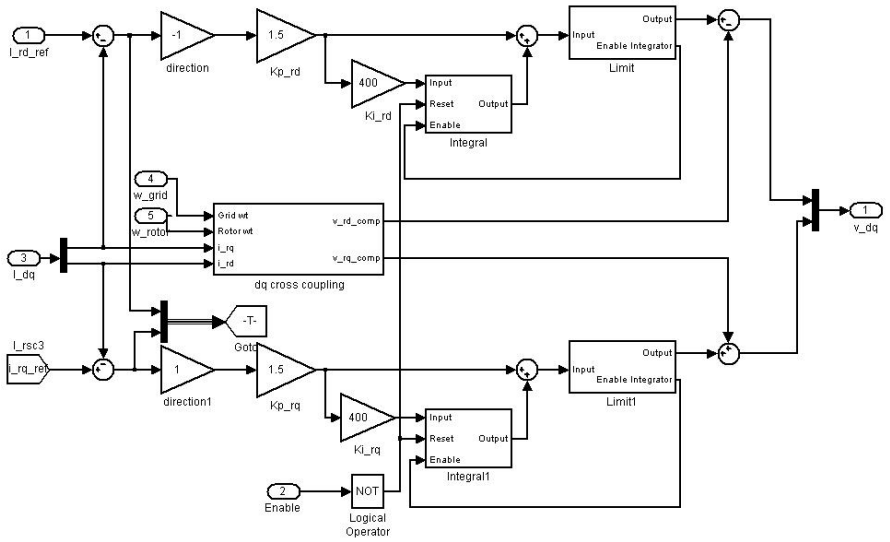

Figure 4.29: Rotor side converter current controllers

4.6.9 Speed controller

The PI speed controller is shown in figure 4.30. It governs the d-axis current which controlles the active power consumed/produced by the DFIG. Since the turbine provides only torque, the speed controller is responsible for keeping the speed at the optimal level.

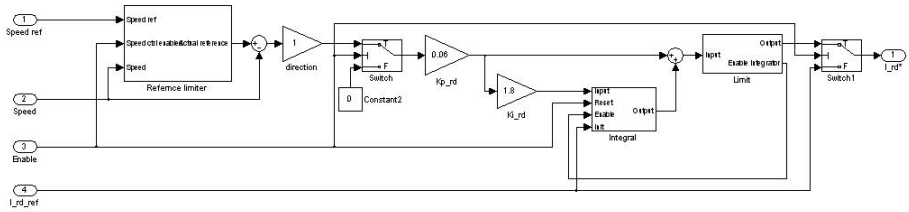

Figure 4.30: Speed controller

Since the turbine is started without the speed controller running, the speed is passed into a block which controls the setpoint of the speed controller. For not having a sudden change in the speed which may require very high torque, a ramp limiter is added. The actual speed at a given time is then used as an initial value for the ramp when speed controller is enabled. This function is shown in figure 4.31.

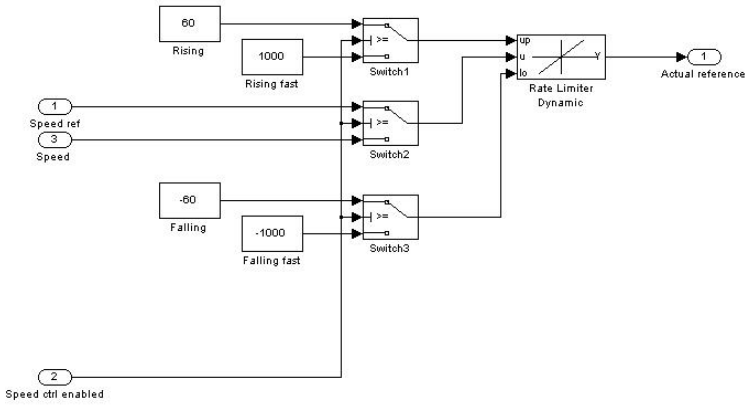

Figure 4.31: Limiter for speed referance

4.6.10 Motor controller

The motor controller is shown in figure 4.32. The control signals from the control panel is input to this block. Both torque limit and reference signals for the motor controller are taken in as values between 0 and 1000. The blue block adds offset and gain to the analog signal so that the 0-1000 range in the control model corresponds to the 0-1000 range in the motor drive. A direction switch is included here. The torque signal is only scaled to fit the 0-5V input of the analog output block. The red block is the digital-to-analog converter configuration block, where number of outputs and voltage range can be set. The four debug lines at output 3-6 is used for the four general debug lines which are connected to the four BNC at the front panel of the control system.

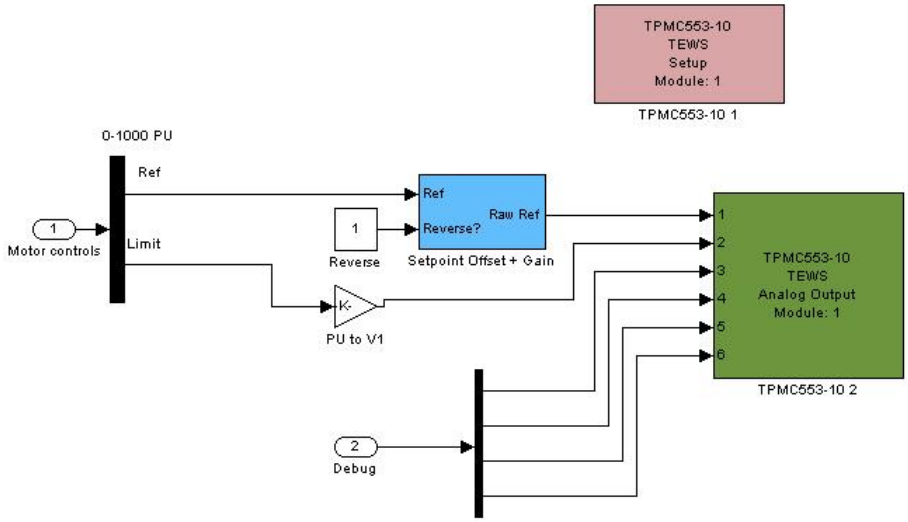

Figure 4.32: Motor controller

4.6.11 System protection

The system needs a protection system for keeping the variables within safe limits during operation. There are four protection mechanisms used in this setup:

- Overspeed protection: When the speed of the machine exceeds the maximum allowable speed, the rotor converter trip signal is generated.
- DC link overvoltage protection: When the DC link exceeds 640 V, a trip signal is sent to the grid converter.
- Rotor side over-current protection: Measurement of the dq components of the rotor side current measurement. Trips the rotor converter if the current increases above the limit.
- Grid side over-current protection: Measurement of the dq components of the grid side current measurement. Trips the grid converter if the current increases above the limit.

For diagnostics, the trip signals are visualized in both the control panel and in the protection block. Each part of the protection block can be reset in the control panel. The protection system is shown in figure 4.33.

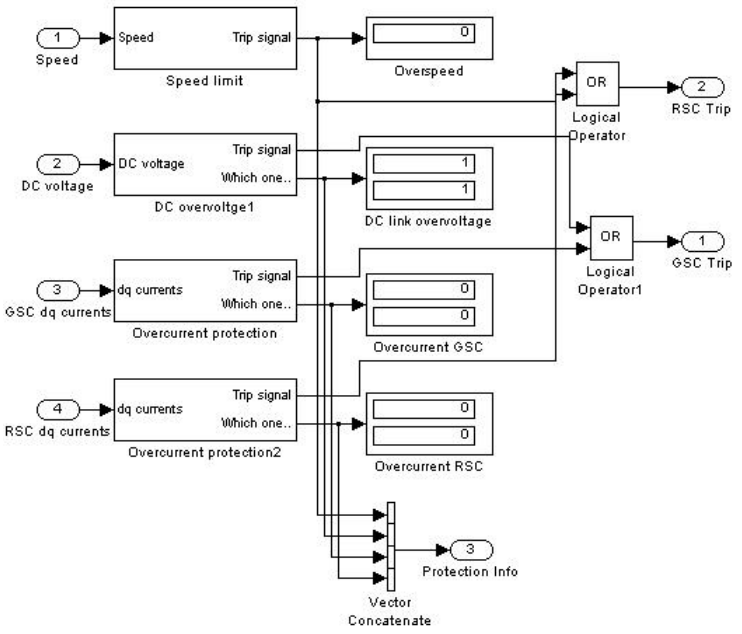

Figure 4.33: Protection system

4.6.12 Control panel

The control panel is shown in figure 4.34. Everyting that should be controlled during operation is located here.

- In the upper left corner the main switch is located. Without this switch enabled, nothing will work.
- Next to the main switch, the converter control is located. The grid side converter, rotor side converter and the speed controller are controlled here. The speed controller can be kept on and controlled by the enable switch for the rotor converter. The DC link voltage converter is controlled by the enable signal for the grid converter.
- Below the converter control, the relay control is located. These controls the breakers for stator, rotor converter and grid converter. Each time the rotor or grid converter breaker is turned on, a signal is sent to the protection system to reset. This signal is delayed by 5s. This is done since the grid converter breaker tends to generate over-current when the main breaker is closed.
- Under the relay controller, the motor controller is placed. The enable switch is used to turn on the motor. The torque reference and torque limit can be adjusted using a slider gain block. There is no trip signal for the motor controller.
- On the top, next to the converter controls, the status display for the protection system is located. If an error occurs, the cause can be read here. What error each column represents, is written in the model.
- To the right of the protection status display, the reset buttons for each protection part are given. A reset ALL switch is also located at the bottom.
- The switching frequency can be set using a constant block to the far right of the model. What number that gives which frequency is listed in the model.
- The setpoint values for all controllers are set at the bottom next to the motor controller. The d-axis current setpoint for both rotor and grid converters are controlled by the speed and DC link voltage controllers. Setting these currents manually can be done by switching the setpoints in each current controller. The q-axis current setpoints can be changed directly for both converters. The setpoint of the speed controller can also be set here.

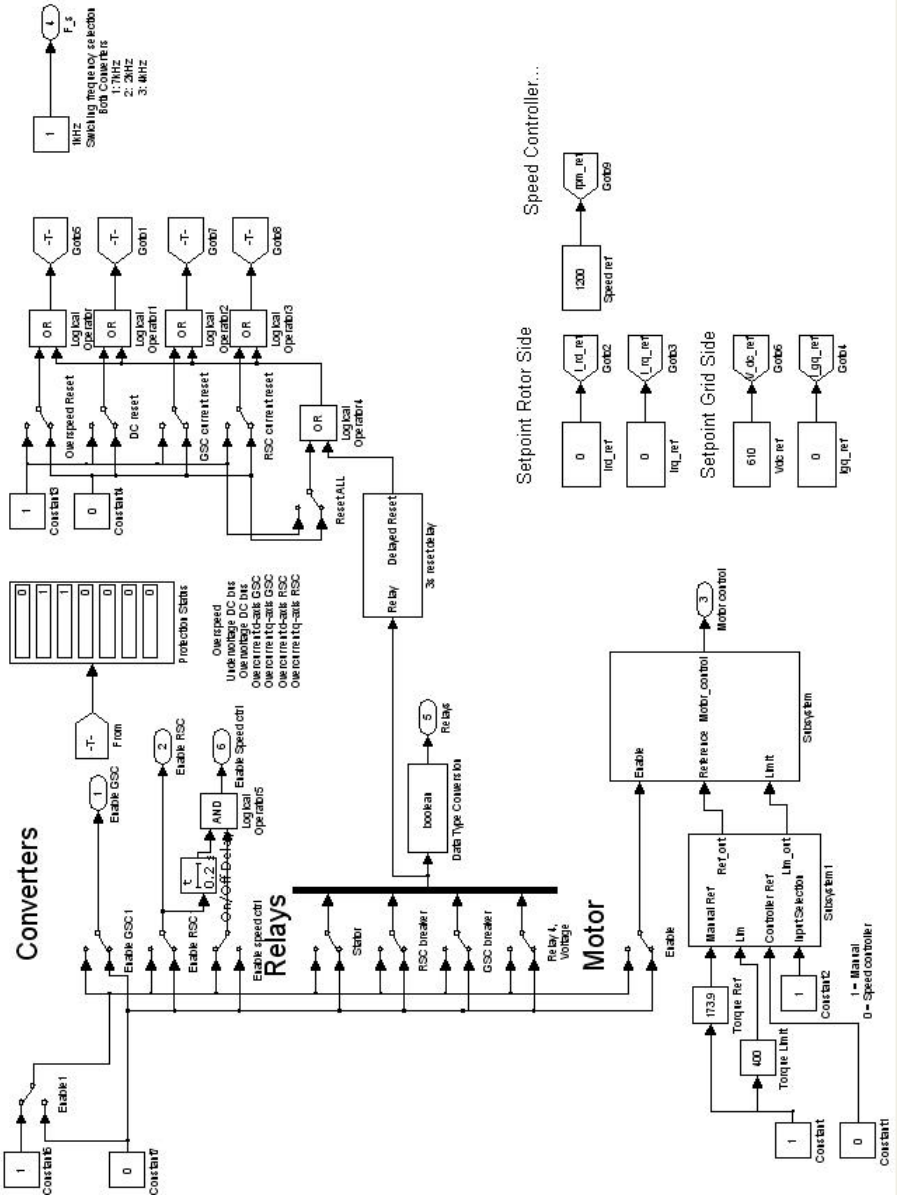

Figure 4.34: Control panel

Chapter 5

Practical problems

A laboratory setup like the one used in this work is exposed to electromagnetic noise and inaccuracies in components. Therefore, the measurements can vary from the theoretical values. To achieve good performance and correct measurements in the setup, noise and inaccuracies must be taken care of by filters and calibration. The setup itself must also be put together in such a way that the noise is reduced to a minimum. This is done by having good and correct grounding for the signal conditioning setup and by adding noise reduction to critical parts. It is also possible to have inverted signals in current and voltage measurements due to transducers used the wrong way around. This can interfere with the direction of the controllers and transformations. All these things must be taken care of to ensure that the system works as expected.

5.1 Calibration

5.1.1 Voltage and current tranducers

The voltage and current measurements are both done with LEM current transducers as described in section 4.4.1 and 4.4.2. These current signals are converted to voltage signals, buffered, offset to 2.5 V and buffered again before they are read by the ADC. This gives a 2.5 V offset which needs to be removed before the signal can be gained up to represent the actual measured signal. The method used for calibration of voltage signals is:

1. A multimeter with true RMS measurement is used for measuring the actual RMS voltage (or DC measurement for pure DC measurements)
2. A temporary mean block is added to the measured signal in the Simulink model. The output is shown numerically in a X-PC scope on the Speedgoat monitor.
3. Using a variac, the voltage is set to zero. This will short circuit the input of the LEM sensor.
4. The offset is adjusted so that the output equals zero.

5. If the voltage is perfectly centered at zero, it should remain zero if the variac is turned to full voltage.

6. With the offset set, the mean block is replaced with a RMS block.

7. The variac is then set to a voltage close to the nominal voltage.

8. The readings from the multimeter is then used as a reference for computing the correct gain for the voltage signal.

9. The calibration can be checked by adjusting the voltage from zero to nominal to see if the multimeter is equal to the measured voltage.

10. The procedure can then be redone for each phase. The offset and gain for the calibration should be about the same, given the same type of transducers.

It is possible to do the very same calibration using the actual waveform of the voltage. This will require an accurate oscilloscope where the accuracy is verified with some known voltage source. However, for this work, where multimeters are easily available, the RMS method should be accurate enough to give good voltage measurements.

The same method descibed over can be used for the DC link voltage measurement and the current measurements. However, since the current measurement is dependent of an actual current in the converters and the converters are current controlled, the calibration must be done after the system is working good enough to have a current flowing. The first guess for the calibration can then be to offset the measurement so when the system is idle, the current is actually zero. The transducer and signal conditioning can then be assumed ideal and the given ratios in the system can be used for calculating what the gain should be. This will be quite accurate and is good enough for having a working control system for the converters. After the system is working, the fine tuning of the signal can be performed using a calibrated current clamp and an oscilloscope.

For ensuring that a signal is not accidently inverted somewhere through the signal conditioning system the measured signal can be routed to one of the auxiliary DAC output ports used for real time debug. By showing the actual voltage and the output of the DAC, the two waveforms should be in phase. It can be some phase shift due to ADC conversion, processing and DAC conversion, but this will be rather small. This is also useful for checking that the waveform of the measured signal is kept during signal conditioning, conversions and processing. A RMS calculation can give good results even if the negative half cycle of the signal is clamped to zero. This is also the drawback of the RMS method.

5.1.2 Rotor converter and the rotor encoder

The mechanical encoder used for obtaining the rotor angle is connected directly to the DFIG rotor shaft. The Z pulse indicating zero for the encoder counter is generated at the point where the zero of the encoder is placed. This may not be at the same angle as the zero for the DFIG. Offset is therefore added to the encoder counter. Since this machine is a part of a fixed lab setup, the calibration is done once, and there is no automatic calibration algorithm used. The method used is based on some trial and error and is given below.

1. The asynchronous motor is started in speed controlled mode giving a fixed speed. The speed is choosen to be about 10 % different from synchronous speed.

2. The grid converter is running as normal controlling the DC link voltage.

3. The rotor converter is started and the d-axis voltage input of the siniusodal PWM modulator is set to a arbitrary level.

4. The stator breaker is kept open. A voltage sensor is measuring the stator voltage.

5. The d- and q-axis voltage components are plotted using an oscilloscope from one of the DAC outputs.

6. The encoder offset is adjusted in such a manner that all the stator voltage is in the d-axis and the q-axis voltage is zero.

7. If the stator is then connected to grid, the rotor converter can be started in current controlled mode, controlling active and reactive power transfer to the grid.

5.1.3 Grid converter and the phase locked loop

The phase locked loop (PLL) is used to obtain the angle of the grid voltage. The PLL used is the built in three phase PLL from the Simpower blockset (Matlab2010b). It synchronize the angle generator with the zero crossing of phase A in the positive sequence. The grid angle is then generated and can be used in Park transformations for obtaining the d and q axis voltage and currents in the system. The grid side converter is controlled by aligning the d-axis to the grid voltage space vector. This implies that if the grid voltage is transformed from abc to dq components using the grid angle obtained from the PLL, the q-axis voltage should be zero. An important point to consider is what voltage the grid voltage sensor is measuring. In this work, the phase-to-neutral voltage is used. That means that the measured voltage must be in phase with the reference voltage at the input of the sinusidal PWM modulator block which is also the phase voltage. If the line-to-line voltage has been used, an offset of 30° must be used. To be sure that the PLL angle is correct, the following test can be performed.

1. Plot the d and q axis of the grid voltage.

2. Adjust the offset of the PLL until the q-axis voltage is zero.

3. The d-axis is then aligned with the grid voltage space vector.

4. Plot the d-axis of the grid phase voltage aginst the d-axis of the reference voltage for the modulator. These two should now be in phase. If not, check if any sensors or phase sequences are wrong.

When the grid converter is tested it is a good idea to use a three phase variac so that it is possible to start with low voltage. To be able to test the converter, a d-axis converter voltage close to the d-axis grid voltage must be applied. For low voltages 0.9 pu is a good choice. For higher voltage close to nominal, 0.95-0.96 pu is good. The grid converter

should now be able to operate. It is a good idea not to include the DC link voltage compensation in the modulator at this point, to keep things simple. If the grid converter is working by setting a fixed d-axis converter voltage, the voltage can be increased. It is a good idea to turn the grid converter on and off to see that no transient currents are tripping the transistor proctection. When the system is running at nominal voltage, the current can reduced to minimum by offsetting the grid angle until the current is at minimum.

5.2 Correction of PI controller directions

All the controllers must operate in the correct direction to work. If the current is increased when the voltage increases, the current controller must increase the voltage if the current should increase. If the sign of the computed error at the input of the PI controller is wrong, the controller will increase the voltage when it is supposed to decrease. Before the controllers can be used, it is important to be sure that the direction of the controller is correct. A gain of -1 can be added to the error if the direction is wrong. For the DC link voltage controller and the speed controller it might be easy to determine the directions, but for the current controllers this may not be trivial. Wrong directions can be caused by wrong phase sequence, inverted current sensors or errors in analog or digital signal conditioning. A test can be performed to determine the directions for the current controllers.

1. Plot the d and q axis currents for the desired converter
2. Start with e.g. the d-axis. Increase the d-axis voltage and see what happends for the d-axis current.
3. Do the same as above for the q-axis.
4. The results can further be used for determining the most likely direction.
5. Then, the current controllers can be connected to the modulator. Start with a pure P regulator with a small proportional gain.
6. Verify the directions by applying steps the current references. When the system seems to have a correct response, the proportional gain can be increased.
7. When the behavior is correct, the controllers can be tuned.
8. Note: Both d- and q-axis controllers must be running at the same time as the d-axis current are dependent of both d- and q-axis voltage components (the same for the q-axis). The controller gains must be equal for both controllers.

5.3 Noise

The setup can be exposed to noise and it is important to try to minimize the impact of noise in analog and digital signals. Some problems encountered in the beginning was related to noise and the solution is included here.

5.3.1 Voltage and current measurements

When the work was initiated, there was some existing signal conditioning from earlier work. The initial plan was to use this system as it was. The earlier work used a dSpace system similar to the Speedgoat system, which had BNC connectors for all analog inputs. The old signal conditioning equipment had BNC connectors for directly connection to the dSpace. An interface box with BNC connectors and single wires for connection to the ADC breakout board was made. At this point, the current signals from the current and voltage transducers was converted to a voltage signal and filtered in a box with BNC connectors for further connections . The BNC cables was then connected to an interface box with single wires for connection to the ADC breakout board. This setup worked well as long as there were no converters running. When the motor drive was started all measured signals had a good amount of noise.

It was desired to create a new signal conditioning system using a signal conditioning board which was a standard board at NTNU. A board with power supply, four signal conditioning boards, connections and breakout boards for the Speedgoat modules was made. Now, all the transducers signals had their own D-SUB connector at the front panel of the signal board. The signal cables were shielded and grounded in the chassis by the connector. Some twisted pair cables went from the D-SUB connectors to the signal conditioning boards. The output signals from the signal conditioning boards was directly connected to the ADC breakout board. The shielding of the cables between the Speedgoat and the breakout board was grounded to chassis as well.

Using this new setup, the noise was reduced to a minimum with no big impact on the measurements in the system.

5.3.2 Digital signals

The same noise phenomena as described for the analog signals was found for the digital signals and especially in the encoder signals. A circuit with a differential signal transceiver was made for testing the encoder functionality. The original idea was to use this circuit on a permanent basis, but after some tests, it was found out that this was a bad idea. The encoder worked very well when it was tested by turning the machine shaft by hand, but as soon as the motor drive was started the encoder signals were totally destroyed by noise. The test circuit was made on a piece of veroboard with a lot of single wires with no shielding. The connector to the encoder consisted of some single wires soildered to a 15 pin D-SUB connector for use with an existing cable.

The signal conditioning boards for the analog signals also had a interface for the gate driver signals and the encoder signals. As for the analog signals, all the digital signals had their connectors in the chassis of the signals condition system. From the respective connectors, flat cables with connectors was used to interface the signal conditioning boards. All these flat cables had ferrite rings for removing high frequency noise. The gate driver signals also have ferrite rings in the converter end of the cable. All signals were monitored with an oscilloscope and most of the harmful noise was gone. The system worked very well with no trouble.

5.4 Torsional resonance

Both the asynchronous motor and the DFIG has its own shaft and bearings. For easy mechanical coupling between the two machines, a mechanical coupling with teeth and a rubber ring is used. This rubber ring provides some damping in the direction of the rotation and can remove vibrations. The alignment of the machines is also easier when the coupling is not stiff. However, this can generate torsional resonance and torque ripple. As a solution for having shorter cables for the encoders, the encoder of the DFIG was used for the motor drive and vice versa. This was no problem when the motor drive was used in torque controlled mode, but when the speed controlled mode was used, the machine started vibrating and made a terrible sound. After some research, it was found out that the soft coupling between the motor and the encoder gave a little offset of the angle when the torque was increased and decreased. The speed controller would then increase the torque for a moment, giving a speed which was above reference speed. The torque was then decreased rapidly, giving a speed below the reference speed. This generated an oscillatory behavior. After the test, a longer cable was used, and the motor drive could use the motor encoder again. It is therefore a good idea to use the encoder which is as close to the machine as possible with as few mechanical couplings as possible to have the best behaviour.

Chapter 6

Laboratory results

6.1 About the measurements

This chapter presents the results from eight tests done with the DFIG lab setup. The first four tests are focusing on the total (rotor + stator) active and reactive power exchanged with the grid during changes in torque, speed or both. The next two tests shows how the total active and reactive power is changed by controlling the q-axis current of the rotor controller. The last two test shows how the active and reactive power flow in the rotor circuit is changed, when torque and speed is changed. For all eight tests, both speed and turbine torque is plotted in addition to the active and reactive powers.

The power measurements are done using a Fluke 434-II three phase analysator which can plot active and reactive power over a given time. The sample rate is a little low for this use and therefore, the transient behavior of the voltage is not very well documented. However, for steady state, the changes in active and reactive power are clear.

The speed and torque are measured at the motor controller. Two of the 16 bit DAC output channels are connected to a oscilloscope giving a small voltage witch is proportional to the actual speed and torque. These values are scaled and offset is added before the actual data is plotted. Matlab is used for plotting the graphs.

The sign convention used, is that the positive active power is supplied to the grid while positive reactive power is consumed from the grid by the DFIG. This is the opposite of the motor convention used in the other chapters of this document.

6.2 Active and reactive power in both rotor and stator

In these four tests, active and reactive power of the DFIG under different operating conditions are tested. The powers are the sum of both rotor and stator. The two first tests are showing the active and reactive power during a change from 0 to 20% torque at fixed speed. The two next tests are showing active and reactive power when both speed and torque is changed.

6.2.1 Test 1: Postive change in torque at 1600 rpm

In this test the speed reference of the speed controller is set to 1600 rpm. The setup is started and is operating steady state at zero turbine torque. At 12 s the turbine torque is increased to 20%. The torque is ramped up with a rate of 10%/s. The q-axis (reactive) currents for both rotor and stator converter are kept at 0. The response of the system is shown in figure 6.1.

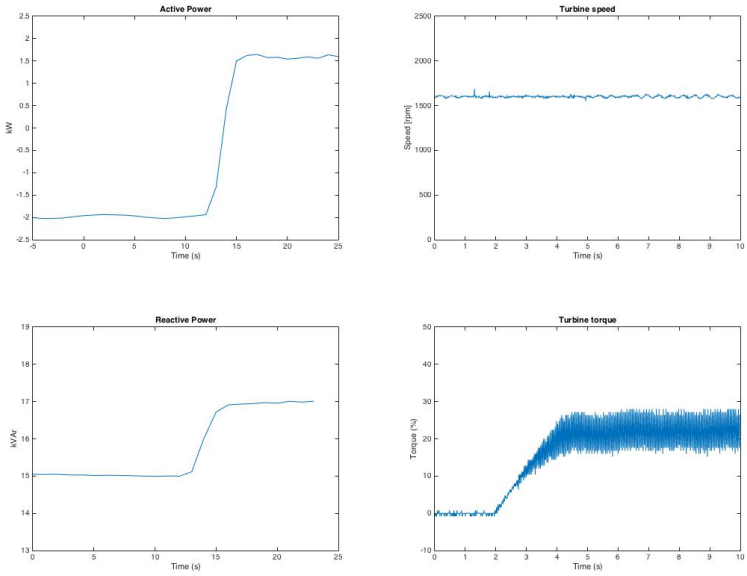

Figure 6.1: Test 1

The active power is increased from below zero, indicating that the DFIG is running as motor, up to about 1.5 kW delivered to the grid. The reactive power is increased by 2 kVAr. The speed is kept very stable at 1800 rpm. The torque from the motor is however oscillating at high frequency. This behavior is equal for all tests running at 1600 rpm.

Note: In figure 6.1, the time axis of torque and speed, has an offset of 10s.

6.2.2 Test 2: Postive change in torque at 1400 rpm

In this test, the speed reference is kept at 1400 rpm. The reactive currents for both converters are kept to zero. The torque is ramped up to 20% with a rate of 10%/s. The response is shown in figure 6.2.

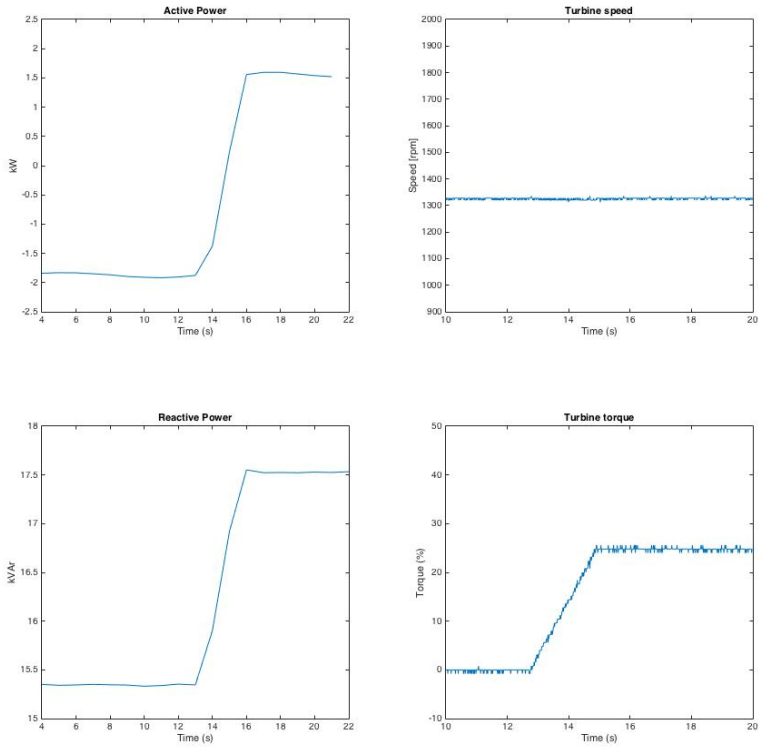

Figure 6.2: Test 2

The active power is slightly lower than for the same test running at 1600 rpm. However, the reactive power has increased with 500-600 VAr when the speed was 1400 rpm compared to 1600 rpm. The reactive power increases with 2.5 kVAr during the torque ramp up. The speed is constant. The torque now has much less ripple compared to running at 1600 rpm.

6.2.3 Test 3: Positive change in both speed and torque

In this test both speed and torque are varied. The speed reference is ramped up from 1400 rpm to 1600 rpm in 2 seconds. At the same time the torque is ramped up from 10% to 25%. Reactive currents for both converters are kept to zero. The results are shown in figure 6.3.

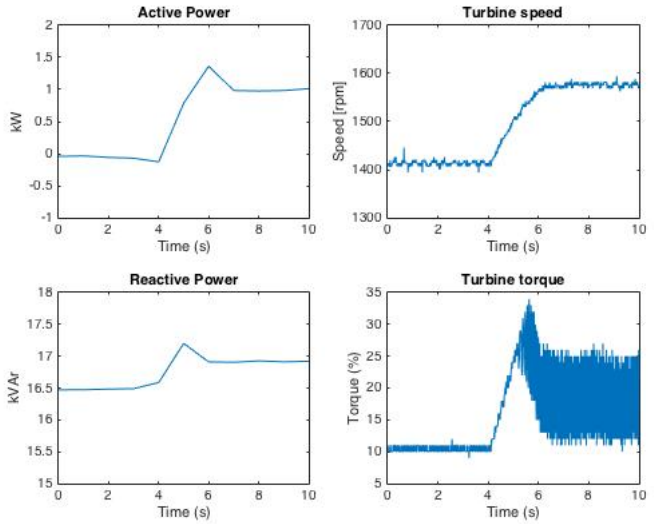

Figure 6.3: Test 3

This test shows that both active and reactive power are having some overshoot when the new speed is reached. Both reative and active power are increased after the change. The turbine speed is following the linear behavior which is set by the speed controller. No overshoot is seen in the speed. The turbine torque is increased and the oscillatory behavior which was seen earlier exists again. It can be noted that the torque has some overshoot at the same time as the active and reactive power.

6.2.4 Test 4: Negative change in both speed and torque

This test is the opposite test of test 3. The machine is operating at 1600 rpm before the speed reference is set to 1400 rpm in 2 seconds. The torque is moved from 25% to 0% Reactive currents for both converters are kept to zero. The response is shown in figure 6.4.

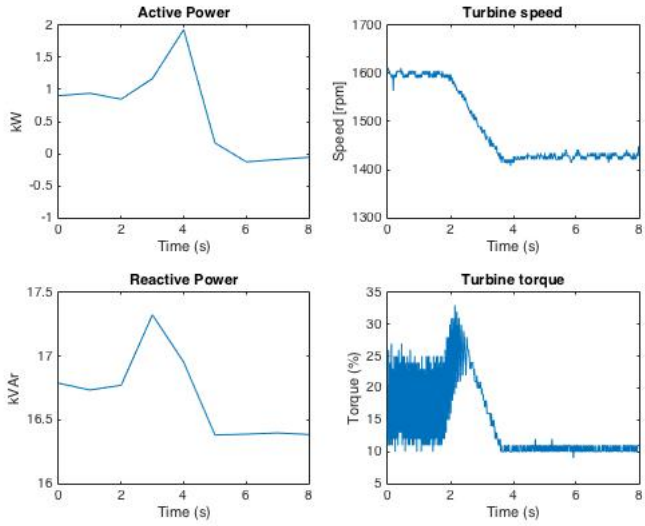

Figure 6.4: Test 4

In this test, the curves look like the opposite of test 3. The active power overshoot is higher than for test 3, which is natural since the machine is loaded more for forcing the speed lower. The reactive power is similiar. The torque have some overshoot that removes the oscillating behavior, an the torque is moved to 10% linearly. The speed have some undershoot, but it is negligible.

6.3 Reactive power control

In these tests, the q-axis current of the rotor converter is adjusted to see the behavior of the reactive power control. These tests are done at constant speed and constant torque.

6.3.1 Test 5: Change in reactive power at 1420 rpm

In this test, the speed is kept constant at 1420 rpm and the torque is constant at 20%. At time equal 2 seconds, the q-axis rotor current is changed to -8 A. The response is shown in figure 6.5.

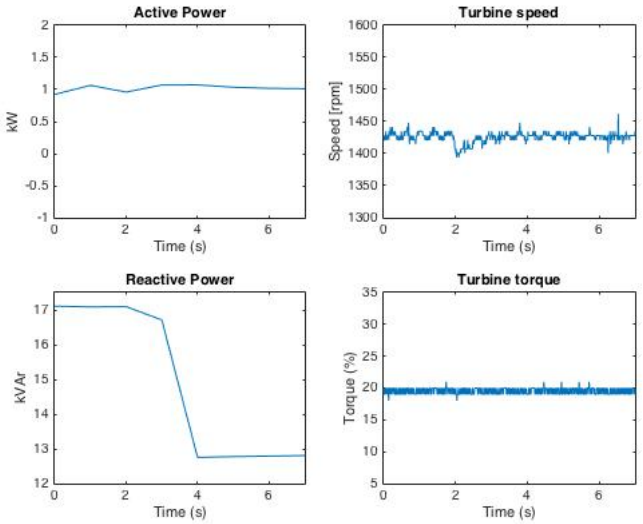

Figure 6.5: Test 5

This gives a significant drop in reactive power from 17 kVAr to about 13 kVAr. Both active power and speed are close to unchanged but a little dip is shown just after the change in q-axis rotor current. The torque is however constant.

6.3.2 Test 6: Change in reactive power at 1600 rpm

This test is the same as test 5, but with at another speed. The speed is kept constant at 1600 rpm and the torque is constant at 20%. At time equal 2 seconds, the q-axis rotor current is changed to -8 A. The response is shown in figure 6.6.

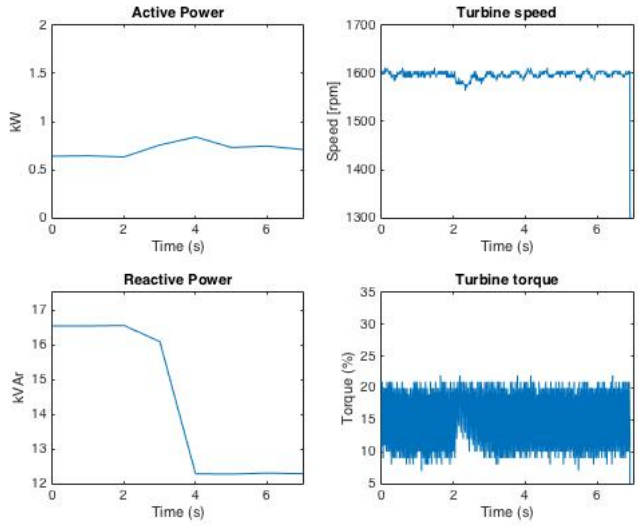

Figure 6.6: Test 6

The response of the reactive power is equal to the same test running at 1400 rpm. The speed has a little dip, and the active power now increases. This is the opposite from test 5. The torque is oscillating as for the other tests running at 1600 rpm, but when the q-axis current is changed, the oscillatory effect decreases for a second before it is back.

6.4 Active and reactive power in the rotor circuit

In these two last tests, the reactive and active power are measured on the terminals of the rotor converter. The speed is varied from hypersynchronous to subsynchronous to verify that the rotor circuit works are expected. The torque is also varied. These tests are the same as test 3 and 4, except for that 7 and 8 are measured at the rotor circuit alone.

6.4.1 Test 7: Positive change for both torque and speed

In this test, the machine is running at 10% load torque and 1400 rpm. Then the speed and torque is ramped up to 1600 rpm and 25% torque in 2 seconds. The response of the rotor powers are given in figure 6.7.

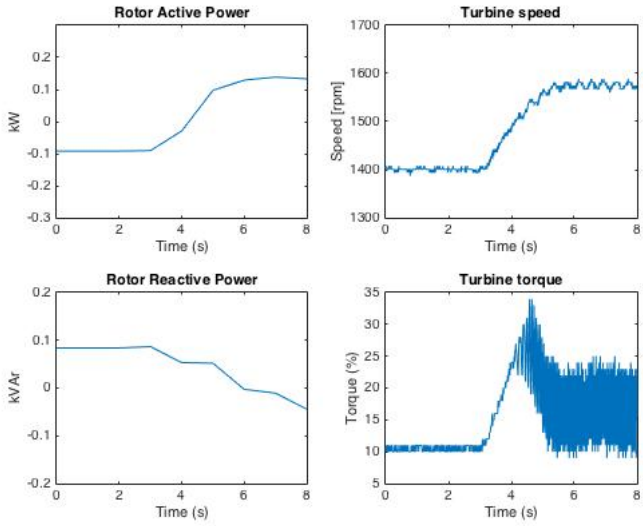

Figure 6.7: Test 7

The rotor power changes from -0.1 kW to 0.15 kW when the speed is increased from 1400 rpm to 1600 rpm. That means that the rotor is delivering active power to the grid when running at hypersynchronous speed and cosuming active power when running at subsynchronous speed. For the reactive power, the characteristic is the inverse of the active power.

6.4.2 Test 8: Negative change for both torque and speed

In this test, the machine is running at 25% load torque and 1600 rpm. Then the speed and torque is ramped down to 1400 rpm and 10% torque in 2 seconds. This is the opposite behaviour as seen in test 7.

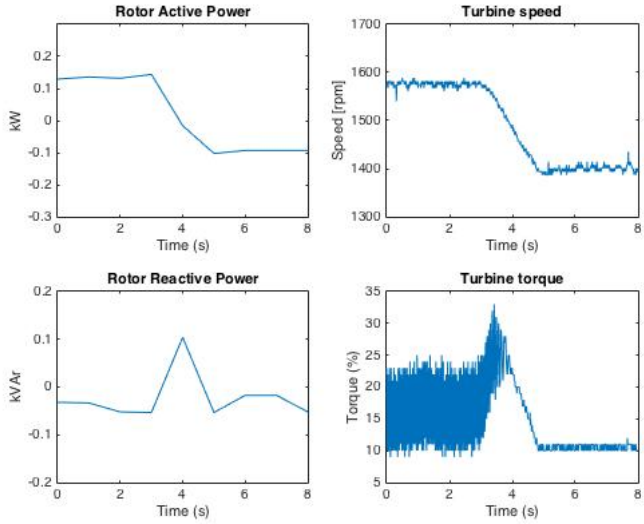

Figure 6.8: Test 8

Also, in this test the active power changes direction when the speed goes from hypersynchronous to subsynchronous. The reactive power a positive peak that is observed during the change of speed and torque.

Chapter 7

Discussion

7.1 Lab results

The lab results is presentes in the previous chapter. These measurements are meant for validating the theoretical descriptions of the machine. Lab tests are very useful for understanding the behavior of the actual systems. However, the results can differ from the theoretial and it is important to understand why this happens.

The lab results obtained in this work has some limitations when it comes to time resolution of the active and reactive powers obtained from the measurements. The measurements can be seen as correct at steady state, while the transient behavior is not shown very well. The choice of measuring equipment was not correct, but at least, the results shows that the setup is working.

Another problem with the lab setup, which is discussed more in detail in the next section, is the limit of loading the machine above 30%. The grid converter trips when the load is larger than 30%. This problem was not solved before the lab tests was done, and the machine was limited to have only small loads.

7.1.1 Active and reactive power in rotor and stator

For the first four lab tests, the focus was to study the behavior of the DFIG during changes in speed reference and turbine torque. The idea was to show that the setup could be controlled by a optimal speed module based on the characteristics of the turbine. However, in the tests, this was done by switching between two pairs of speed and torque refereneces and the optimal speed module was not considered in these tests.

For the first two tests, the speed was kept constant while the torque was increased over time. For both these tests, the active and reactive power increased. This behaviour is normal since the current increases through the inductances in the equivalent circuit. The active power is increased to keep the speed at the defined setpoint. It can also be seen that the speed controller is working properly since the speed is not varied during the torque changes. However, this is not verified for a step change in turbine torque. There

is no overshoot in the torque, meaning that the motor alone controls the torque in a good manner. For speeds above synchronous speed and 10% torque, the torque measured at the motordrive starts to oscillates making it hard to determine the actual torque. However, the torque reference for the motor drive is set to 25%.

For test 3 and 4, the speed was varied with the torque. The same active and reactive power behavior as for the fixed speed operation, is shown. At the point where the speed is correct, the speed controller increase the active power for stopping the increase in speed. This makes the power peak at the end of the torque and speed ramp. The same phenomena is shown when the speed should be decreased. A load peek is occuring to slow down the rotating mass.

7.1.2 Reactive power control

In test 5 and 6, the speed and torque references was kept constant to see what happens when the q-axis current in the rotor was increased. In theory, this should decrease the reactive power produced by that machine. This behavior is verified in the tests. At both subsynchronous and hypersynchronous speed, the reactive power is reduced from about 17 kVAr to 12 kVAr. At the point of change in q-axis current, the speed drops a about 100 rpm. This can be due to a small misalignment of the dq frame, making the active power slightly dependent of the q-axis current. For subsynchronous speed, the active power drops, while for the hypersynchronous speed, the active power increases. However, the reactive power change is large compared to the active power change and the theory is thereby verified.

7.1.3 Rotor circuit behavior

In test 7 and 8, the power flow of the rotor circuit is studied. The idea was to show that the direction of the power flow was changed when the speed was increased from subsynchronous to hypersynchronous. The torque was increased with the speed.

The theory is verified when the speed is increased. The rotor consumes 100 W when it is operated at subsynchronous speed and produces 150 W when the speed is increased to hypersynchronous. The difference in magnitudes before and after the change is due to increase in torque at the motor. The reactive power is opposite. Negative reactive power for subsyncronous speed while it is positive for hypersynchronous speed.

7.1.4 Large torque ripple for speeds above synchronous speed

For all tests that runs at 1600 rpm and torque over 10%, the torque becomes oscillatory. The speed controller for the DFIG is not tuned with very high gain and the speed measurement for the controller is filtered with a time constant larger than the oscillation frequency of the torque. The speed measurement at the motor drive (which is used for plotting) does show some oscillations, but the frequency is small compared to the torque oscillations.

A possible explaination for this is the mechanical coupling between the motor and generator. It contains a rubber ring which will add some elasticity in the coupling. The natural oscillation frequency of this coupling seems to be somewhere above, but close to 1600 rpm. This can cause the torque ripple.

7.2 Lab setup considerations

The lab setup is built, tested and its functionality is proven to work somewhat close to the theory. However, there are some limitations of the setup which are not correct. The known limitations can be summed up as follows:

- The current controllers are not very well tuned. They work, but the optimal response is not validated. One of the major problems with the current controllers is that the ADC sampling is not synchronized with the PWM, enabling the possibility to sample at the top and the bottom of the current ripple. Instead, a sampling running at 10 kHz is sampling a current signal which runs at 7 kHz giving a very noisy current signal. This signal is filtered, but the time constant of the filter must be small enough so the dynamic behavior of the current is kept intact. This introduces noise which is fed through the proportional term of the current controllers, and the proportional gain must be chosen so that the noise is satisfyingly low at the input of the PWM modulator.

- The setup is limited by the grid converter at this point. When the DFIG is loaded by increasing the d-axis current of the rotor converter, the transistor protection of the grid converter trips. This makes the setup only usable for small active powers at about 20-30% of the rated values. This makes it impossible to really examine the system behavior at heavy load.

- The current controllers of the rotor circuit trips when the stator breaker is open. For any d-axis current different from zero, this is normal as the active power have no place to go, when the stator breaker is open. However, it should be possible to start the machine, adjust the magnitude, phase and frequency of the stator voltage and synchronize it to the grid before the stator breaker is closed. At this point, this is not possible. One possible reason is that the time constant of the rotor circuit is lower when the stator is not connected, since the stator leakage inductance is gone. With a slow, badly tuned controller, the system would not necessary behave perfectly.

- The DFIG used in the setup is rated 220/380 V (Δ/Y). In the laboratory, the voltage is above 400 V giving a possibilty for saturation of the DFIG. When the stator breaker is closed, the machine consumes reactive power at about 15-16 kVAr. The machine ratings say 32 A stator current and 15 kW active power. This means that if the machine is running at rated active power and current, the reactive power can be up to around 15 kVAr. What the reactive power is at rated reactive power without reactive compensation in the rotor, is unknown due to not being able to fully load the machine without tripping the grid converter.

- The grid converter has some reactive power flowing which cannot be modified with the reactive current of the grid converter. A possible explanation is that the LC filter used between the converter and the grid is consuming reactive power to some degree. This is not verified by calculations or measurements. This reactive power is included in all the lab results regarding the total power of the DFIG.

- It can be mentioned that the converter power ratings is four times larger than required for supplying the rotor circuit at speed variations of $\pm 30\%$. This can introduce higher losses than for a perfectly dimensioned converter.

7.3 DFIG used in mini hydro power plants

In this work, the main idea was to increase the efficiency of the hydro turbine by introducing the possiblilty to vary the rotational speed. The speed was determined by the Hill diagram of the Francis turbine which used flow and speed as parameters. This does not take the head into consideration. The best point of efficiency is defined for a specific head, flow and speed. The Hill diagram used in this work assumes that the head is optimal and constant for all operating points. Reasons for change in head can be different levels in the dam, or head loss in the penstock. To be able to to say whenever the head variations are important, must be studied in each case. This will define whenever the choice of DFIG is a good idea or not, when it comes to efficiency improvement.

The use of DFIG opens new possibilities when it comes to motor operation which is used in pump to storage power plants. Depending of the capacity of the rotor converter, the speed can be varied making it possible to change the flow when the machine is operated as pump. In turbine mode, the water flow is changed by controlling the angle of the guide vanes in the turbine. However, in pump mode the guide vanes must be set to fixed angle, making flow variations rather difficult. If the speed can be varied, the flow of pump turbine can be controlled. The DFIG can be used for making it easier to go from turbine mode to pump mode and also control the water flow of the pump. In this case, the improvement of the efficiency in turbine mode is a bonus feature.

An interesting advantage of the DFIG is the fast response to rapid change in power demand. The synchronous machine must wait for the turbine to open the guide vanes before the power can be increased and this process can take seconds to do. The DFIG can change the speed and utilize the rotating mass while the guide vanes are opened. This makes the use of DFIG smart for applications where fast power characteristics is useful. An typical application can be to increase stability in the grid by being able to supply power faster than conventional methods.

Chapter 8

Conclusion

The objective of this work was to continue the work done in an earlier Master thesis where the topic was to implement a DFIG in a small scale hydro power plant. The main goal of doing so, was to introduce the possiblitiy of operating a Francis turbine at variable speed, and thereby possibly increase the efficiency of the turbine. In the thesis this work is based on, control strategies were developed and simulations were done to see if variable speed operation could increase the efficiency of the turbine. A lab setup was made for verifying the simulated results.

The lab setup was developed further in this work. The existing setup consisted of a DFIG connected to an asynchronous motor. In addition, a rack with voltage source converters for controlling the rotor circuit and a motor drive for controlling the asynchronous motor existed. The control system for two existing back-to-back connected converters, was made from scratch. The instrumentation required for measurements of speed, currents and voltages were redone, and the control algorithm was made from scratch.

Working in the lab with so many components that should work together takes time. Therefore, it was impossible to make a lab setup where everything was working 100%. However, the result is a lab setup with complete instrumentation, controllers and a control platform that should be easy for others to develop further.

The tests showed that the setup operates close to the theory. By the use of vector control, the active and reactive power in both stator and rotor circuit was controlled. The machine worked as both motor and generator. Speed control was implemented in the control system by controlling the power flow of the DFIG. Finally, the machine could be operated at both subsynchronous and hypersynchronous speed with bidirectional power flow of the rotor circuit.

8.1 Further Work

As mentioned in the conclusion, the lab setup is working. However, there are a few problems that can be solved and thereby improve the performance of the setup. This is a list of improvements that can be made to the lab setup:

- Do a better tuning of control system for the grid converter. When the active power flow of the rotor circuit reaches a threshold of about 30%, the transistor protection trips the converter.
- The encoder and PLL offsets should be recalibrated to be sure that the alignment of the dq reference frames are correct.
- The reactive power provided by the grid converter, when the reactive current is zero, should be examined and minimized.
- If possible, PWM synchronized ADC conversion should be implemented. This will remove noise from the current measurement, and can be used to improve the tunings of the current controllers.
- The rotor controller should be modified in such a manner that it is possible to run it with open stator breaker. At this point, the current protection will trip the converter once the stator breaker is opened.
- By adding a CAN-bus module into the Speedgoat controller, it is possible to control the motor drive by digital control. This will increase accuracy and remove potential problems with noise on the analog signals.

In addition to the improvements, some new features can be implemented in the setup:

- Implement a turbine characteristic for the motor controller. By doing so, it is possible to examine the actual result of using a hydro turbine connected to a DFIG.
- If the controller of the rotor converter is corrected, it is possible to implement a proper algorithm for synchronizing the machine to the grid. This can reduce the current in-rush when the stator breaker is closed.
- If possible, a DFIG should be connected to a real Francis turbine. This might require a larger DFIG.

If the DFIG technology is to be used in hydro power applications, its advantages compared to using a synchronous generator with a full power converter must be determined. The price of power electronic components is decreasing and their power ratings are increasing for every year. However, if the DFIG is to be used, the following points can be taken into consideration:

- Include the head variations in the optimal speed calculation.
- Examine how the DFIG can be used in pump to storage power plants so that the flow in the pump can be varied by adjusting the speed.
- Due to the fast power response of the DFIG, it can be used for stabilizing the grid.

Bibliography

[1] Aggarwal Archna, Saini Lalit Mohan, Singh Bhim, 2014. Modeling and Control for Wind Energy Generation. YMCA University of Sc. & Technology, Faridabad, Haryana, India.

[2] Gonzalo Abad, Jesus Lopez, Miguel Rodriguez, Luis Marroyo, Grzegorz Iwanski, 2011. Doubly Fed Induction Machine. Wiley, IEEE press.

[3] Iversen, B., 2015. Project work: Doubly-fed induction generator for use in mini-hydro power plants. NTNU.

[4] Kjell Ljøkelsøy, H. K., 2001. Beskrivelse: Måleinnsamlingskort, v1.0.

[5] Kjell Ljøkelsøy, H. K., 2002. Arbeidsnotat: 20 kW IGBT omformer. Beskrivelse.

[6] Ljøkelsøy, K., 2014. Project Memo: Control system for a three phase grid connected converter.

[7] Rafique, R., 2015. Master thesis: Doubly-fed induction generator for use in mini-hydro power plants. NTNU.

[8] Speedgoat, 2010. Modular-large real-time target machine, user's manual. URL `www.speedgoat.ch`

Appendix A - Speedgoat pinouts

311 - Grid side FPGA Card

- PCI-bus: 4.10
- Reset pin is not used since the measurement board does not support it.
- OK PCB is ok signal for measurement board power supply.

Speedgoat 311 FPGA Grid side converter

Function	Pin nr	Board pin nr	IO	Euroconnector	Color	Notes
PWM A	1	1	O	8C	Brown	
PWM A'	2	2	O	7C	Red	
PWM B	4	4	O	8B	Orange	
PWM B'	5	5	O	7B	Yellow	
PWM C	7	7	O	8A	Green	
PWM C'	8	8	O	7A	Blue	
GND		18		2ABC	Black	
GND		19		2ABC	Black	
Reset	33	37	O			Not used
Enable	34	38	O	6B	Purple	
OK signal	49	53	I	4C	Grey	
Status T3	50	54	I	5A	Yellow	
Status T2	51	55	I	5B	Orange	
Status T1	52	56	I	5C	Red	
Status T0	53	57	I	6A	Brown	
OK PCB	54	58	I	4B	Green	Power ok
Enc A	14	14	I	10B	Brown	
Enc B	15	15	I	11A	Red	
Enc Z	16	16	I	10A	Orange	

311 - Rotor side FPGA Card

- PCI-bus: 4.14
- Reset pin is not used since the measurement board does not support it.
- OK PCB is ok signal for measurement board power supply.

Speedgoat 311 FPGA Rotor side converter

Function	Pin nr	Board pin nr	IO	Euroconnector	Color	Notes
PWM A	1	1	O	8C	Brown	
PWM A'	2	2	O	7C	Red	
PWM B	4	4	O	8B	Orange	
PWM B'	5	5	O	7B	Yellow	
PWM C	7	7	O	8A	Green	
PWM C'	8	8	O	7A	Blue	
GND		18		2ABC	Black	
GND		19		2ABC	Black	
Reset	33	37	O			Not used
Enable	34	38	O	6B	Purple	
OK signal	49	53	I	4C	Grey	
Status T3	50	54	I	5A	Yellow	
Status T2	51	55	I	5B	Orange	
Status T1	52	56	I	5C	Red	
Status T0	53	57	I	6A	Brown	
OK PCB	54	58	I	4B	Green	Power ok

203 - Digital IO card

- Relay 1-3 controls the breakers for stator, rotor side converter and grid side converter
- Relay 4 controls a breaker used for measuring the output voltage at the rotor side converter.
- Relay 5 is included in the relay driver, but no relay is connected.
- Red wire is 1 in the flat cable.
- The colors of the wires between the breakout card for the 203 and the DSUB9 is represented in the last column.

Speedgoat 203 Digital IO

Function	Pin nr	Board pin nr	IO	DSUB9	Flatcable	Color
Relay 1 Stator Breaker	1	1	O	6	2	Green
Relay 2 RSC Breaker	2	35	O	2	3	Blue
Relay 3 GSC Breaker	3	2	O	7	4	Red
Relay 4 Volt.M	4	36	O	3	5	Purple
Relay 5 Not used	5	3	O	8	6	
GND		9		1	1	Black

106 - Analog-to-digital card

- All voltage measurements are centered around 2.5V
- V_{ga} is meaured at the grid side of the stator breaker
- V_{sa} is meaured at the stator side of the stator breaker
- #MPCB denotes which measurement board that is used.

Speedgoat 106 ADC

Function	Pin nr	Board pin nr	Voltage	#MPCB	Euro	Color
V_{ga}	1	1	0-5V	4	23C	Brown
V_{gb}	2	2	0-5V	4	23B	Red
V_{gc}	3	3	0-5V	4	23A	Orange
V_{dc}	4	4	0-5V	4	22C	Yellow
GND		5		4	2ABC	Black
I_{ra}	5	6	0-5V	1	23C	Brown
I_{rb}	6	7	0-5V	1	23B	Red
I_{rc}	7	8	0-5V	1	23A	Orange
GND		10		1	2ABC	Black
I_{ga}	9	11	0-5V	2	23C	Brown
I_{gb}	10	12	0-5V	2	23B	Red
I_{gc}	11	13	0-5V	2	23A	Orange
GND		15		2	2ABC	Black
V_{sa}	13	16	0-5V	3	23C	Brown
V_{sb}	14	17	0-5V	3	23B	Red
V_{sc}	15	18	0-5V	3	23A	Orange
GND		20		3	2ABC	Black

110 - Digital-to-analog card

- Analog control signals for the motor controller.
- Voltage is centered around 2.5V and both positive and negtive torque can be controlled.

Speedgoat 110 DAC

Function	Pin nr	Board pin nr	Voltage
Motor Torque Ref	1	1	0-5V
Motor Torque Limit	2	2	0-5V
GND		35	

Appendix B - Running the lab setup

Part 1: Inital settings

This appendix describes how to manually and automatically run the lab setup. First, the basic settings for both modes are given before each mode is discussed in detail. The following steps are the necessary steps for powering up the setup.

Note: Please read this document before trying to start the system. Keep out of the reach of children.

1. Connect the three phase 63 A 400 V connector for the motor drive to the outlet at the wall.

2. Connect the single phase power for the electronics of the motor drive to a outlet in the lab bench, and turn the 63A curcuit breaker on.

3. Press the green button on the motor controller to energize the DC link of the motor drive. Be sure that the motor drive is in `Torque` controlled mode and that the torque reference is set to `Potmeters`. How to do so, is given in the lab chapter of this document. The motor drive is now ready. DO NOT turn on the enable switch yet..

4. Connect the three phase 63 A 400 V connector for the converter rack to the outlet at the wall. This also supplies the stator of the DFIG. Do not power up the control system for the converter rack yet.

5. Turn on the computer running MATLAB2010b (or a) and load the Simulink model named `control_system_v4.mdl` in Simulink.

6. Turn on the Speedgoat controller. An ethernet cable should be connected between the computer and the Speedgoat controller as described in the Speedgoat documentation. The computer must have the Speedgoat block set installed.

7. The model can now be loaded into the Speedgoat controller. This is done by pressing `CTRL + B` on the keyboard of the computer running Matlab. Have a look at the Matlab commandline. Something should happen! This will take about 30-40 seconds. If nothing happens, please try again.

8. When the model is downloaded to the Speedgoat, the screen of the Speedgoat changes and is ready for operation. Set the mode of the Simulink model to `External` and the play button should be pressed to start the model. Now the model is running on the Speedgoat, but it can be controlled by the computer running Matlab. To verify that the system is running, make sure that the measurements have become active at the screen of the Speedgoat.

9. Now, connect the control system power for the converter rack to an available outlet.

10. Be sure that the normal Elko lampswitch with white wires marked `Drivers` is on.

11. The system is now ready for start up. Please proceed to either manual or automatic control.

Part 2a: Manual mode

In this mode, all controls must be done manually. If part 1 is done, it is ready for start the setup. The control panel block in the model is located at the bottom left of the Simulink model and has a red distinct color. Open this block and it should look like figure 8.1. In this mode, both the file named `control_system_v3.mdl` and `control_system_v4.mdl` should work. The start procedure can now start.

1. Be sure that everything in part 1 is OK. Please be sure that all switches in the model is off (pointing downwards).

2. If using the file named `control_system_v4.mdl`, ensure that the parameter named `Automode?` is set to 0.

3. First, the global enable switch in the upper left corner must be switched on.

4. Then, the grid and rotor converter breakers can be closed by turning on the two switches named `RSC breaker` and `GSC breaker`. Usually, the grid breaker is closed first. The DC link will now charge in about 3 seconds.

5. Now the grid converter can be enabled. This is done by turning on the switch named `Enable GSC 1`. The grid converter should now start humming. If not, check the protection status display in the Simulink model.

6. Then, the motor can be started. Flip over the Enable button of the motor drive (located at the driver rack). The motor should now start humming.

7. The motor is started by enabling the `Enable` button below `Motor` in Simulink. A good startup torque is about 17 (=1.7%) and can be set using the slider gain named `Torque Ref`. The torque limit must be set to a value above zero e.g. 400 (40%).

8. While the speed increases, the button named `Enable speed ctrl` should be enabled. Nothing will happen by doing so. It will just make it ready for later use.

9. When the speed reaches about 1100 rpm, the stator breaker can be closed using the switch named `Stator`.

10. Now, the rotor side converter can be started directly. To enable the rotor converter and the speed controller, enable the switch named `Enable RSC`. The machine should now go the speed set by the `Speed ref` box under the point named `Speed controller`.

11. The setup should now be working. The following things can be done while the machine is running:

    - The speed reference can be changed using the `Speed ref` constant block.
    - The reactive current references for both converters can be controlled by `I_rq_ref` and `I_gq_ref`.
    - The DC link voltage can be changed by modifying `Vdc_ref`

12. The shutdown sequence are as follows:

    - Disable rotor converter
    - Open the stator breaker
    - Stop the motor
    - Disable the grid converter
    - Open the rotor and grid converter breakers
    - Turn off enable switch of the motor drive.
    - Stop the Simulink model.

If something does not work, please check the protection status display in Simulink and the status codes/ok-signals at the Speedgoat screen. See Appendix C for status codes of the converters. Each term of the protection system can be reset by the use of reset buttons in the control panel. The protection is reset each time the grid converter breaker is closed. It is also a good idea to start with the reactive currents at zero.

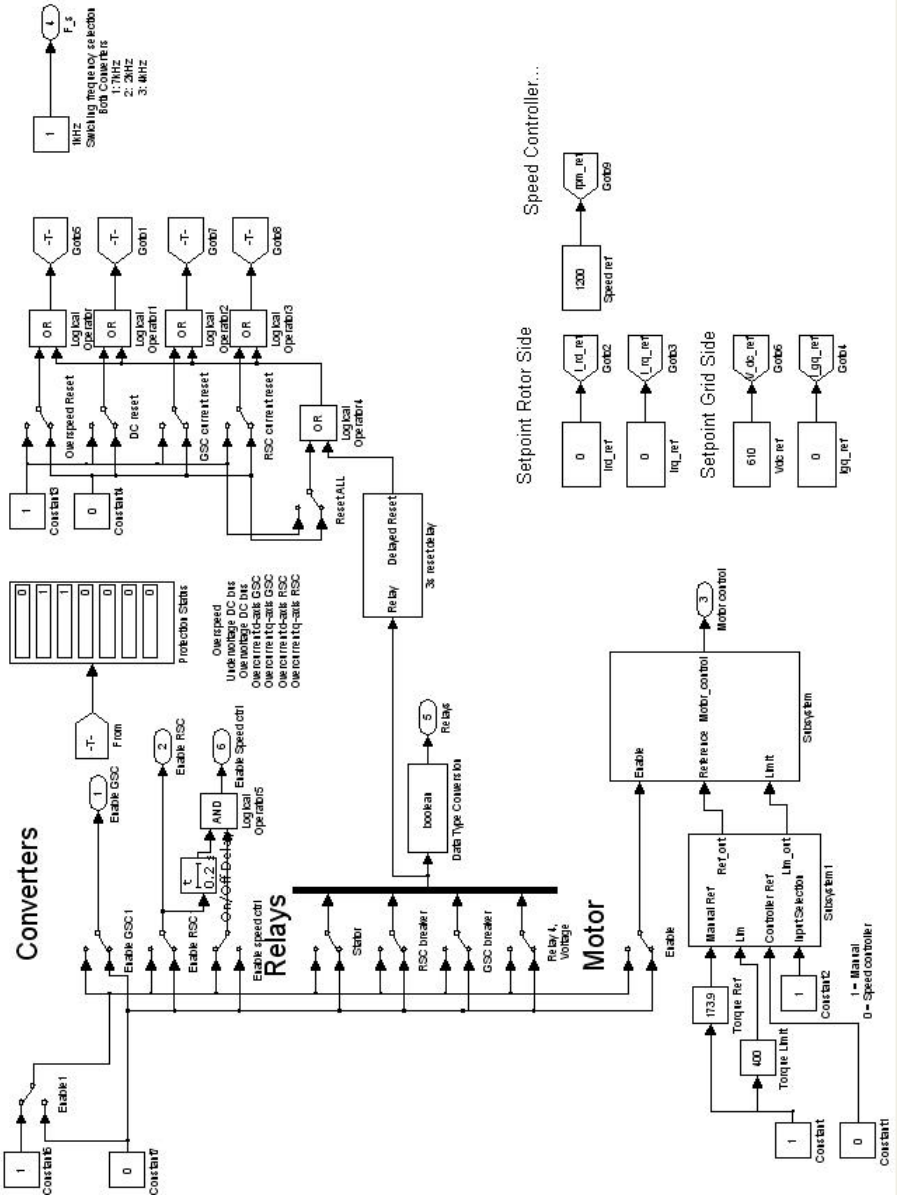

Figure 8.1: Simulink control panel

Part 2b: Automatic mode

If automode is enabled, the setup is started and stopped automatically. For being able to use the automode, it is necessary to use the following file `control_system_v4.mdl` in Simulink. The automatic control of the system is shown in figure 8.2 and the following steps must be done to control the machine:

1. Part 1 must be done (as for Manual mode).
2. Ensure that the parameter named `Automode?` is set to 1.
3. Be sure that the switch named `Trip` is off.
4. Be sure that the switch named `Enable speed ctrl` is on.
5. To start the machine, enable the switch `Start`. The machine starts in the following order:
    - Close the grid convert breaker
    - Wait 3s, close the rotor converter breaker
    - Wait 3s, enable the grid converter (inkl DC link controller) and start the motor.
    - When the speed reaches 1100 rpm, wait 0.5s and close the stator switch.
    - Wait 0.5s, the rotor converter (and then speed controller) is enabled.
    - System is now running at nominal operation
6. The machine is now running normally. Motor torque and speed reference can be set by user.
7. To stop the machine, simply turn off `Start`. This will stop the machine in the following order:
    - Disable rotor converter
    - Open stator breaker
    - Stop motor
    - Wait 1s, turn off grid converter
    - Wait 1s, open rotor converter breaker
    - Open grid converter breaker
    - System is now standby
8. Turn off enable switch of the motor drive.
9. If the system must be shut down immediately, the `Trip` switch is used. Please note that the trip function is not connected to the protection system at this point.

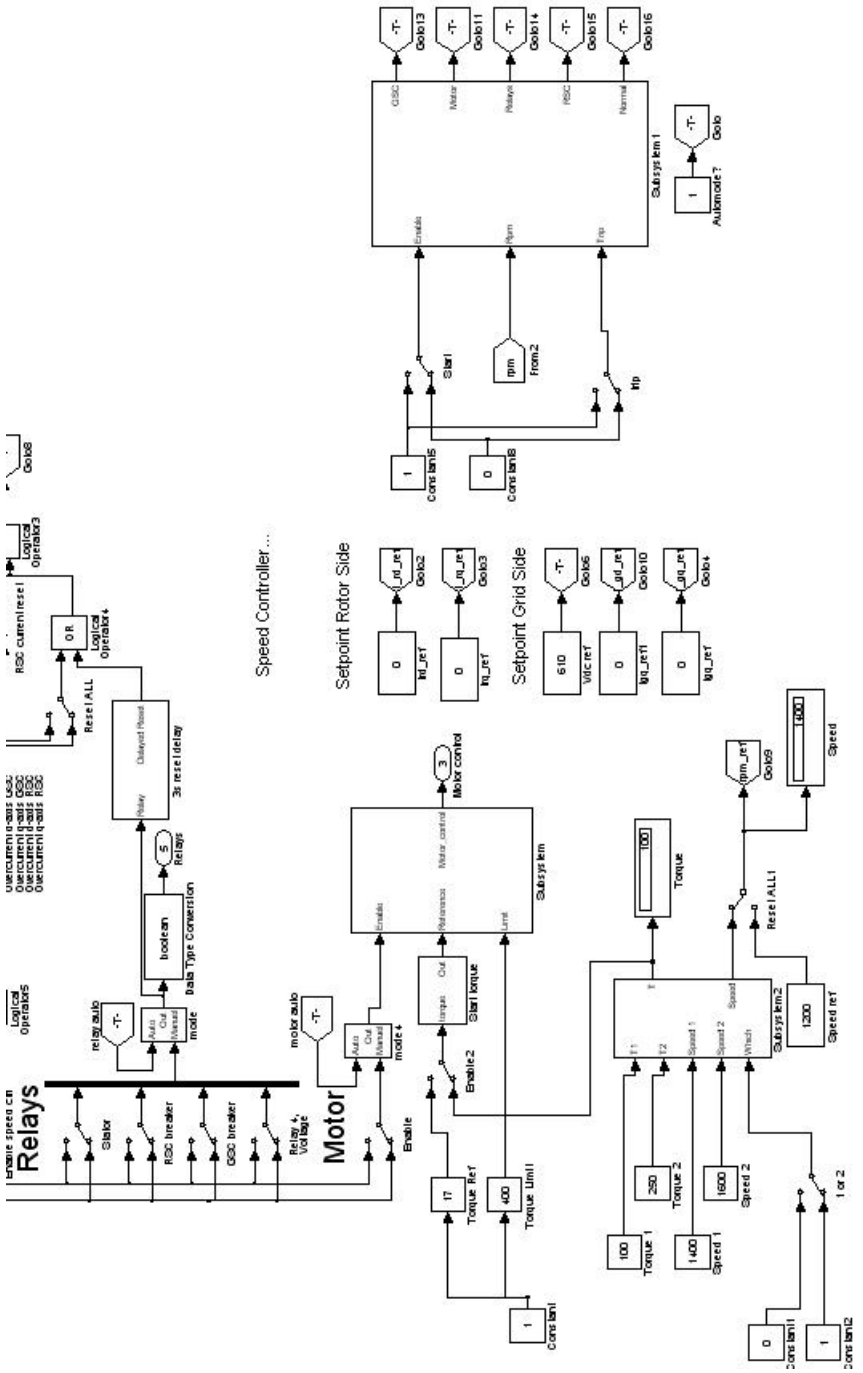

Figure 8.2: Automatic mode

File location for the files in the lab computer:

```
Documents ->
Matlab2010b ->
Control_system_v0 ->
    - control_system_v3.mdl
    - control_system_v4.mdl

A lot of other files exist in this folder.
However, only the one of the two given above is
necessary to open.
```

Appendix C - Converter status codes

Converter status codes

Status code	Message
F	5V error
E	Overcurrent Transitor A+ trip
D	Overcurrent Transitor B+ trip
C	Overcurrent Transitor C+ trip
B	Overcurrent breaking chopper
A	Overcurrent Transitor A- trip
9	Overcurrent Transitor B- trip
8	Overcurrent Transitor C- trip
7	Not used
6	Overtemp. Heat sink
5	Not used
4	Not used
3	Overvoltage DC link
2	Not used
1	Main breaker open
0	Converter OK